Modeling of Phase Equilibria for Paint-Related Polymer Systems

Kouskoumvekaki, Eirini; Kontogeorgis, Georgios; Michelsen, Michael Locht

Publication date:
2004

Document Version
Publisher's PDF, also known as Version of record

Modeling of Phase Equilibria for Paint-Related Polymer Systems

Irene Kouskoumvekaki

2004

Ph.D. Thesis

DTU

TECHNICAL UNIVERSITY OF DENMARK
DEPARTMENT OF CHEMICAL ENGINEERING

Modeling of Phase Equilibria

For Paint-Related Polymer Systems

Irene A. Kouskoumvekaki

Ph.D Dissertation, January 2004

Center for Phase Equilibria and Separation Processes (IVC-SEP)

Department of Chemical Engineering

Technical University of Denmark

DK-2800 Lyngby, Denmark

Printed by Book Partner, Nørhaven Digital, Copenhagen, Denmark
ISBN 87-91435-01-3

To my parents, for their
continuous support, even though
they have never really understood
the reason I got to all this trouble…

PREFACE

The thesis is submitted in partial fulfillment of the requirements for the Ph.D. degree at the Technical University of Denmark (Danmarks Tekniske Universitet).

This work has been carried out from February 2001 to January 2004 at the Department of Chemical Engineering (Institut for Kemiteknik) under the supervision of Georgios M. Kontogeorgis and Michael L. Michelsen.

The project has been financed by the Danish Research Council in the framework of a grant entitled: '*Thermodynamic properties of polymer solutions related to paints and coatings*', as well as by the J. C. Hempel foundation. The author gratefully acknowledges their support.

Furthermore, I would like to thank a number of people that played a key role in my Ph.D studies and contributed positively in one way or another:

- Erling Stenby for having given me the opportunity to be a member of the IVC-SEP group.
- My two supervisors, for the enormous help and support that they have provided me, as well as their great guidance and their ability to transfer their enthusiasm and knowledge to the people they are working with.
- Gerard Krooshof and the whole ACES group of DSM for our great collaboration and their hospitality during my external stay in their company.
- Samer Derawi, Thomas Lindvig and Nicolas von Solms for being always there whenever I had a question.
- Dani Merino Garcia for being an excellent co-traveler from the very first to the very last day of our Ph.D. studies.
- Christian Jensen and Natascha Mikkelsen for having given me the idea to apply to IVC-SEP in the first place.

Irene Kouskoumvekaki

January 30, 2004

CONTENTS

SUMMARY

There has been an increasing interest in the recent years from industries that deal with polymeric materials (e.g. producing paints, polymeric fibers etc.) for powerful thermodynamic tools. These tools should free them from costly and time-consuming experiments, losses of chemicals due to inaccurate process design, or errors in prediction of phase equilibria whenever a change in the process -either in the temperature or pressure, or in the number and type of the components- is required.

The target of this thesis is to evaluate and develop such thermodynamic tools, in terms of activity coefficient models or equations of state, capable of describing qualitatively – and to a high extend quantitatively – vapor-phase and liquid-phase equilibria of multicomponent polymer systems containing non-polar, polar and associating solvents.

With this focus, the free-volume term of the Entropic-FV activity coefficient model has been modified based on the performance of the model in athermal systems with high asymmetry (high differences in molecular size). The applied modification corrects the underestimation of the original Entropic-FV model in the prediction of activity coefficients of both solvent and solute and can be theoretically justified by the values of packing densities of polymers and organic solvents, based on their geometrical structure.

Furthermore, the simplified PC-SAFT equation of state has been evaluated in more demanding areas of industrial interest, such as polymers with complex structure (nylons), and systems containing components that self- and cross-associate. Special attention has been given in two points: a) the development of an efficient algorithm for the calculation of liquid-liquid equilibria in polymer systems and b) the regression of the pure-polymer parameters that are required as input from simplified PC-SAFT.

The overall performance of the simplified PC-SAFT equation of state in the studied cases is quite promising and is our wish that the present thesis will provide the ground for further improvement and development of the model.

RESUMÉ

I de senere år har industrier, der beskæftiger sig med polymermaterialer (f.eks. producenter af maling, polymerfibre osv.) vist en øget interesse i kraftige termodynamiske redskaber. Disse redskaber skulle befri dem for dyre og tidskrævende eksperimenter, tab af kemikalier på grund af unøjagtigt procesdesign eller fejl i forudsigelsen af faseligevægte, når en ændring i processen – enten i temperatur eller tryk, eller i antal og type komponenter – er påkrævet.

Formålet med denne afhandling er at evaluere og udvikle sådanne termodynamiske redskaber, i form af aktivitetskoefficientsmodeller eller ligevægtsligninger, der er i stand til at beskrive kvalitativt – og i stor udstrækning kvantitativt – dampfase og flydende fase ligevægte i multikomponent polymersystemer, der indeholder ikke-polære, polære og associerende opløsningsmidler. Med fokus herpå, er Entropic-FV aktivitetskoefficientsmodellens fri masse term blevet modificeret på grundlag af modellens præstation i atermiske systemer med stor asymmetri (store forskelle i molekylær størrelse). Den anvendte modificering korrigerer den oprindelige Entropic-FV models undervurdering i forudsigelsen af både opløsningsmiddels og opløst stofs aktivitetskoefficienter og kan teoretisk godtgøres ved værdierne af polymerers og organiske opløsningsmidlers pakningstæthed, ud fra deres geometriske struktur. Endvidere er den forenklede PC-SAFT ligevægtsligning blevet evalueret på mere krævende områder af industriel interesse, såsom polymerer med kompleks struktur (nyloner) og systemer med komponenter, der selv- og krydsassocierer. To punkter har fået særlig opmærksomhed: a) udvikling af en effektiv algoritme til beregning af væske-væske ligevægte i polymersystemer og b) renpolymerparametres regression, der kræves som input fra forenklet PC-SAFT.

Den forenklede PC-SAFT ligevægtslignings generelle præstation i de undersøgte cases er temmelig lovende, og det er vort ønske, at nærværende afhandling vil danne grundlag for videre udvikling af modellen.

Chapter 1

Introduction

Paints are complex materials comprising of one or more polymers dissolved in one or more solvents, while other compounds are also typically present (additives, pigments). In paint formulation, as well as in polymer production, knowledge of phase equilibria of the system is essential in accurate process design and control as well as in solvent selection and substitution. Current industrial practice is often based on a variety of empirical models and rules of thumb that may quite accurately describe a process, but cannot be used as predictive tools or give trustworthy guidelines, when changes in the process or formulation are required.

At the same time, it is very attractive to use thermodynamic models in order to minimize experimental effort, especially because such experiments are either expensive or too laborious. For this reason, and as industrial products and processes become more advanced, there is an industrial need for a thermodynamic tool that is able to describe complex, multicomponent polymer mixtures. This tool could be either an activity coefficient model or an equation of state that, above all, is able to handle the difference in the free volume and size between the large polymer molecule and the small solvent, as well as able to describe the energetic interactions (e.g. polar, associating) between components with complex structure. Furthermore, it should be able to fulfill the following requirements:

1. Predict satisfactorily pure-compound properties, as well as two-phase binary systems.
2. Predict very low values of polymer vapor pressures ($P^s \approx 0$).
3. The method for estimating the polymer parameters should be readily available for many polymers (e.g. use of standard available properties such as liquid densities).
4. Predict, to a satisfactory extend, liquid-liquid equilibria with parameters taken from vapor-liquid equilibrium correlations.
5. Be applied satisfactory to both low and high pressures.
6. Be successful in correlating the more complex multicomponent, multiphase systems that are more representative of paint solutions.

Activity coefficient models that are based on the group-contribution approach have the great advantage that they are purely predictive and can provide a qualitative answer very fast, based solely on the molecular structure of all the components of a mixture. However, previous investigations have shown that their development and application has reached its limit for systems with high asymmetry (large difference in size), unless the difference of the free-volume of the components is taken into account. For this reason, some selected free-volume activity coefficient models are evaluated in the first part of this study.

In the second part of this study, the simplified PC-SAFT equation of state has been selected among the equations of state that have been developed in the recent years for polymer systems, as the more promising one for further improvement and evaluation. Simplified PC-SAFT belongs to the SAFT family of equations of state, which are segment based –in contrast to the cubic equations of state- and therefore, can be readily adapted in any process that involves polymeric or complex components.

The thesis is accordingly divided into the following chapters:

- **Chapter 2:** *Evaluation of Free-Volume Activity Coefficient Models in Alkane and Polymer Systems*

  Selection of four free-volume activity coefficient models and evaluation of their performance in athermal and nearly athermal alkane systems. Evaluation of the Entropic-FV model in prediction of activity coefficients of dendrimer solutions. Modification of the free-volume term of the Entropic-FV model.

  (I.A. Kouskoumvekaki, M.L. Michelsen, G.M. Kontogeorgis, *Fluid Phase Equilibria* **2002**, 202 (2), 325 & I.A. Kouskoumvekaki, R. Giesen, M.L. Michelsen, G.M. Kontogeorgis, *Ind.Eng.Chem.Res.* **2002**, 41 (19), 4848)

- **Chapter 3:** *Non-Cubic Equations of state for polymer systems – The Simplified PC-SAFT Equation of State*

  Brief presentation of the theoretical background and the main equations of the simplified PC-SAFT equation of state.

- **Chapter 4:** *Application of the Simplified PC-SAFT Equation of State in Binary Vapor-Liquid Equilibria of Polymer Mixtures*

  Comparison of the simplified PC-SAFT equation of state with the original model and evaluation of the former in vapor-liquid equilibria of binary polymer systems that include a variety of non-associating (esters, cyclic hydrocarbons), polar (ketones) as well as associating (amines, alcohols) solvents.

  (I.A. Kouskoumvekaki, N. von Solms, M.L. Michelsen, G.M. Kontogeorgis, *Fluid Phase Equilibria* **2004**, 215, 71)

- **Chapter 5:** *Application of the Simplified PC-SAFT Equation of State in Binary Liquid-Liquid Equilibria of Polymer Mixtures*

  Development of an algorithm for the calculation of liquid-liquid equilibria of polymer mixtures, with application to the simplified PC-SAFT equation of state. Evaluation of the model in binary mixtures of polymers with non-associating as well as associating solvents.

  (N. von Solms, I.A. Kouskoumvekaki, T. Lindvig, M.L. Michelsen, G.M. Kontogeorgis, *Fluid Phase Equilibria* **2004**, accepted for publication)

- **Chapter 6:** *Application of the Simplified PC-SAFT Equation of State in the Manufacturing Process of Polyamide 6*

  Development of a method for obtaining pure-component parameters for polyamides. Application of simplified PC-SAFT in vapor-liquid equilibria of binary and ternary mixtures of polyamide 6.

  (I.A. Kouskoumvekaki, G. Krooshof, M.L. Michelsen, G.M. Kontogeorgis, *Ind.Eng.Chem.Res.* **2004,** 43 (3), 834)

- **Chapter 7:** *Development of a Method for the Estimation of Pure-Component Parameters for Polymers, with Application to the Simplified PC-SAFT Equation of State*

  Improvement and extension of the method for obtaining pure-component parameters for polymers. Evaluation of the method in a variety of binary polymer mixtures, exhibiting both vapor-liquid and liquid-liquid phase equilibria.

(I.A. Kouskoumvekaki, N. von Solms, T. Lindvig, M.L. Michelsen, G.M. Kontogeorgis, *Ind.Eng.Chem.Res.* **2004**, accepted for publication)

- **Chapter 8:** *Conclusions and Future Challenges with the Application of Simplified PC-SAFT Equation of State in Polymer Systems*

  Brief presentation of the main conclusions that have derived from the present work. Suggestions and preliminary results on subjects that could be considered as future challenges for simplified PC-SFT, like the application of the model in aqueous polymer solutions, polymer blends etc.

Chapter 2

Evaluation of Free-Volume Activity Coefficient Models in Alkane and Polymer Systems

In polymer solutions, the combinatorial and free-volume (comb/FV) effects are very important and every thermodynamic model should account for them. This is usually done with a separate contribution term. Finding, however the correct comb/FV term is not a trivial issue and many expressions have been proposed and evaluated. One way of evaluating these terms is via comparison with experimental data from athermal polymer and size-asymmetric non-polymer solutions. In this work we have performed such an evaluation for four promising free-volume activity coefficient models, namely UNIFAC-FV, Flory-FV, Zhong-Masuoka and Entropic-FV. Entropic-FV, which has shown the best behavior in athermal systems, has then been evaluated in phase equilibria for dendrimer systems. The free-volume term of the Entropic-FV model has been modified based on the statement by Bondi and others that due to the packing of molecules, a higher than the van der Waals volume (V_w) inaccessible volume represents more adequately the hard-core volume. Using experimental phase equilibrium data for athermal polymer (and other asymmetric) solutions, we show that the optimum V^*/V_w ratio is equal to 1.2, which is very close to the value expected based on the packing density at 0 K for organic systems.

2.1 Introduction

The concept of free-volume is rather loose but very important especially in polymer systems, since the free-volume percentages of solvents and polymers are different and this difference is usually responsible for the non-ideal thermodynamic behaviour of such systems. In the typical case, the free-volume percentage of solvents is greater (40-50%) than that of polymers (30-40%)[1].

Many combinatorial–free volume expressions have been proposed the last 20 years for polymer solutions, e.g UNIFAC-FV[2], UNIFAC-ZM[3] and Entropic-FV[1].

Oishi and Prausnitz[2] proposed the *Unifac-FV* model for polymer solutions. The activity coefficient is given by the expression:

$$\ln \gamma_i = \ln \gamma_i^{comb} + \ln \gamma_i^{fv} + \ln \gamma_i^{res} \qquad (2.1)$$

$\ln \gamma_i^{comb}$ and $\ln \gamma_i^{res}$ account for the combinatorial and energetic effects, respectively and are obtained from the Unifac[4] group contribution method.

The free-volume term is derived from the Flory equation of state[5],

$$\ln \gamma_i^{fv} = 3c \ln\left(\frac{\widetilde{V}_i^{1/3} - 1}{\widetilde{V}_m^{1/3} - 1}\right) - c\left[\left(\frac{\widetilde{V}_i}{\widetilde{V}_m} - 1\right)\left(1 - \frac{1}{\widetilde{V}_i^{1/3}}\right)^{-1}\right] \tag{2.2}$$

where the reduced volumes are defined as

$$\widetilde{V}_i = \frac{V_i}{bV_{i,w}} \tag{2.2a}$$

$$\widetilde{V}_m = \frac{\sum w_i V_i}{b\sum w_i V_{i,w}} \tag{2.2b}$$

and $c = 1.1$ and $b = 1.28$ for all solvents and polymers. In the residual term, the revised by Hansen et al.[6] temperature independent parameters are employed.

The *Entropic-FV* model is given by the expression:

$$\ln \gamma_i = \ln \gamma_i^{comb-fv} + \ln \gamma_i^{res} \tag{2.3}$$

The combinatorial-free volume expression used in the Entropic-FV model is somewhat simpler than that of Unifac-FV and has been originally suggested by Hildebrand[7] and many years later put into a working form and tested by Elbro et al.[1]:

$$\ln \gamma_i^{\text{comb-fv}} = \ln \frac{\varphi_i^{fv}}{x_i} + 1 - \frac{\varphi_i^{fv}}{x_i} \tag{2.4}$$

where

$$\varphi_i^{fv} = \frac{x_i V_i^{fv}}{\sum_j x_j V_j^{fv}} \qquad (2.4_a)$$

and

$$V_i^{fv} = V_i - V_i^* = V_i - V_{iw} \qquad (2.4_b)$$

Eq. (2.4) is essentially identical to the well-known Flory-Huggins expression[8-9], except that free-volume fractions are used instead of segment or volume fractions. The van der Waals volume (V_w) is estimated from the group increments of Bondi[10]. Elbro et al.[1] showed that the Entropic-FV model performs much better than Flory-Huggins (segment or volume-based) for nearly athermal polymer solutions. When Entropic-FV is applied to non-athermal systems, the same residual term as in the Unifac-FV model is used[2] to account for the energetic effects. The Entropic-FV model has been applied to polymer-solvent VLE[11], LLE[12], copolymers VLE[13] and SLE[14]. However, as shown by a number of researchers[15-19], the Entropic-FV formula has –despite its success- a number of deficiencies:

i. The solvent activities in athermal polymer solutions are systematically underestimated by, often, 10% or more. Such an error cannot be entirely attributed to the small interaction effects present in such systems.

ii. The activities of heavy alkanes in short-chain ones (hereafter denoted γ_2), compared with data available from SLE measurements, are in significant error, especially as the size difference increases. Due to the lack of experimental data for polymer activities, such data can test the model's applicability at the other (than solvent activity) concentration end. Activities of short alkanes (γ_1) are much easier to predict.

iii. The model's performance is rather sensitive to the values used for the polymer density.

To account for one or more of these deficiencies, a number of entropic formulas have been proposed over the last years.[3, 15-18]

The model of Zhong and Masuoka, *Unifac-ZM*,[3] has the advantage that the density of the components is not required. Several of the other models (p-FV [13], Chain-FV[17] and R-Unifac[18]) yield improved results over Entropic-FV for both γ_1 and γ_2, but as shown previously[20], they cannot be extended rigorously to multicomponent systems. Thus, they will not be further considered in this work.

An interesting model originally suggested in[21] and shown later[16-19] to yield very good SLE for alkane solutions, is the so-called *Flory-FV* model, which is given by Eq. (2.4), but the free-volume fractions are based on the free-volume definition by Flory[21]:

$$V_i^{fv} = (V_i^{1/3} - V_{iw}^{1/3})^{3c_i} \quad (c_i = 1.1) \tag{2.5}$$

$3c_i$ is the number of external degrees of freedom per solvent molecule and for c_i=1.1 the model was shown to have the best performance[15]. This value was chosen in agreement with the development of Unifac-FV, but it should noted that when a c-value different than unity is applied in Eq. (2.5), the free-volume term has no longer dimensions of volume. This is a theoretical limitation of Eq. (2.5), although there is no inconsistency when Eq. (2.5) is used together with the free-volume fractions shown in Eq. (2.4).

A common feature for all free-volume activity coefficient models is that they require the volumes of solvents and polymers (at the different temperatures that the application requires). This can be a problem in those cases where the densities are not available experimentally and have to been estimated using a predictive group-contribution or other method, e.g. GCVOL or van Krevelen methods.

2.2 Athermal Systems

2.2.1 Database

The models Unifac-FV, Entropic-FV, Unifac-ZM and Flory-FV were evaluated against experimental data, both at infinite dilution and intermediate concentrations. Due to the

lack of experimental data on polymer activity coefficients, the predicted values were compared with values obtained from methods based on molecular simulation studies.
The database used in this work is presented in Tables 2.1 and 2.2 and includes:

- Mole based activity coefficients of the solvent in short-chain alkane (C_{4-10}) and long-chain alkane (C_{24-36}) solutions at infinite dilution (γ_1^{∞})[22,23].
- Mole based activity coefficients of the solute in long-chain alkane (C_{16-36}) and short-chain alkane (C_{5-12}) solutions at infinite dilution (γ_2^{∞})[24,25] and intermediate concentrations (γ_2)[19]. The following distinction is adopted: *S:* symmetric systems ($\gamma_2 > 0.8$), *MA:* medium asymmetric systems ($0.7<\gamma_2<0.8$); *A:* asymmetric systems ($\gamma_2 < 0.7$).
- Weight based activity coefficients of solvents (Ω_1^{∞})[26,27] in various nearly athermal polymer solutions.
- Molecular simulation data of polymer infinite dilution activity coefficients (Ω_2^{∞}) calculated by a previously developed method[28].

Table 2.1 Database of experimental data for infinite dilution activity coefficients.

Type of systems	N_{sys}	N_{DP}	*T*-Range (K)	*MW*-Range (polymer)
Short n-alkane/long alkane	21	60	333-373	
Short branched, cyclic-alkane / long alkane	19	55	328-373	
Alkane / PE	25	68	373-473	$7.4 \cdot 10^3$-$10.5 \cdot 10^4$
Alkane / PIB	10	22	298-373	$24.5 \cdot 10^3$-10^6
Organic solvent / PDMS, PS, PVAc	8	27	298-483	$3.5 \cdot 10^3$-$9.7 \cdot 10^4$
Symmetric long / short alkanes	15	16	220-285	
Medium asymmetric long / short alkanes	7	7	257-281	
Asymmetric long / short alkanes	19	19	218-295	
PE / alkane	20	20	373-473	$7.4 \cdot 10^3$-$10.5 \cdot 10^4$
PIB / alkane	10	10	298-373	$24.5 \cdot 10^3$-10^6
PDMS, PS, PVAc / organic solvent	6	6	298-483	$3.5 \cdot 10^3$-$9.7 \cdot 10^4$

Two versions of Flory-FV are considered, where c_i in Eq. (2.5) is taken equal to 1.0 and 1.1 respectively. Since the final target is the optimization of the free-volume expression (Eq. (2.5)), it is necessary to check the performance of the model independently of the c_i parameter. The value 1.1 is the outcome of an optimization and it is thus not desirable that it influences the current optimization.

The results of our evaluation are presented in Table 2.3**,** in the form of absolute average percentage deviations between the calculated and the experimental values.

Table 2.2 Database of experimental data for activity coefficients at intermediate concentrations.

Type of systems	N_{sys}	N_{DP}	***C*- Range (component 1)**	***T*- Range (K)**	***MW* Range (polymer)**
Alkane / HDPE, PP	5	40	0.01-0.1	353-458	$5 \cdot 10^4$
Short n-alkane / PIB	18	139	0.01-0.89	298-338	$1.17 \cdot 10^3$-$2.2 \cdot 10^6$
Short branched alkane / PIB	4	26	0.01-0.13	298-308	10^6
Short cyclic alkane / PIB	9	91	0.02-0.99	281-338	$4 \cdot 10^4$-10^5
Organic solv. / PDMS, PS, PVAc	8	70	0.01-0.90	283-403	$5.9 \cdot 10^2$-$2.7 \cdot 10^5$
Symmetric long / short alkanes	26	455	0.004-1.000	268-317	
Medium asymmetric long / short alkanes	12	251	0.001-1.000	259-331	
Asymmetric long / short alkanes	13	241	$9.3 \cdot 10^{-5}$-1.000	278-334	

For those models, where the volumes are required, the experimental values were used, for short and long-chain alkanes calculated via the correlations taken by the DIPPR database[29], whereas those of the polymers by the Tait correlation[30].

2.2.2. Results and Discussion

From the results shown in Table 2.3 we conclude:

Generally:

i. The models perform clearly better for γ_1 (activity of low molecular weight alkane) than for γ_2 (activity of heavy alkane).

ii. Entropic-FV is the best model for γ_1 and Flory-FV for γ_2. Unifac-ZM performs rather poorly for γ_2.

Table 2.3 % Absolute average percentage deviation between experimental and calculated activity coefficients.

% AAD	Entropic-FV	Unifac-ZM	Unifac-FV	Flory-FV (c=1.0)	Flory-FV (c=1.1)
γ_1^∞ (Ω_1^∞ for polymers)	12	14	19	60	26
Ω_1	11	20	14	-	19
γ_2^∞	38	56	-	20	20
γ_2	26	32	-	-	11
Ω_2^∞	11	7	-	49	70
OVERALL	**20**	**26**	**17**	**43**	**29**

(-): not evaluated

More specifically:

i. Entropic-FV performs very accurately for both γ_1^∞ and Ω_1 and is the best among the evaluated models. The good performance of the model when compared to the molecular simulation data (Ω_2^∞), adds positively to this remark, though only indicatively. As stated also by Kontogeorgis et al.[11], there is no difference on results between solutions containing normal, branched and cyclic alkanes. The opposite trend is observed for γ_2 and γ_2^∞ data, where, with increasing asymmetry the model tends to overcorrect for the non-ideality and thus, yielding higher deviations. This remark is in agreement with the conclusions of Polyzou et al.[19] and Coutinho et al.[16] based on solid-liquid equilibrium studies. The overall lower deviations compared to those shown in the paper of Voutsas et al.[18], are due to the use of the DIPPR and Tait methods for calculating long-chain alkane and polymer volumes respectively in this work, instead of GCVOL, which is an estimation method.

ii. Flory-FV (c = 1.1) is the best model for γ_2^∞ and γ_2. However, it has increased deviations at elevated temperatures and low molecular weights of the polymer. This may explain the higher deviations for γ_1^∞, where the experimental data for alkane and polymer systems were measured in a variety of temperatures and

molecular weights. Flory-FV is the only among the evaluated models that overestimates γ_1^{∞} data. The observed performance of the model is in accordance with previous results in the literature[15-16]. The influence of the *c*-parameter is not significant when the model is applied to alkane systems. However, the model becomes very sensitive to the *c*-value, when polymer systems are involved (Ω_1^{∞} and Ω_2^{∞}). The higher deviations for polymer solutions with $c = 1$ (Ω_1^{∞}) limit the chances for a successful optimization.

iii. Unifac-ZM was primarily derived for polymer solutions. However, it is interesting to notice that it performs rather well for short-alkane / long-alkane solutions (γ_1^{∞}), especially for lower asymmetries, which is a field that the model had not been previously evaluated. This could be due to the fact that since it contains no free-volume expression term, the n-mer modification minimizes the underestimation that would have otherwise been more apparent. As it was also shown by the developers of the model[3], it gives worse results than Unifac-FV for alkanes in PIB and its performance for γ_2^{∞} of long alkanes in short alkanes, is very poor. However, it shows the lowest deviation when it comes to Ω_2^{∞} calculations. The increased error of Unifac-ZM in PIB, PDMS, PS and PVAc compared with the good results in PE, may indicate that the model cannot predict the branching effect. Furthermore, the lack of a free-volume term leads to higher deviations with the size of the solute molecules and to a temperature independent behavior of the model. Temperature has a small influence even for nearly athermal solutions. The overall performance of this model indicates that the free-volume fractions account more satisfactorily for the non-energetic effects than the segment fractions.

iv. The Unifac-FV model of Oishi and Prausnitz has not been systematically evaluated for athermal alkane solutions in the past. Its performance is shown to be poor for γ_1^{∞} for most cases considered. However, it gives very good predictions of solvent activity coefficients, both at infinite and intermediate concentrations, for alkane – PIB solutions. In the case of PE systems, the values are underestimated, whereas for PIB solutions they are overestimated. This behavior has been discussed previously[11].

2.3 Dendrimer Systems

2.3.1 Dendrimers: A Novel Family of Polymers – Applications

Dendrimers (also called cascade polymers) are a special type of highly branched macromolecules with a branch point at each monomeric unit. They consist of a central core and an external surface. The branches (dendrons) are built of repeat units or cells, which are connected in a precise architectural arrangement that produces a series of regular, radially concentric layers, called generations, organized around the core, as can be seen in Figure 2.1.

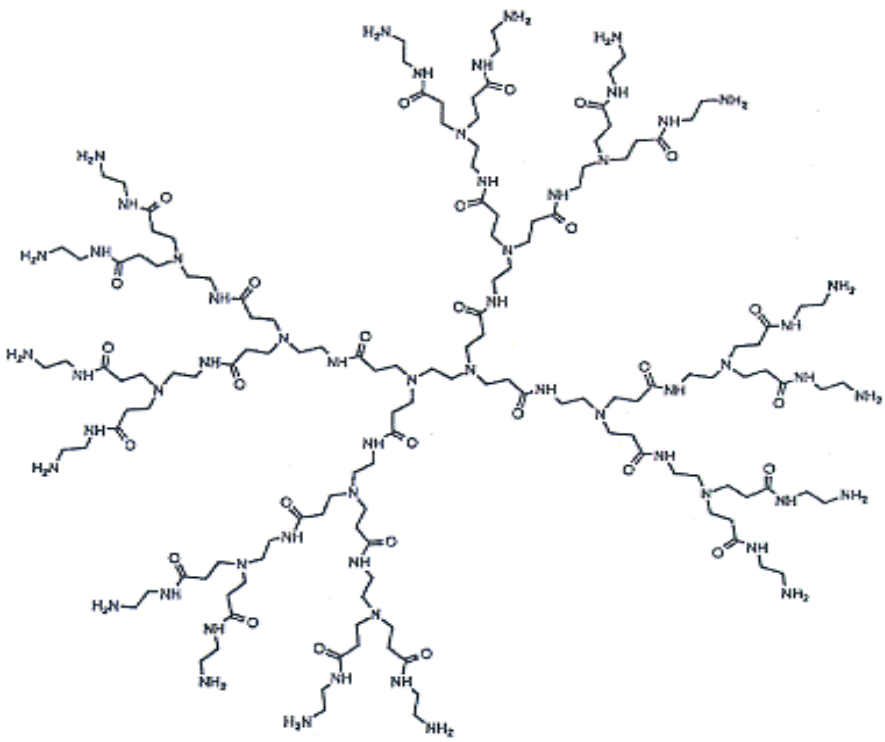

Figure 2.1 Schematic representation of the structure of the dendrimer PAMAM, generation 2.

Due to such an organized architecture, dendrimers can be prepared with a high degree of synthetic control and monodispersity and thus provide a unique combination of high molecular weights and molecular shapes similar to ideal spherical particles[31]. This unusual combination is responsible for their unique properties, such as perfectly Newtonian flow even at high molecular weights[31], high reactivity and good solubility in

solvents[32]. As a consequence of these properties, dendrimers have found applications in a variety of fields such as photovoltaic devices, medicine and biotechnology.

Previous efforts for modeling dendrimer solutions have been orientated towards modifying the mean-field theory of Flory-Huggins[32-34]. Other developments focus on the lattice cluster theory (LCT)[35]. Mio et al.[33] used a simplified version of this theory with one adjustable parameter to correlate VLE data of dendrimer / solvent systems. Lieu et al.[34] used a more complex version of LCT for similar correlations, again using one adjustable parameter. Jang et al.[32] proposed a lattice model based on LCT, which, using three adjustable parameters, takes into account the specific interactions encountered between solvent and end groups of the dendrimer. Earlier studies have been reviewed recently[33] and thus they are not repeated here.

The purpose of this work is to evaluate the performance of the Entropic-FV activity coefficient model in this new category of systems, as well as to estimate the influence of the dendrimer's density in the performance of the model. Since experimental densities are usually not known, we are interested in evaluating the performance of the model based on predicted values of densities. Under this scope, the predictive capabilities of the van Krevelen method for estimating dendrimer densities are also evaluated. Furthermore, since many of the dendrimers have newly characterised groups in their molecules, for which not all the interaction parameters have been estimated, the influence of assigning zero values to all the missing interaction parameters is also investigated.

2.3.2 Database

The Entropic-FV model was evaluated against experimental data of certain dendrimer solutions at intermediate concentrations, obtained by Mio et al.[33] and Lieu et al.[34].

The database used in this work includes:

- Benzyl Ether dendrimers with aromatic termination ring (AR) of generations 3-5 with polar and non-polar solvents
- Poly(amidoamine) (PAMAM) dendrimers of generations 1, 2 and 4 with polar solvents

- A-series poly(imidoamine) dendrimers (A) of generation 4, with polar and non-polar solvents.
- Benzyl Ether dendrimers with dodecyl alkane termination ring (C12) of generation 3 with polar and non-polar solvents.

Entropic-FV requires, as can be seen by Eqs. (2.4), the knowledge of the molar volumes of all the components of a system. For the solvents, these values were calculated from the correlations in the DIPPR database[29]. For the dendrimers, since the performance of the model may be very sensitive to the value of the molar volume[36] and since experimental data are not always available, three different approaches were considered:

1. In the papers of Lieu et al.[34] and Tande et al.[37], all dendrimers were assumed to have a density of 1 g/cm^3. The influence of this rather simplified assumption in the performance of the models is evaluated.
2. Use of a predictive method for the calculation of the molar volume such as:

The van Krevelen method[38]:

$$V=V_w(1.3+10^{-3}T) \tag{2.6}$$

where the van der Waals volume (V_w) is estimated from the group increments of Bondi[10].

or the GCVOL method[39]:

$$V = \sum n_i (A_i + B_i T + C_i T^2) \tag{2.7}$$

where, the A_i, B_i, C_i parameters are taken from the GCVOL parameter table[39]. For the dendrimers studied here, however, not all necessary group parameters are included in the GCVOL table. The evaluation is thus limited to the van Krevelen method.

3. Use of the experimental molar volume of the dendrimer, but such data are scarce and limited to few types of dendrimers. The experimental density data for PAMAM dendrimers provided by Uppuluri et al.[31] and for AR dendrimers provided by Hay et al.[40] are used in this work in order to evaluate both the effect of density on the predictions of both activity coefficient models, as well as the accuracy of the van Krevelen method in

predicting the density of these systems. The performance of the van Krevelen method is shown in Table 2.4 and Figure 2.2.

Table 2.4 Absolute average percentage deviation between experimental and predicted (by the van Krevelen method) densities the AR and PAMAM dendrimers at 20°C.

Dendrimer	d_{exp}	d_{pred}		d=1
	g/cm^3	g/cm^3	% AAD	% AAD
ARG-3	1.197	1.145	4	16
ARG-4	1.227	1.154	6	18
ARG-5	1.237	1.158	6	19
ARG-6	1.196	1.160	3	16
PAMAMG1	1.196	1.048	12	16
PAMAMG2	1.214	1.052	13	17
PAMAMG4	1.224	1.054	16	18

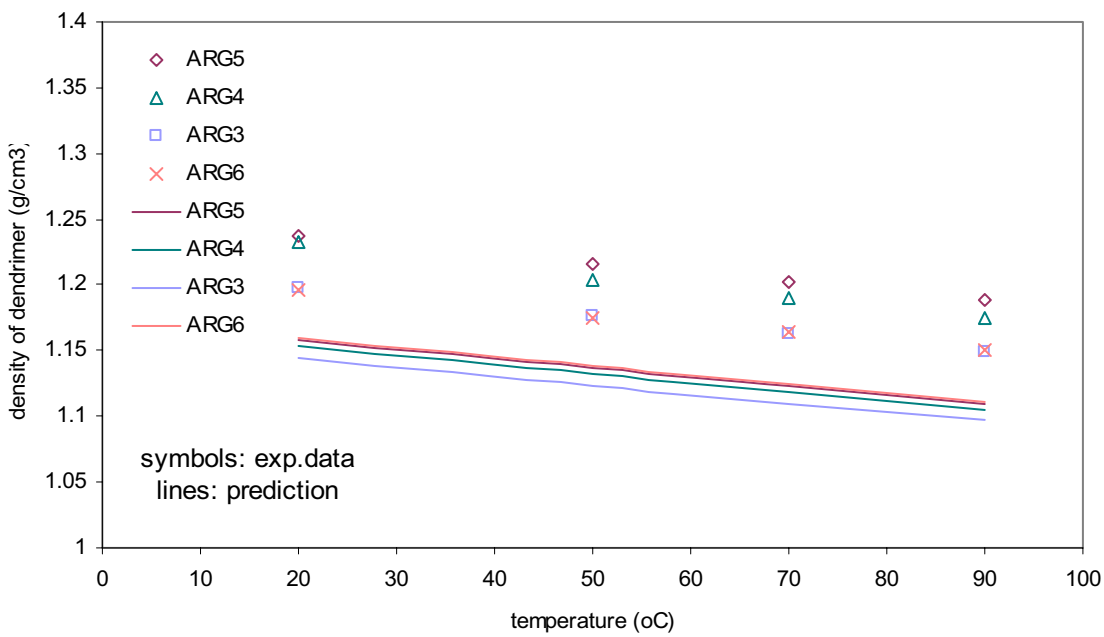

Figure 2.2 Temperature dependence of experimental[31,40] and predicted via the van Krevelen method densities of AR dendrimers.

The results of the evaluation, for both predicted and experimental density of the dendrimer (when the latter is available), are presented in Figures 2.3 - 2.4 and Tables 2.5

- 2.7, in the form of absolute average percent deviations (%AAD) between the calculated and the experimental activities:

$$\%\text{AAD} = 100 \left(\frac{\left| \alpha_{\text{exp}} - \alpha_{cal} \right|}{\alpha_{\text{exp}}} \right) \tag{2.8}$$

The values of the experimental solvent activities were obtained by the relation (assuming ideal vapor phase):

$$\alpha_i = \frac{P}{P^s} \tag{2.9}$$

where P^s is the saturated pressure and P the pressure of the system.

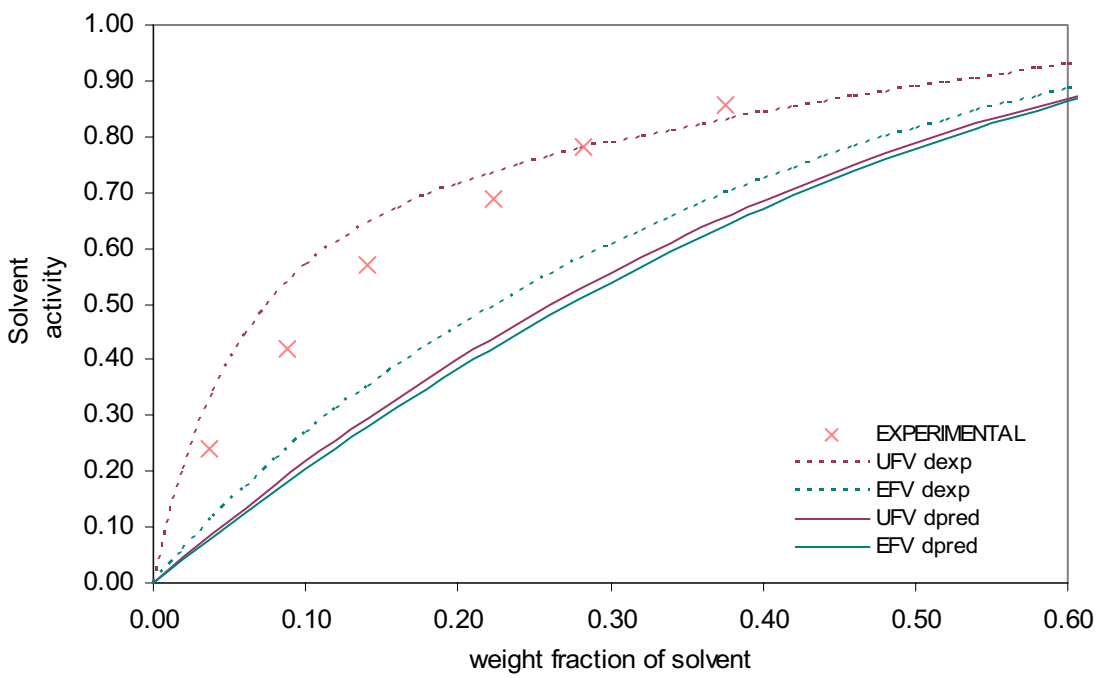

Figure 2.3 Experimental[33] and predicted activities of methanol in PAMAM-G2 with the Entropic-FV and the Unifac-FVmodels.

2.2.3. Results and Discussion

Based on the results shown in Tables 2.4 - 2.7 and Figures 2.2 - 2.4, the following summarize our conclusions:

1. Prediction of the dendrimer density: The predicted densities with the van Krevelen method are in the area between unity and the experimental density of the PAMAM and AR dendrimers (Table 2.4). The deviation from the experimental values increases for increasing generation number. This could be attributed to the characteristic structure of dendrimers, which, unlike other polymers, are flexible and allow a more compact packing. However, although the experimental density of the AR dendrimer increases from G-3 to G-5, it suddenly decreases for G-6. This is attributed by the authors[40] to the fact that a structural rearrangement occurs on an increase in the dendrimer molecular weight and hence the generation number. This packing is much closer to the packing of linear polymers and this may be the reason that the van Krevelen method can predict the density in this case with much accuracy. From the plot of the dendrimer's volume against temperature (Figure 2.2), we see that the van Krevelen method overestimates the volume, but has the same T-dependence as the experimental data. The assumption that the density is equal to unity is, thus, a rather crude simplification. The use of a predictive tool, such as the van Krevelen equation seems more appropriate.

2. Sensitivity of the model to the value of density: Figures 2.3 and 2.4 show that Entropic-FV is weakly influenced by the value of density. The performance of the model is quite similar when the experimental density, the predicted density or a value equal to unity is employed. However, Entropic-FV performs best when the value of the experimental density is employed. This weak density-dependency permits the application of the model in systems where the density of the dendrimer is not known. For comparative purposes the performance of Unifac-FV is presented in the same figures. It is shown that Unifac-FV has a greater dependence on the value of the dendrimer density. An extensive evaluation and comparison of the two models in dendrimer systems appears in literature[41].

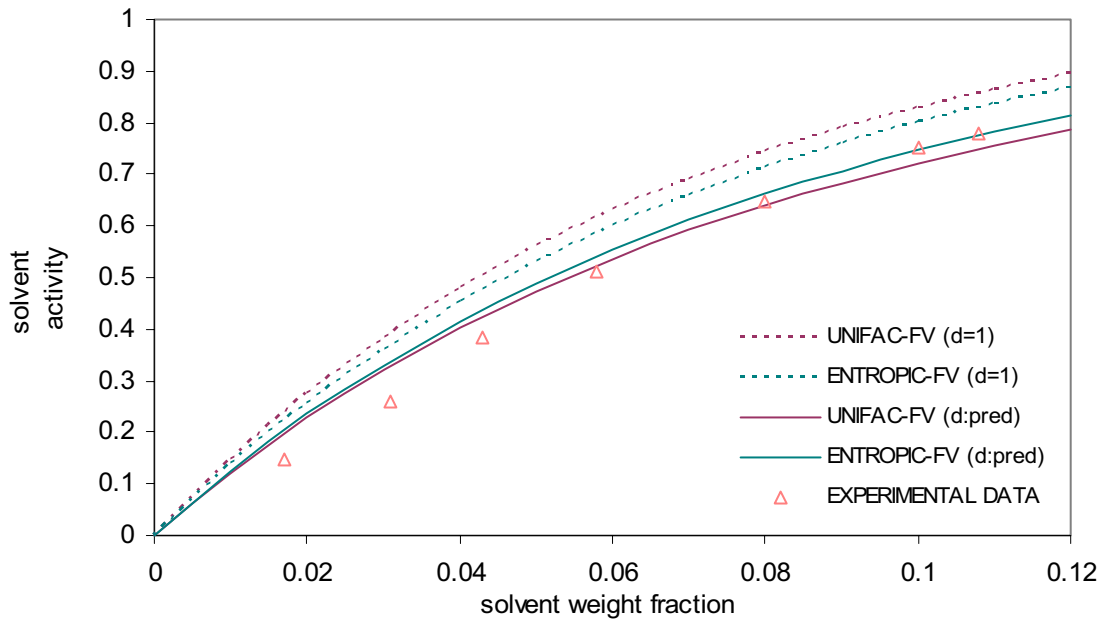

Figure 2.4 Experimental[34] and predicted activities of acetone in A4 with the Entropic-FVand the Unifac-FV models.

3. There is no influence of the dendrimer's generation number on the performance of the model. The differences in the deviation among systems with the same solvent and dendrimer of different generation number are mainly due to the different concentration range of the experimental data. As expected, when the concentration of the solvent in the system approaches the infinite dilution region, maximum non-ideality is encountered and higher deviations are expected.

4. Due to solvent induced crystallization (SINC) phenomena present in some of the studied systems (ARG3 / acetone, ARG3 / chloroform, ARG3 / toluene), the dendrimer rejects the solvent, when the solvent mass fraction exceeds a certain value, leading to a two-phase liquid system. The model cannot predict this behavior and this leads to higher deviations than the model's average performance, as can be seen in Table 2.5.

5. The predictions of the solvent activity in systems with a non-polar solvent are more accurate than in systems with polar solvents. This could be due to interactions (e.g.

hydrogen bonding) present in polar systems, which are not explicitly taken into account in the Entropic-FV model.

6. Table 2.7 presents systems, where experimental densities are known, but some of the interaction parameters between the groups of the solute and the solvent are missing (e.g. $CHCl_3$-CON, CHOH-CH_2NH_2) and were assigned here the value of zero. The results show that there is an increase in the deviations from the experimental data due to the missing interaction parameters.

Table 2.5 Absolute average percentage deviation (%AAD) between predicted and experimental solvent activities. d_{pred} is the density of the dendrimers predicted via the van Krevelen method.

	d_{exp} (g/cm^3)	d_{pred} (g/cm^3)	T (^{o}C)	ENTROPIC-FV	
				d_{exp}	d_{pred}
ARG3-acetone	1.176	1.124	50	58*	61*
ARG4-acetone	1.204	1.132	50	34	40
ARG4-acetone	1.189	1.119	70	31	39
ARG5-acetone	1.216	1.137	50	34	41
ARG3-chloroform	1.176	1.124	50	82*	83*
ARG4-chloroform	1.204	1.132	50	38	43
ARG4-chloroform	1.189	1.119	70	49	54
ARG5-chloroform	1.216	1.137	50	44	49
ARG5-chloroform	1.202	1.123	70	38	44
ARG3-toluene	1.162	1.110	70	84*	86*
ARG4-toluene	1.189	1.119	70	30	37
ARG4-toluene	1.175	1.106	89	12	17
ARG5-toluene	1.202	1.123	70	36	38
ARG4-tetrahydrofuran	1.189	1.119	70	4	6
ARG5-tetrahydrofuran	1.202	1.123	70	48	22
overall				**41**	**44**
overall (SINC excluded)				**30**	**33**

*SINC of the dendrimer

Table 2.6 Absolute average percentage deviation (%AAD) between predicted and experimental solvent activities. d_{pred} is the density of the dendrimers predicted via the van Krevelen method.

	d_{pred} (g/cm^3)	T (^{o}C)	ENTROPIC-FV
			% ADD
A4-acetone	0.963	50	13
A4-chloroform	0.963	50	11
A4-hexane	0.954	65	19
A4-heptane	0.954	65	18
A4-octane	0.954	65	27
A4-nonane	0.954	65	40
overall			**21**
C12G3-acetone	0.952	50	25
C12G3-chloroform	0.952	50	20
C12G3-cyclohexane	0.946	60	8
C12G3-pentane	0.958	40	19
C12G3-toluene	0.941	70	15
overall			**17**

Table 2.7 Absolute average deviation (%AAD) between predicted and experimental solvent activities for the PAMAM dendrimers, with missing interaction parameters set to zero. d_{pred} is the density of the dendrimers predicted via the van Krevelen method.

		ENTROPIC-FV		
	T **(°C)**	d_{exp}	d_{pred}	***d*=1**
		% ADD		
PAMAMG1-methanol	35	33	44	47
PAMAMG2-methanol	35	34	46	49
PAMAMG4-methanol	35	38	50	54
overall		***35***	***47***	***50***
PAMAMG1-propylamine	35	73	80	82
PAMAMG2-propylamine	35	66	76	78
PAMAMG4-propylamine	35	73	81	83
overall		***71***	***79***	***81***
PAMAMG1-acetone	35	61	70	73
PAMAMG2- acetone	35	59	70	73
PAMAMG4- acetone	35	67	77	79
overall		***62***	***72***	***75***
PAMAMG1-acetonitrile	40	71	80	82
PAMAMG2- acetonitrile	40	73	81	83
PAMAMG4- acetonitrile	40	77	84	86
overall		***74***	***82***	***84***
PAMAMG1-chloroform	35	65	71	73
PAMAMG2- chloroform	35	71	77	78
PAMAMG4- chloroform	35	72	78	80
overall		***69***	***75***	***77***

2.4 Modification of the Entropic-FV Activity Coefficient Model

2.4.1 Background

The proposed modification of the Entropic-FV model was based on optimizing the relation of the hard-core volume to the vdW volume of Eq. (2.1_b), considering the statement of Bondi that due to the packing of molecules, a higher than V_w 'inaccessible' volume represents more adequately the hard-core volume. The hard-core volume V^*, that corresponds to the molecular volume at 0 K and the van der Waals volume V_w could be,

thus, related through the packing density at 0 K (ρ_o^*). This leads to an expression of the type $V^* = \alpha V_w$ ($1 < \alpha < 2$). Values of the *a*-parameter in this range were introduced in the equation $V^* = \alpha V_w$ and the results of the evaluation are shown in Table 2.8 and summarized in Figures 2.5 and 2.6.

2.4.2 Results and Discussion

The Entropic-FV model, as was revealed in the first part of the investigation, was the most promising model for athermal systems. The results, which are shown in Table 2.8 and Figures 2.5 - 2.6, lead to the following general conclusions:

- The *a*-parameter ($a = V^*/V_w$), which yields lowest deviations for both γ_1 and γ_2, is higher than unity and in the range of 1.2-1.3. A bit higher values are required for γ_2.
- γ_2 calculations are more sensitive to *a*-values than γ_1. This is shown by the steeper γ_2-*a* curves (Figure 2.6) compared to γ_1-*a* curves (Figure 2.5).
- Although a completely unique value for all systems and both γ_1 and γ_2 is difficult to obtain, a value of $a = 1.2$ is a reasonable compromise. The Entropic-FV model for $a = 1.2$ is now the best model in all situations, since it is comparable to Flory-FV for γ_2 (where the latter was better when *a* was set equal to 1).

2.4.3. Theoretical Interpretation of the Result

The conclusion that a value of *a* equal to 1.2 improves the performance of the Entropic-FV model increases in significance when it is considered in the light of previous empirical attempts and theoretical investigations on the concept of the hard-core volume.

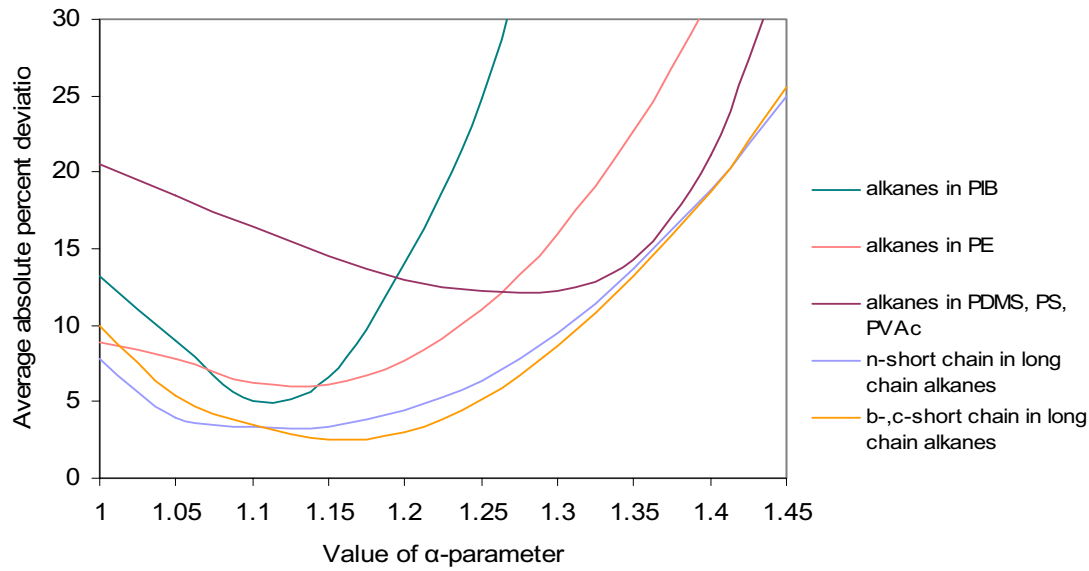

Figure 2.5 % Absolute average percentage deviation between experimental[26-42] and calculated solvent infinite dilution activity coefficients, versus the *a*-parameter in Entropic-FV ($V_f = V - aV_w$)

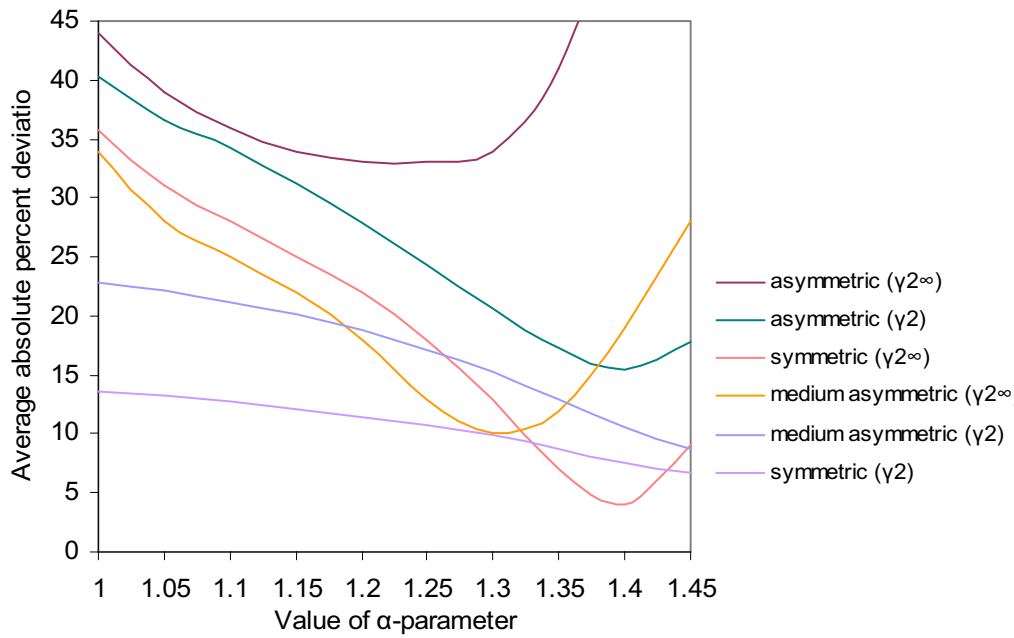

Figure 2.6 % Absolute average percentage deviation between experimental[19,24-25] and calculated activity coefficients of the solute, versus the *a*-parameter in Entropic-FV ($V_f = V - aV_w$)

Table 2.8 % Absolute average percentage deviation between experimental and calculated activity coefficients with the optimum value of the *a*-parameter. Results of original Entropic-FV (*a*=1.0) are shown for comparison.

	Entropic-FV	
	(*a*=1.0)	**(*a*=1.2)**
γ_1^∞ (Ω_1^∞)	**% Absolute Average Deviation**	
Short n-alkane / long alkane	8	4
Short b-c- alkane / long alkane	10	3
Alkane / PE	9	8
Alkane / PIB	16	13
Organic solv. / PDMS, PS, PVAc	20	13
OVERALL	**13**	**8**
γ_2^∞		
Symmetric long / short alkanes	36	22
Medium asymmetric long / short alkanes	34	18
Asymmetric long / short alkanes	44	33
OVERALL	**38**	**24**
Ω_1		
Alkane / HDPE, PP	19	17
Short n-alkane / PIB	5	10
Short b-alkane / PIB	20	7
Short c-alkane / PIB	4	3
Organic solv. / PDMS, PS, PVAc	7	6
OVERALL	**11**	**9**
γ_2		
Symmetric long / short alkanes	14	11
Medium asymmetric long / short	23	19
Asymmetric long / short	40	28
OVERALL	**26**	**19**

As Bondi[10] mentions, a more general free-volume expression has the form:

$$V_f = V - V_j \tag{2.10}$$

where V_j is the so-called inaccessible or occupied volume. Usually, V_j is represented by the hard-core volume V^* or the co-volume parameter b, the latter especially in the terminology of equations of state.

A first approximation of this inaccessible volume is the van der Waals volume. However, it is clear that, due to the packing of the molecules, a higher than V_w, inaccessible volume is maybe more adequate, as also stated by Bondi.

One interpretation of the inaccessible volume, which includes the effects of packing density, is the molecular volume at 0 K denoted as V_o, where $V_o / V_w = 1/\rho_o^*$ with ρ_o^* being the so-called packing density of the molecules at 0 K.

The packing density is a dimensionless parameter that depends on the shape and the structure of the molecule. Table 2.9 gives, some values for both the packing density and the parameter a in the equation $V^* = V_o = a\,V_w$.

From this table, we conclude that most organic molecules including polymers (e.g. polyethylene) have an a-parameter between 1.2 and 1.4, which nearly corresponds to the closed-packed cubic structure of spheres. For long molecules however, a mean value for the a-parameter may be somewhat lower (1.1 for close-packed arrays of infinite cylinders). But even in this case, the a-parameter for the mixture is expected to be in the range of 1.2.

Another way to look at V_o is by taking the limit of volume equations at 0 K. Using two models for the prediction of the liquid volume of polymers (the van Krevelen and GCVOL equations) and taking the limit at T=0 K, the following relations between the V_w and the volume at 0 K (V_o=V^*) are obtained:

- The van Krevelen method Eq.(2.6): ($T = 0$) → $V_o = 1.3 V_w$

- The GCVOL method Eq.(2.7)

The A_i, B_i, C_i parameters are taken from the GCVOL parameter table[39].

When applied for polyethylene (2*CH_2), Eq. (2.7) gives:

$$V = 2*(12.52+12.94*10^{-3}T)$$

And at $T = 0$ K: $V_o = 25.04$ (cm^3/gmol)

or equivalently: $V_o = 1.22 V_w$

since: V_w(2*CH_2) = 2*0.6744*15.17 = 20.46 cm^3/gmol

Unlike the van Krevelen method, the GCVOL method is valid for both solvents and oligomers / polymers.

The above values are also close to the values indicated on Table 2.9 for the packing density.

Table 2.9 Values of packing density[10] (ρ_o^*) and corresponding V_j/V_w ratios for a variety of structures.

Structure/Compound	ρ_o^*	$a = V_o/V_w$
Open-packed cubic structure of spheres	0.52	1.923
Closed-packed cubic structure of spheres	0.74	1.35
Open-packed arrays of infinite cylinders	0.785	1.273
Close-packed arrays of infinite cylinders	0.903	1.107
Polyethylene	0.762	1.312
Most organic compounds	0.7 …. 0.78	1.43 …. 1.28

Additional indications for the use of a higher, than V_w, inaccessible volume in the free-volume expressions are provided by several 'hard-core (inaccessible) volume definitions' in several thermodynamic models previously proposed in the literature. Some examples are included in Table 2.10.

Table 2.10 Empirical modifications of the hard-core volume

ACM/EoS	V^*	Method
Unifac-FV[1]	$1.28V_w$	Fitted from phase equilibrium data
GC-Flory[13]	$1.448V_w$	No explanation is provided
Holten-Andersen[43]	$1.4V_w$	No explanation is provided
Flory[44]	$1.4\text{-}1.48V_w$	Liquid densities
VdW[44]	$1.5\text{-}1.6V_w$	Fitted to vapor pressures and liquid densities
Sako[45]	$1.3768V_w$	No explanation is provided
Schotte[46]	$1.3\text{-}1.4V_w$	Liquid densities
CPA[47]	$1.5V_w$	Fitted to vapor pressures and liquid densities
PR[48]	$1.3\text{-}1.4V_w$	Fitted to volumetric data

Even though all these literature attempts should be considered as partially empirical, all of them indicate that the hard-core volume used in the thermodynamic models should be higher than V_w by a constant in the area of 1.2 – 1.5.

This picture seems to be in agreement with both the need of using another form of the inaccessible volume instead of V_w, as well as with the packing density range shown in Table 2.9.

2.5 Conclusions

Four free-volume expressions were tested for nearly athermal alkane and polymer solutions. The Entropic-FV model was found to be the best and it was further applied in dendrimer systems. The Entropic-FV model, with no extra fitting parameters, can predict the solvent activity in dendrimer systems with acceptable accuracy in many cases. However, due to the special structure of dendrimers, dependable tools such as the van Krevelen method are necessary for the prediction of their molar volume, which is a parameter that influences significantly the overall performance of free-volume models.

The free-volume expression of the Entropic-FV model employs the van der Waals volume (V_w) as a measure of molecules' hard-core volume (V^*). Much literature and theoretical evidence indicates that $V^* > V_w$. We have thus investigated the performance of Entropic-FV by optimizing the hard-core volume, i.e. finding a in the $V^* = a \cdot V_w$ expression. The optimum a-value obtained from experimental data is very close to values stated by Bondi for this type of systems (organic solvents in polymers), which are based on packing densities. This finding strengthens further the optimization and justifies the implementation of the modified free-volume definition: $V_f = V - 1.2V_w$ in the Entropic-FV model. The comparison with experimental data for athermal systems showed that this modification corrects the underestimation of the original Entropic-FV model in the prediction of both activity coefficients of the solvent and the solute in infinite dilution, as well as at intermediate concentrations.

References

1. H. S. Elbro, Aa. Fredenslund and P. Rasmussen, A New Simple Equation for the Prediction of Solvent Activities in Polymer Solutions, Macromolecules **1990,** 23, (21) 4707.
2. T. Oishi and M. Prausnitz, Estimation of Solvent Activities in Polymer Solutions Using a Group-Contribution Method, *Ind. Eng. Chem. Process Des.* **1978,** 17 (3), 333.
3. C. Zhong, Y. Sato, H. Masuoka and X. Chen, Improvement of Predictive Accuracy of the UNIFAC Model for Vapor-Liquid Equilibria of Polymer Solutions, *Fluid Phase Equilibria* **1996**, 123, 97.
4. Aa. Fredenslund, R. L. Jones, J. M. Prausnitz, Group-Contribution Estimation of Activity Coefficients in Nonideal Liquid Mixtures, *AlChEJ.* **1975,** 21, 1086.
5. J. M. Prausnitz, R. N. Lichtenthaler, E. G. de Azevedo, *Molecular Thermodynamic of Fluid Phase Equilibria*, 3rd Ed., **1999.**
6. H. K. Hansen, P. Rasmussen, Aa. Fredeslund, M. Schiller, J. Gmehling, Vapor-Liquid Equilibria by UNIFAC Group Contribution. 5. Revision and Extension, *Ind. Eng. Chem. Res.,* **1991,** 30, 2352
7. J. H. Hildebrand, R. L. Scott, *The Solubility of Nonelectrolytes.* Dover, New York, **1964.**
8. P. J. Flory, Thermodynamics of High Polymer Solutions, *J. Chem. Phys.* **1941,** 9, 660.
9. M. L. Huggins, Solutions of Long Chain Compounds, *J. Chem. Phys.* **1941,** 9, 440.
10. A. Bondi, Physical Properties of Molecular Crystals, Liquids and Glasses, Wiley, New York, **1968**.
11. G. M. Kontogeorgis, Aa. Fredenslund and D. P. Tassios, Simple Activity Coefficient Model for the Prediction of Solvent Activities in Polymer Solutions, *Ind. Eng. Chem. Res.* **1993**, 32 (2), 362.
12. G. M. Kontogeorgis, A. Saraiva, Aa. Fredenslund and D. P. Tassios, Prediction of Liquid-Liquid Equilibrium for Binary Polymer Solutions with Simple Activity Coefficient Models, *Ind. Eng. Chem. Res.* **1995**, 34 1823.

13. G. Bogdanic and Aa. Fredenslund, Revision of the Group-Contribution Flory Equation of State for Phase Equilibria Calculations in Mixtures with Polymers. 1. Prediction of Vapor-Liquid Equilibria for Polymer Solutions, *Ind. Eng. Chem. Process Des. Dev.* **1994**, 33, 1331.
14. V. I. Harismiadis, A. R. D. van Bergen, A. Saraiva, G. M. Kontogeorgis and Aa. Fredenslund, D. P. Tassios, Miscibility of Polymer Blends with Engineering Models, *AlChE J.* **1996,** 42 (11), 3170.
15. G. M. Kontogeorgis, P. Coutsikos, D. P. Tassios and Aa. Fredenslund, Improved Models for the Prediction of Activity Coefficients in Nearly Athermal Mixtures: Part I. Empirical Modifications of Free-Volume Models, *Fluid Phase Equilibria* **1994,** 92, 35.
16. J. A. P. Coutinho, S. I. Andersen and E. H. Stenby, Evaluation of ACM in Prediction of Alkane SLE, *Fluid Phase Equilibria* **1995**, 103, 23.
17. G. M. Kontogeorgis, G. I. Nikolopoulos, Aa. Fredenslund and D. P. Tassios, Improved Models for the Prediction of Activity Coefficients in nearly Athermal Mixtures. Part II. A theoretically based G^E-Model based on the van den Waals Partition Function, *Fluid Phase Equilibria* **1997,** 127 103.
18. E. C. Voutsas, N. S. Kalospiros and D. P. Tassios, A Combinatorial Activity Coefficient Model for Symmetric and Asymmetric Mixtures, *Fluid Phase Equilibria* **1995**, 109, 1.
19. E. N. Polyzou, P. M. Vlamos, G. M. Dimakos, I. V. Yakoumis and G. M. Kontogeorgis, Assessment of ACM for Predicting SLE of Assymetric Binary Alkane Systems, *Ind. Eng. Chem. Res.* **1999**, 38, 316.
20. E. C. Voutsas and D. P. Tassios, On the Extension of the p-Unifac and R-Unifac Models to Multicomponent Mixtures, *Fluid Phase Equilibria,* **1997,** 128, 271.
21. P. J. Flory, Thermodynamics of Polymer Solutions, *Discuss. Farad. Soc.* **1970,** 49 7.
22. J. F. Parcher, P. K. Weiner, C. L. Hussey and T. N. Westlake, Specific Retention Volumes and Limiting Activity-coefficients of C_4-C_8 Alkane Solutes in C_{22}-C_{36}, *J. Chem. Eng. Data* **1975,** 20, 145.
23. Y. B. Tewari, D. E. Martire and J. P. Sheridan, Gas-Liquid Partition Chromatographic Determination and Theoretical Interpretation of Activity

Coefficients for Hydrocarbon Solutes in Alkane Solvents, *J. Phys. Chem.* **1970,** 74, 2345.

24. K. Kniaz, Influence of Size and Shape Effects on the Solubility of Hydrocarbons. The Role of the Combinatorial Entropy, *Fluid Phase Equilibria*, **1991,** 68, 35.
25. K. Kniaz, Solubility of normal-Docosane in normal-Hexane and Cyclohexane, *J. Chem. Eng. Data,* **1991**, 36, 471.
26. R. N. Lichtenhaler, D. D. Lieu and J. M. Prausnitz, *Ber. Bunsenges. Phys. Chem.* **1974,** 78, 470.
27. J. D. Newman and J. M. Prausnitz,, Polymer – Solvent Interactions from Gas – Liquid Chromatography, *J. Paint Technol*. **1973,** 45, 33.
28. G. M. Kontogeorgis, E. Voutsas and D. P. Tassios, A Molecular Simulation-Based Method for the Estimation of Activity Coefficients for Alkane Solutions, *Chem. Eng. Science*, **1996,** 51 (12), 3247.
29. R. P. Danner, M. S. High, Handbook of Polymer Solution Thermodynamics, Design Institute for Physical Property Data, **1993**.
30. P. A. Rodgers, PVT Relationships for Polymeric Liquids: A Review of Equations of State and their Characteristic Parameters for 56 Polymers, J. Appl. Polym. Sci. **1993,** 48, 1061.
31. S. Uppuluri, S. E. Keinath, D.A. S. Tomalia, P. R. Dvornic, Rheology of Dendrimers. I. Newtonian flow Behavior of Medium and Highly Concentrated Solutions of Polyamidoamine (PAMAM) Dendrimers in Ethylenediamine (EDA) Solvent, *Macromolecules* **1998,** 31, 4498.
32. J. G. Jang, Y. C. Bae, Vapor-liquid Equilibria of Dendrimer Solutions: the Effect of Endgroups at the Periphery of Dendrimeric Molecules, *Chemical Physics* **2001,** 285.
33. C. Mio, S. Kiritsov, Y. Thio, R. Brafman, J. Prausnitz, C. Hawker, E.E. Malmstrøm, Vapor-Liquid Equilibria for Solutions of Dendritic Polymers, *J. Chem. Eng. Data* **1998**, 43, 541.
34. J. G. Lieu, M. Liu, J. M. J. Frechet, J. M. Prausnitz, Vapor-Liquid Equilibria for Dendritic-Polymer Solutions, *J. Chem. Eng. Data* **1999**, 44, 613.

35. A. M. Nemirovsky, M. G. Bawendi, K. F. Freed, Lattice Models of Polymer Solutions: Monomers Occupying Several Lattice Sites, *Journal of Chemical Physics.* **1987,** 87, 12, 7272.
36. G. D. Pappa, E. C. Voutsas, D. P. Tassios, Prediction of Activity Coefficients in Polymer and Copolymer Solutions Using Simple Activity Coefficient Models, *Ind. Eng. Chem. Res.* **1999,** 38, 4975.
37. B. M. Tande, R. W. Jr. Deitcher, S. I. Sandler, N. J. Wagner, Unifac-FV Applied to Dendritic Macromolecules in Solution: Comment on 'Vapor-Liquid Equilibria for Dedritic-Polymer Solutions', *J. Chem. Eng. Data* **2002,** 47, 2, 376.
38. Van Krevelen, Properties of Polymers. Their Correlation with Chemical Structure; their Numerical Estimation and Prediction from Additive Group Contributions, Elsevier, **1990**.
39. H. S. Elbro, Aa. Fredenslund and P. Rasmussen, Group Contribution Method for the Prediction of Liquid Densities as a Function of Temperature for Solvents, Oligomers and Polymers, *Ind. Eng. Chem. Res.* **1991,** 30, 2576.
40. G. Hay, E. Mackay, C. J. Hawker, Thermodynamic Properties of Dendrimers Compared with Linear Polymers: General Observations, *J. Pol. Science* **2001,** 39, 1766.
41. I. A. Kouskoumvekaki, R. Giesen, M. L. Michelsen, G. M. Kontogeorgis, Free-Volume Activity Coefficient Models for Dendrimer Solutions, *Ind. Eng. Chem. Res.* **2002**, 41 (19), 4848.
42. W. Hao, H. S. Elbro and P. Alessi, Polymer Solution Data Collection Part 1-2, DECHEMA, Chemistry Data Series XIV, **1992.**
43. J. Holten-Andersen, P. Rasmussen and Aa. Fredenslund, Phase Equilibria of Polymer Solutions by Group Contribution. 1. Vapor-liquid Equilibria, *Ind. Eng. Chem. Res.* **1987**, 26 (7), 1382.
44. G. M. Kontogeorgis, V. I. Harismiadis, Aa. Fredenslund and D. P.Tassios, Application of the van der Waals Equation of State to Polymers. I. Correlation, *Fluid Phase Equilibria* **1994,** 96, 65.

45. T. Sako, A. H. Wu and J. M. Jr. Prausnitz, A Cubic Equation of State for High-Pressure Phase Equilibria of Mixtures Containing Polymers and Volatile Fluids, *Appl. Polym. Sci.* **1989,** 38, 1839.
46. J. L. Liu and D. S. H. Wong, Application of Wong-Sandler Mixing Rules to Polymer Solutions, *Fluid Phase Equilibria* **1996,** 117, 92.
47. I. Yakoumis, G. M. Kontogeorgis, E. Voutsas and D. P. Tassios, Vapor-liquid Equilibria for Alcohol/Hydrocarbon Systems Using the CPA Equation of State, *Fluid Phase Equilibria* **1997**, 130 31.
48. N. Orbey and S. I. Sandler, VLE of Polymer Solutions Using a Cubic Equation of State, *AIChE J.* **1994,** 40 (7), 1203.

Chapter 3

Non-Cubic Equations of State for Polymer Systems - the Simplified PC-SAFT Equation of State

Cubic equations of state have been traditionally employed in the oil and chemical industry and during the last decade they have been also extended to polymer applications Since then, they have been competing with a novel family of non-cubic equations of state that are based on statistical mechanics, namely SAFT and its many versions. PC-SAFT is a version of STAFT that has been especially developed to handle systems with polymeric chains and components that strongly self- and cross-associate. The simplification that we have applied on the model is based on the assumption that all the segments in the mixture have the same mean diameter d that gives a mixture volume fraction identical to that of the actual mixture. This simplification reduces greatly the computational time and makes the model more attractive for industrial applications. Simplified PC-SAFT requires, like the original PC-SAFT, three pure-component parameters for a non-associating compound and two additional parameters for an associating compound.

3.1 Introduction

Activity coefficient models can only provide low pressure information, e.g. regarding the activity coefficient of the solute and the solvent, either at infinite dilution, or at intermediate concentrations. Such calculations are useful for some applications, eg. for determining suitable solvents for a polymer. However, there are many other areas in polymer thermodynamics, such as phase equilibria at elevated pressures that activity coefficient models cannot cover. On the other hand, equations of state offer many advantages over activity coefficient models: they can be applied to both low and high pressures and also for properties other than phase equilibria.

A novel family of non-cubic equations of state that is derived from statistical mechanics is the SAFT equation of state and its many modifications. The SAFT equation of state has been developed by Chapman et al.[1] and is based on the perturbation theory of Wertheim[2]. Perturbation theories divide the interactions of molecules into a repulsive part and a contribution due to the attractive part of the potential. To calculate the repulsive contribution, a reference fluid in which no attractions are present is defined. Each

perturbation is a correction that results in the model resembling more closely the actual mixture.

Non-cubic equations of state that are derived from statistical mechanics contain separate terms for the various effects (dispersion, polar, chain, hydrogen bonding). The development of SAFT starts by considering the reference system as a mixture of hard spheres. The first perturbation is the introduction of dispersive attractions. Then, follows the connection of the hard spheres, leading to the formation of hard-sphere chains. This perturbation accounts for the non-sphericity of the molecules, which is particularly pronounced for polymers. Finally, if the mixture contains associating compounds, the system is perturbed by the introduction of association sites, leading to the formation of association complexes.

3.2 Non-Cubic versus Cubic Equations of State

Cubic equations of state have been traditionally employed in the oil and chemical industry and during the last decade they have been also extended to polymer applications[3-12]. Correlation and prediction of VLE data at low and high pressures, is a field that most cubic EoS have been evaluated for certain industrial applications (binary systems of common industrial polymers with polar and non-polar organic solvents) and have shown to be quite successful.

A drawback, however, is that the extension of cubic equations of state to polymer applications possesses some theoretical limitations and weaknesses and is, therefore, mainly accomplished in an empirical way. To begin with, chain formation, which is of outmost importance in polymer solutions, is not explicitly taken into account. Furthermore, the a and b parameters that in the case of low molecular compounds are obtained via the critical pressure and temperature, now have to be calculated either through empirical correlations or from some fixed values of 'critical' polymer properties that are the same for all polymers. As a result, extra parameters are usually needed in the correlation equations, which are adjusted to a specific set of experimental data, -depending on the desired application of the equation of state- and, thus, cannot be

considered universal. Furthermore, cubic equations of state with conventional mixing rules are not adequate for systems with polar or associating compounds (e.g. water) that present high deviations from ideality in the liquid phase, since, in the cubic equations of state, only the dispersive interactions are taken into account.

On the other hand, the development of segment-based non-cubic equations of state obtained from statistical mechanics is performed in a more rigorous and systematic way. There are separate terms for each contribution and the association term that is included, strengthens the application of these equations of state to systems containing water, alcohols and other hydrogen-bonding components. Moreover, the segment-based approach makes it far easier to treat components with varying MW, which is frequently the case in polymer systems.

It is worth mentioning that in the various SAFT modifications, different attractive terms are proposed, i.e. different terms for the dispersion term of the equation of state, while the chain and association terms remain unchanged.

One recent successful SAFT modification is the PC-SAFT equation of state[13]. The main difference between SAFT and PC-SAFT is the perturbation sequence: PC-SAFT takes the reference system to be the mixture of hard-sphere chains and then introduces the dispersive attractions. The PC-SAFT equation of state is an attempt to model asymmetric and highly non-ideal systems and the results so far are rather promising. PC-SAFT has been previously applied to high-pressure liquid-liquid equilibria of mixtures of polymers and polymer blends with various hydrocarbon solvents[13,14,15], where it has shown improved performance over the original SAFT[16,17]. It has also recently been applied to associating mixtures of alcohols in short-chain hydrocarbons[18], where both vapor-liquid and liquid-liquid equilibrium were simultaneously described with a single binary interaction parameter. Most recently it has been extended to copolymer systems[19].

The purpose of the work shown in the following chapters is to improve the performance of PC-SAFT and extend its ability to calculating vapor-liquid and liquid-liquid equilibria of complex polymer systems with polar and associating solvents. Special emphasis is given in the parameterization of the model when it comes to the pure-polymer parameters.

3.3 The PC-SAFT Equation of State

3.3.1 Model Description

The PC-SAFT equation of state can be formulated in terms of the reduced residual Helmholtz energy, which is made up of the following contributions:

$$\tilde{a} \equiv \frac{A}{NkT} = \tilde{a}^{hc} + \tilde{a}^{disp} + \tilde{a}^{assoc} \tag{3.1}$$

The hard-sphere chain contribution is made up by the hard-sphere and the chain formation contributions:

$$\tilde{a}^{hc} = \overline{m}\tilde{a}^{hs} + \tilde{a}^{chain} = \overline{m}\tilde{a}^{hs} - \sum_i x_i (m_i - 1)\rho \frac{\partial \ln g_{ii}^{hs}}{\partial \rho} \tag{3.2}$$

where $\overline{m}$ is the average number of segments per chain:

$$\overline{m} = \sum_{i=1}^{NC} x_i m_i \tag{3.3}$$

The hard-sphere term is given by the mixture version of the Carnahan-Starling equation of state for hard-spheres.

$$\tilde{a}^{hs} = \frac{1}{\zeta_0}\left[\frac{3\zeta_1\zeta_2}{1-\zeta_3} + \frac{\zeta_2^3}{\zeta_3(1-\zeta_3)^2} + \left(\frac{\zeta_2^3}{\zeta_3^2} - \zeta_0\right)\ln(1-\zeta_3)\right] \tag{3.4}$$

where ζ_n are the partial volume fractions defined by:

$$\zeta_n = \frac{\pi\rho}{6}\sum_i x_i m_i d_i^n \qquad n \in \{0, 1, 2, 3\} \tag{3.5}$$

and d_i is the Chen and Kreglewski[20] temperature-dependent segment diameter of component i:

$$d_i = \sigma_i \left[1 - 0.12 \exp\left(-\frac{3\varepsilon_i}{kT} \right) \right] \tag{3.6}$$

where σ is the segment diameter and ε the depth of pair potential.

The temperature-dependent segment diameter of component i, is the outcome of the integration of the equation for the effective hard-collision diameter of the chain segments, developed by Barker and Henderson[21]:

$$d(T) = \int_0^{\sigma} \left[1 - \exp\left(-\frac{u(r)}{kT} \right) \right] dr \tag{3.7}$$

which is based on the modified square well potential for segment-segment interactions.
The chain term in Eq. (3.2) depends also on the radial distribution function at contact, which is given by:

$$g_{ij}^{hs}(d_{ij}) = \frac{1}{1-\zeta_3} + \left(\frac{d_i d_j}{d_i d_j} \right) \frac{3\zeta_2}{(1-\zeta_3)^2} + \left(\frac{d_i d_j}{d_i + d_j} \right)^2 \frac{2\zeta_2^2}{(1-\zeta_3)^3} \tag{3.8}$$

The radial distribution function denotes the probability density for finding a hard-sphere belonging to a j-molecule at a distance d from a hard sphere belonging to an i-molecule.
The dispersion contribution in PC-SAFT is based on second order perturbation theory, i.e. the attractive part of the chain interactions is calculated from a first and a second order perturbation. Basically, these are calculated by integrating the intermolecular interactions over the entire mixture volume, which leads to:

$$\tilde{a}^{disp} = -2\pi\rho I_1 m^2 \varepsilon \sigma^3 - \pi\rho\bar{m}\left(1 + \tilde{a}^{hc} + \rho \frac{\partial \tilde{a}^{hc}}{\partial \rho}\right)^{-1} I_2 m^2 \varepsilon^2 \sigma^3 \tag{3.9}$$

The required integrals are approximated by power-series in density *n*, where the coefficients of the power series are functions of the chain length:

$$I_1 = \sum_{i=0}^{6} a_i(\overline{m})\eta^i \tag{3.10}$$

$$I_2 = \sum_{i=0}^{6} b_i(\overline{m})\eta^i \tag{3.11}$$

The dependency of the coefficients $\alpha_i(m)$ and $b_i(m)$ upon segment number is described by the equations:

$$a_i(\overline{m}) = a_{01} + \frac{\overline{m}-1}{\overline{m}} a_{1i} + \frac{\overline{m}-1}{\overline{m}} \frac{\overline{m}-2}{\overline{m}} a_{2i} \tag{3.12}$$

$$b_i(\overline{m}) = b_{01} + \frac{\overline{m}-1}{\overline{m}} b_{1i} + \frac{\overline{m}-1}{\overline{m}} \frac{\overline{m}-2}{\overline{m}} b_{2i} \tag{3.13}$$

and:

$$m^2 \varepsilon^y \sigma^3 = \sum_{i=1}^{NC} \sum_{j=1}^{NC} x_i x_j m_i m_j \left(\frac{\varepsilon_{ij}}{kT}\right)^y \sigma_{ij}^3 \qquad \text{where: y = 1, 2} \tag{3.14}$$

The cross-parameters are obtained from the combining rules:

$$\sigma_{ij} = \frac{\sigma_i + \sigma_j}{2} \tag{3.15}$$

$$\varepsilon_{ij} = (\varepsilon_{ii}\varepsilon_{jj})^{1/2}(1 - k_{ij}) \tag{3.16}$$

The association contribution is only included for systems containing components capable of self-associating and cross-associating (e.g. alcohols and acids). The association contribution is:

$$\tilde{a}^{assoc} = \sum_i x_i \sum_{A_i} \left(\ln X_{A_i} - \frac{1}{2} X_{A_i} + \frac{1}{2} \right) \tag{3.17}$$

where X_{A_i} is the fraction of A-sites on molecule *i* that do not form associating bonds with other active sites. This number is found through the solution of the non-linear system of equations:

$$X_{A_i} = \frac{1}{1 + N_A \sum_j \rho_j \sum_{B_j} X_{B_j} \Delta^{A_i B_j}} \tag{3.18}$$

where ρ_j is the molar density of component j and $\Delta^{A_i B_j}$ is a measure of the association strength between site *A* on molecule *i* and site *B* on molecule *j*. This parameter in turn is a function of the association volume $\kappa^{A_i B_j}$, the association energy $\varepsilon^{A_i B_j}$ and the radial distribution function as follows:

$$\Delta^{A_i B_j} = \sigma_{ij}^3 g^{hs}(d_{ij}) \kappa^{A_i B_j} \left[\exp\left(\frac{\varepsilon^{A_i B_j}}{kT} \right) - 1 \right] \tag{3.19}$$

where $\Delta^{A_i B_j}$ is the so-called association strength.

3.3.2 The Simplified PC-SAFT Equation of State

In the simplified PC-SAFT equation of state[22], the expression for the contributions from dispersion ($\tilde{a}^{disp}$) are identical to Eqs. (3.9) – (3.16) of the original PC-SAFT presented in the previous paragraph.

The targets of the modification are Eqs. (3.4) and (3.8) and the motivation is that sine the segment diameters of the species in the mixture are frequently very similar to each other, Eqs. (3.4) and (3.8) will reduce to the much simpler pure-component versions. This, in turn, makes the computation of the derivatives in phase-equilibrium calculations simpler and less computational intensive, both for the hard-sphere chain term (Eq. (3.2) and for the association term (Eq. (3.17)).

Therefore, by assuming that all the segments in the mixture have a mean diameter d that gives a mixture volume fraction identical to that of the actual mixture, the volume

fraction $\zeta_3 = \frac{\pi\rho}{6}\sum_i x_i m_i d_i^3$ is now based on the diameter of a one-component mixture having a volume, η, corresponding to the fraction ζ_3:

$$\zeta_3 \equiv \eta = \frac{\pi\rho}{6} d^3 \sum_i x_i m_i \tag{3.20}$$

This average diameter is then given by the following expression:

$$d = \left(\frac{\sum_i x_i m_i d_i^3}{\sum_i x_i m_i} \right)^{1/3} \tag{3.21}$$

When this modification is applied to Eqs. (3.4) and (3.8), they are reduced to:

$$\tilde{a}^{hs} = \frac{4\eta - 3\eta^2}{(1-\eta)^2} \tag{3.22}$$

and

$$g^{hs}(d^+) = \frac{1 - \eta/2}{(1-\eta)^3} \tag{3.23}$$

When it comes to the association term, the modification yields a composition-independent expression for the radial distribution faction used in Eq. (3.19), which means that this complex contribution to $\Delta^{A_i B_j}$ is factored out of the component summation of Eq. (3.18).

The overall reduction in the computational time of the simplified PC-SAFT compared to the original is shown in Table 3.1.

Table 3.1 Comparison of computing times for 36-component phase envelope calculation with PC-SAFT and with simplified PC-SAFT. Computations were performed on a 2.0 GHz Pentium IV machine with DVF compiler[21].

Calculation	***Computing times (ms)***
Phase envelope calculation, 36 component mixture, *full PC-SAFT*	48
Phase envelope calculation, 36 component mixture, *simplified PC-SAFT*	32

3.3.3 Pure-Component Parameters for the Simplified PC-SAFT Equation of State

The simplified PC-SAFT requires, like the original PC-SAFT, three pure-component parameters for a non-associating compound: the segment number (m/MW), the interaction energy (ε/k), often expressed in Kelvin, and the hard core segment diameter (σ), expressed in Å. For associating compounds, simplified PC-SAFT needs two additional parameters: the association energy (well-depth, ε_{AB}) and the dimensionless association co volume (well-width, κ_{AB}). For volatile substances, the values for these parameters can be obtained by fitting experimental data, e.g. vapor pressures and liquid densities. For polymers, the current practise is to estimate the pure-component parameters from volumetric (PVT) data and experimental binary data. Alternatively, for polyolefins the parameters can be estimated by extrapolating the n-alkane parameters.

Good initial values are important in the optimization of the parameters based on experimental data, because the dispersive and associating forces are intercorrelated. For example, the estimated value of the liquid density can be increased by increasing the association energy, but also by decreasing the hard core radius. Thus, the five parameters are largely intercorrelated and multiple solutions can be obtained.

The parameters for a variety of low molecular non-associating and associating substances and polymers are reported in the literature.[13,14,18,19]

References

1. W. G. Chapman, K. E. Gubbins, G. Jackson and M. Radosz, SAFT: Equation-of-State Solution Model for Associating Fluids, *Fluid Phase Equilib.* **1989**, 52, 31.
2. M. S. Wertheim, Thermodynamic Perturbation Theory of Polymerization, *J. Chem. Phys.* **1987**, 87, 7323.
3. G. M. Kontogerogis, V. I. Harismiadis, Aa. Fredeslund and D. P. Tassios, Application of the van der Waals Equation of State to Polymers. I. Correlation, *Fluid Phase Equilibria* **1994**, 96, 65.
4. V. I. Harismiadis, G. M. Kontogerogis, Aa. Fredeslund and D. P. Tassios, Application of the van der Waals Equation of State to Polymers. II. Prediction, *Fluid Phase Equilibria* **1994**, 96, 93.
5. V. I. Harismiadis, G. M. Kontogerogis, A. Saraiva, Aa. Fredeslund and D. P. Tassios, Application of the van der Waals Equation of State to Polymers. III. Correlation and Prediction of Upper Critical Solution Temperatures for Polymer Solutions, *Fluid Phase Equilibria* **1994**, 100, 63.
6. A. Saraiva, G. M. Kontogerogis, V. I. Harismiadis, Aa. Fredeslund and D. P. Tassios, IV. Correlation and Prediction of Lower Critical Solution Temperatures for Polymer Solutions, *Fluid Phase Equilibria* **1996**, 115, 73.
7. V. Louli and D. Tassios, Vapor-Liquid Equilibrium in Polymer-Solvent Systems with a Cubic Equation of State, *Fluid Phase Equilibria*, **2000**, 168, 165.
8. N. Kalospiros and D. Tassios, Prediction of vapor-liquid equilibria in polymer solutions using an equation of state/excess Gibbs free energy model, *Ind. Eng. Chem. Res*. **1995**, 34, 2117.
9. N. Orbey and S. Sandler, Vapor-Liquid Equilibrium of Polymer Solutions Using a Cubic Equations of State, *AlChE J.* **1994**, 40, 1203.
10. H. Orbey, C. C. Chen and C. Bokis, An Extension of Cubic Equations of State to Vapor-Liquid Equilibria in Polymer-Solvent Mixtures, *Fluid Phase Equilibria* **1998**, 145, 169.
11. A. Bertucco and C. Mio, Prediction of Vapor-Liquid Equilibrium for Polymer Solutions by a Group-Contribution Redlich-Kwong-Soave Equation of State, *Fluid Phase Equilibria* **1996**, 117, 18.

12. T. Sako, A. H.Wu and J. M. Prausnitz, A Cubic Equation of State for High-Pressure Phase Equilibria of Mixtures Containing Polymers and Volatile Fluids, *J.Appl.Chem.Sc.* **1989,** 38, 1839.
13. J. Gross and G. Sadowski, Perturbed-Chain SAFT: An Equation of State Based on Perturbation Theory for Chain Molecules, *Ind. Eng. Chem. Res.* **2001,** 40, 1244.
14. J. Gross and G. Sadowski, Modeling Polymer Systems Using the Perturbed-Chain Statistical Associating Fluid Theory Equation of State Equation of State, *Ind. Eng. Chem. Res.* **2002,** 41, 1084
15. F. Tumakaka, J. Gross and G. Sadowski, Modeling of Polymer Phase Equilibria using Perturbed-Chain SAFT, *Fluid Phase Equilib.* **2002**, 194, 541.
16. W. G. Chapman, K. E. Gubbins, G. Jackson and M. Radosz, New reference equation of state for associating liquids, *Ind. Eng. Chem. Res.* **1990**, 29, 1709.
17. S. H. Huang and M. Radosz, Equation of State for Small, Large, Polydisperse, and Associating Molecules**,** *Ind. Eng. Chem. Res.* **1990**, 29, 2284.
18. J. Gross and G. Sadowski, Application of the Perturbed-Chain SAFT Equation of State to Associating Systems, *Ind. Eng. Chem. Res.* **2002,** 41, 5510.
19. J. Gross, O. Spuhl, F. Tumakaka and G. Sadowski, Modeling Copolymer Systems Using the Perturbed-Chain SAFT Equation of State, *Ind. Eng. Chem. Res.*, **2003**, 42, 1266.
20. S. S. Chen and A. Kreglewski, Applications of Augmented van der Waals Theory of Fluids .I. Pure Fluids. *Ber. Bunsen. Phys. Chem.* **1977,** *81*, 1048.
21. J. A. Barker and D. Henderson, *J. Chem. Phys.* **1967,** *47*, 4714.
22. N. von Solms, M. L. Michelsen and G. M. Kontogeorgis, Computational and Physical Performance of a Modified PC-SAFT Equation of State for Highly Asymmetric and Associating Mixtures, *Ind. Eng. Chem. Res.* **2003**, 42, 1098.

Chapter 4

Application of the Simplified PC-SAFT Equation of State in Binary Vapor-Liquid Equilibria of Polymer Mixtures

The simplified perturbed-chain SAFT (PC-SAFT) equation of state is applied to polymer systems that include a variety of non-associating (esters, cyclic hydrocarbons), polar (ketones) as well as associating (amines, alcohols) solvents. The solvent pure-component parameters that are not available in the literature are estimated by correlating vapor pressure and liquid density data. The performance of the simplified PC-SAFT is compared to the original PC-SAFT equation of state for polymer systems of varying complexity. It is shown that the applied simplification is not at the expense of the accuracy of the equation of state, while the computational time and complexity are significantly reduced, especially for associating systems. With no binary interaction parameter, simplified PC-SAFT is able to successfully predict vapor-liquid equilibria of polymers with non-associating solvents. In the case of associating solvents, a small binary interaction parameter k_{ij} is usually needed for the satisfactory correlation of the experimental data.

4.1 Introduction

The recent development of a simplified PC-SAFT model has been described in detail in the previous section. This simplified version is both simpler to implement and improves computational performance compared with original PC-SAFT, -and as will be shown in the chapter- without sacrificing physical accuracy. The present work focuses on the evaluation of the simplified PC-SAFT for more complex systems than those previously considered, namely polymer solutions with polar and associating solvents.

The method of obtaining pure-component parameters for associating solvents is then described. Sample comparative results with the original and the simplified PC-SAFT equation of state are presented. The capabilities of the simplified PC-SAFT model in a variety of polymer-solvent systems are then illustrated and discussed. Finally, some conclusions are drawn based on the results presented.

4.2 Database

*T*he pure component parameters of the polymers studied in this work were taken from Tumakaka et al.[1] and of the solvents from Gross et al.[2]. While the effect of solvent self-association is considered in this work, the effects of polarity are not considered explicitly. Thus we would expect that modeling polar systems using only 3 pure-component parameters might not be as successful, especially for polymers that contain polar groups. Nevertheless, for VLE, these systems have been successfully correlated with (in most cases) a small value of the binary interaction parameter.

The pure-component parameters that were not available in the literature were estimated from experimental liquid-density and vapor-pressure data extracted from the DIPPR correlations[3].

Table 4.1 Pure component parameters of PC-SAFT for non-polar, polar and associating compounds. (Experimental data from DIPPR electronic database[3]).

Compound	**Parameters**					**% Error**		**T-range *(K)***
	σ *(A)*	ε/k *(K)*	*m (-)*	ε^{AB} *(K)*	κ^{AB}	P^s	V_L	
chloroform	3.4709	271.625	2.5038	-	-	0.78	0.38	250-490
carbon tetrachloride	3.8055	292.134	2.32521	-	-	0.48	0.32	260-510
acetone	3.2557	253.406	2.77409	-	-	0.99	1.95	250-480
methyl ethyl ketone	3.4473	260.07	2.9093	-	-	1.47	1.86	200-490
diisopropyl ketone	3.5532	251.843	3.70638	-	-	0.48	1.36	250-540
diethyl ketone	3.4778	252.726	3.35652	-	-	1.28	1.39	280-530
1-propanol	3.3085	236.343	2.81484	2370	0.01457	0.18	0.57	250-490
2-propanol	3.2088	204.214	3.05279	2331	0.02642	0.39	0.29	250-480
1-butanol	3.5574	252.149	2.8317	2504	0.00966	0.36	0.42	250-520
2-butanol	3.2683	227.61	3.55377	2168	0.00775	0.37	0.43	240-520
2methyl1propanol	3.3746	242.937	3.26813	2554	0.00293	0.68	0.95	260-510
1-propylamine	3.4039	234.769	2.71851	820	0.06576	0.96	0.48	250-480
2-propylamine	3.5031	232.569	2.5438	961	0.02330	0.12	0.1	250-440

Table 4.1 shows the parameters for the ketones, amines and alcohols studied, where the associating components were all assigned two association sites. This is the 2B model of association in the terminology of Huang and Radosz[4]. While it is true that a three-site model is a better physical description of an alcohol, it was felt that the extra complexity involved in using a three-site model was not justified, particularly in view of the fact that

it is still necessary to regress five pure-component parameters to experimental vapor pressure and liquid density data. Furthermore, since the first parameterization of SAFT appeared in 1990[4] the majority of researchers in the field have followed this convention – see for example the recent paper of Gross and Sadowski[5]. Ketones are considered to be non-associating and therefore, only three pure-component parameters were used.

4.3 Comparison with the Original PC-SAFT Equation of State

The PC-SAFT and the simplified PC-SAFT equations of state were evaluated against vapor pressure experimental data of binary polypropylene, polystyrene and poly(vinyl acetate) solutions with cyclic and aromatic hydrocarbons, chlorinated hydrocarbons, esters, ketones, amines and alcohols. The intention was to consider systems with a variety of solvents, ranging from non-polar to polar and associating.

Figures 4.1 – 4.3 show comparative pressure predictions of the simplified and the original PC-SAFT models, for three different polymer systems. As mentioned by von Solms et al.[6] the differences between the two versions become noticeable, as the segment size asymmetry increases. It may be noted here that in the case of a pure component, the simplified version of PC-SAFT is identical to original PC-SAFT. In the case of Figure 4.1 (polypropylene-diisopropylketone), simplified PC-SAFT predicts higher pressures than the original model. Simplified PC-SAFT in fact shows a maximum in the vapor pressure curve, which indicates the onset of liquid-liquid demixing.

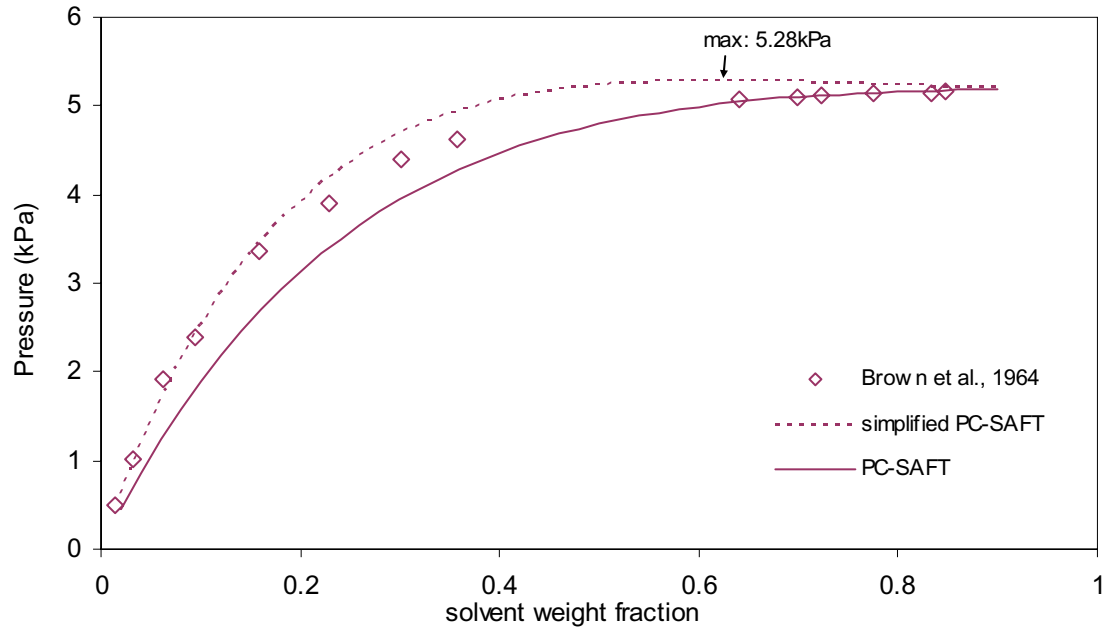

Figure 4.1 Pressure-weight fraction plot of polypropylene – diisopropyl ketone at T = 318 K. Polypropylene molecular weight = 20 000. Comparison of experimental data with the predictions of original (solid line) and the simplified version (dotted line) of PC-SAFT. In both curves the interaction parameter k_{ij}=0. Experimental data are from Brown et al.[8].

This is typically the case, whenever the two curves do not coincide, as can be seen in the next two Figures 4.2 and 4.3. Figure 4.2 shows the vapor pressure curve for the system polystyrene – ethyl benzene and Figure 4.3 for the system polystyrene – methyl ethyl ketone. The differences between the predictions of the two equations of state are very small in both cases. In Figure 4.3 the predictions are indistinguishable. This implies that when a positive binary interaction parameter (k_{ij}) is required by original PC-SAFT for correlating the system, the simplified version will usually require a smaller positive or negative k_{ij}. As shown further in Table 4.2, the simplified version is either better than or as successful as the original PC-SAFT in predicting vapor-liquid equilibria of many polymer-solvent systems.

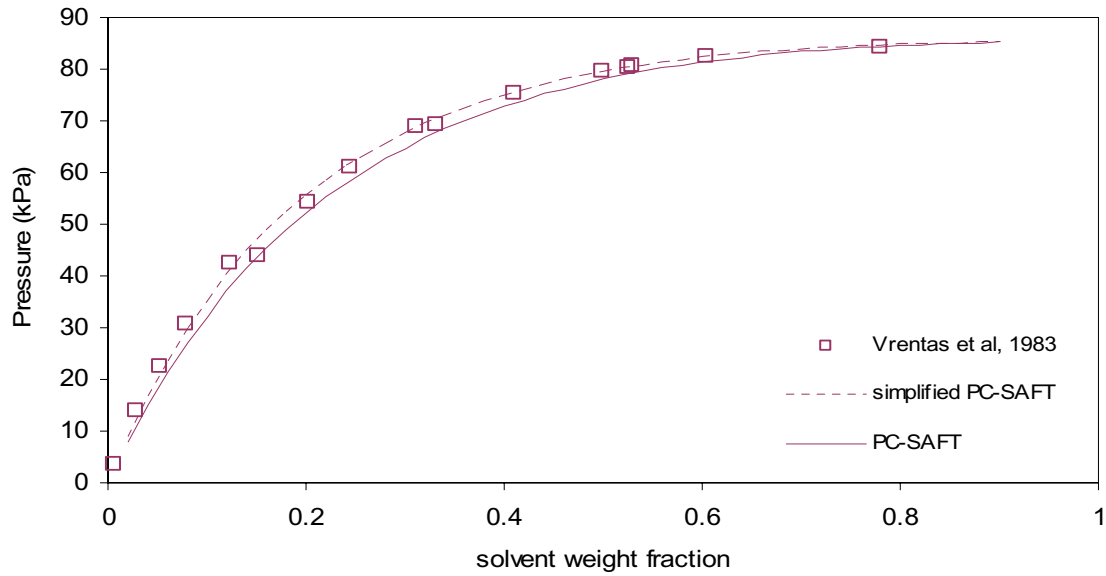

Figure 4.2 Pressure-weight fraction plot of polystyrene – ethyl benzene at T = 403 K. Polystyrene molecular weight = 275 000. Comparison of experimental data with the predictions of original (solid line) and the simplified version (dotted line) of PC-SAFT. In both curves the interaction parameter k_{ij}=0. Experimental data are from Vrentas et al.[9].

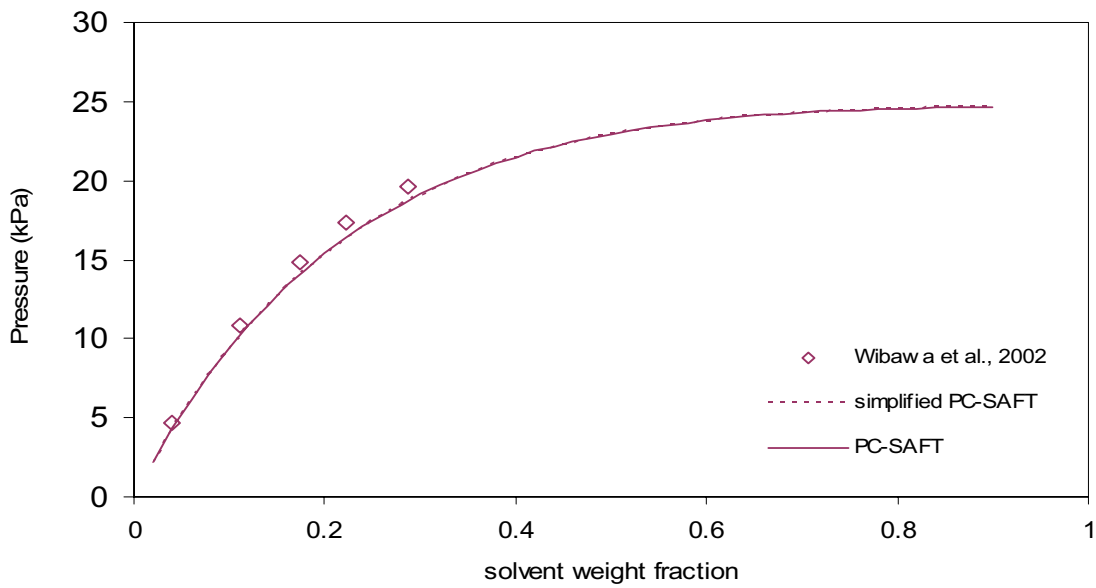

Figure 4.3 Pressure-weight fraction plot of poly(vinyl acetate) – methyl ethyl ketone at T = 313 K. Poly(vinyl acetate) molecular weight = 167 000. Comparison of experimental data with the predictions of original (solid line) and the simplified version (dotted line) of PC-SAFT. In both curves the interaction parameter k_{ij}=0. Experimental data are from Wibawa et al.[10].

Table 4.2 Comparison of the performance of the simplified against the original PC-SAFT in predicting vapor-liquid equilibria of polymer solutions (k_{ij} = 0 in all cases). Average percentage deviation between experimental and predicted equilibrium pressure curves.

%AAD	PC-SAFT (Simplified version)	PC-SAFT (Original version)
Cyclic hydrocarbons		
PS – cyclohexane	13	16
PS – benzene	28	13
PS – ethyl benzene	3	6
PS – m-xylene	25	16
PS – toluene	18	7
PVAc – benzene	6	10
Chlorinated hydrocarbons		
PS – carbon tetrachloride	18	12
PS – chloroform	30	11
PP – dichloromethane	59	74
PP – carbon tetrachloride	55	47
Esters		
PS – propyl acetate	5	21
PS – butyl acetate	3	25
PVAc – methyl acetate	3	2
PVAc – propyl acetate	19	18
Ketones		
PS – acetone	6	26
PS – diethyl ketone	7	28
PS – methyl ethyl ketone	14	12
PVAc – acetone	4	7
PP – diethyl ketone	16	27
PP – diisopropyl ketone	4	11
PVAc – methyl ethyl ketone	7	6
Amines		
PVAc – propylamine	4	3
PVAc – isopropyl amine	17	16
Alcohols		
PVAc – 1-propanol	56	54
PVAc – 2-propanol	84	73
PVAc – 1-butanol	59	59
PVAc – 2-butanol	39	36
PVAc – 2methyl-1propanol	29	29
Overall	***23***	***24***

4.4 Results and Discussion

Figures 4.4 and 4.5 show two different polymer systems with ester solvents. In Figure 4.4 the vapor-liquid phase diagram for the system poly(vinyl acetate) - propyl acetate is

presented at three different temperatures. This system is very well predicted by simplified PC-SAFT at all three temperatures. Deviations increase, however, as the temperature increases. In Figure 4.5 the phase diagram of polystyrene – butyl acetate is shown, where again the prediction is very accurate.

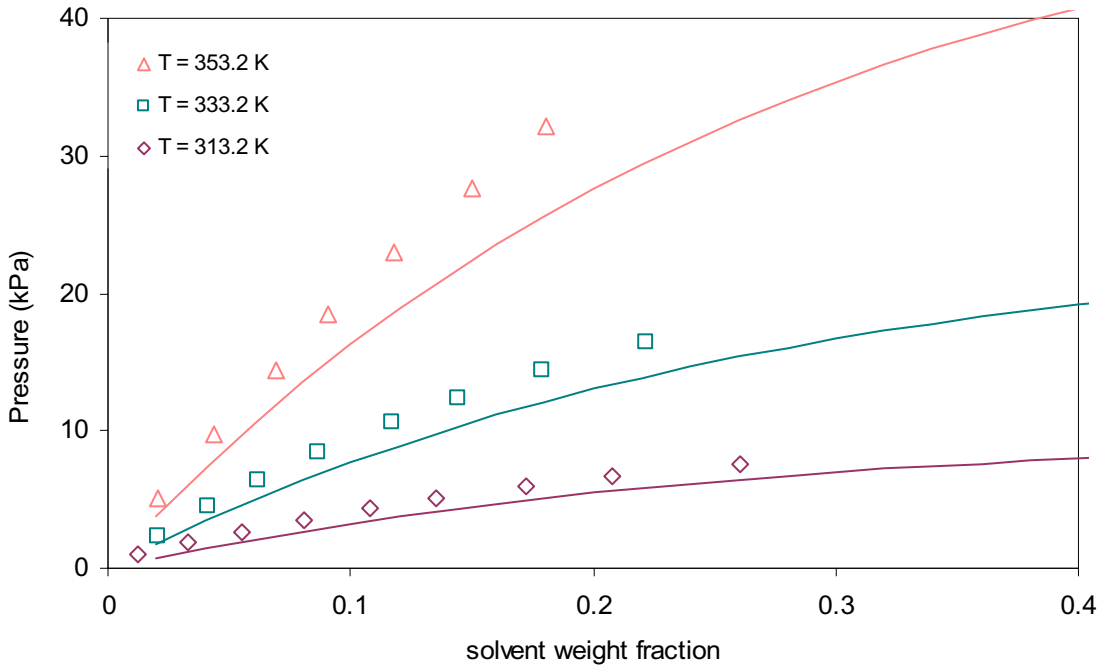

Figure 4.4 Pressure-weight fraction plot of poly(vinyl acetate) – propyl acetate. Poly(vinyl acetate) molecular weight = 167 000. Comparison of experimental data with the predictions of simplified PC-SAFT (solid line). In all curves the interaction parameter k_{ij}=0. Experimental data are from Wibawa et al.[10].

The last three Figures 4.6 – 4.8 present results for systems with self-associating solvents. Figure 4.6 shows the vapor-liquid phase diagram for the systems poly(vinyl acetate) – 1-propylamine and poly(vinyl acetate) – 2-propylamine. The aim of this combined plot is to investigate the ability of the model to capture the differences between isomers. The poly(vinyl acetate) – 1-propylamine system is very well predicted by simplified PC-SAFT, although there is a slight underestimation of the vapor pressure in the case of the poly(vinyl acetate) – 2-propylamine system (that is corrected by a small positive k_{ij}). This underestimation cannot be attributed to the pure component parameters of 2-propylamine reported in Table 4.1, since the properties (liquid density and vapor pressure) of the pure 2-propylamine are very well described with these parameters.

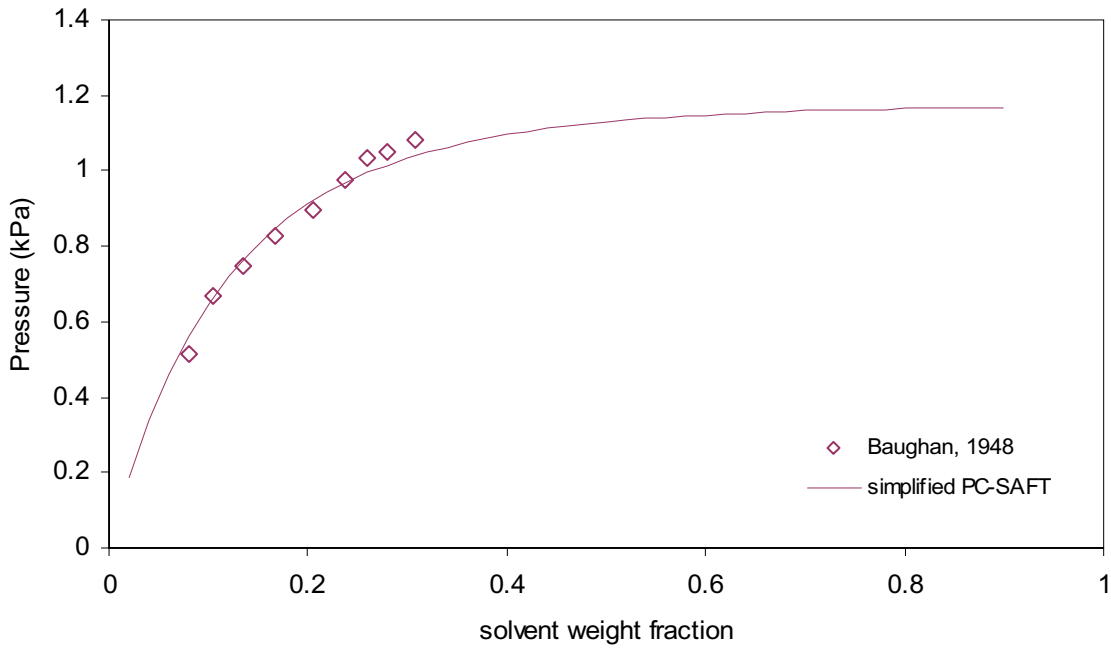

Figure 4.5 Pressure-weight fraction plot of polystyrene – butyl acetate at T = 293 K Polystyrene molecular weight = 500 000. Comparison of experimental data with the predictions of simplified PC-SAFT. The interaction parameter k_{ij}=0. Experimental data are from Baughan[11].

Figure 4.7 shows the phase diagram of poly(vinyl acetate) – 2-methylpropanol, which is another system that contains a self-associating solvent. The prediction of simplified PC-SAFT is satisfactory, although, a small, negative k_{ij} is now required for a good correlation. Finally, Figure 4.8 shows the polymer – associating solvent system poly(vinyl acetate) – 2-propanol. In this case, even though the overestimation of the prediction is somewhat corrected by a small, negative k_{ij}, the correlation is not satisfactory. As in Figure 4.1, simplified PC-SAFT without a binary interaction parameter predicts a maximum in the vapor-pressure curve, indicating incipient liquid-liquid phase separation, whereas the experimental data do not show this. Rather than calculating this liquid-liquid coexistence (which does not occur in the data), a small binary interaction parameter is used to correlate the data.

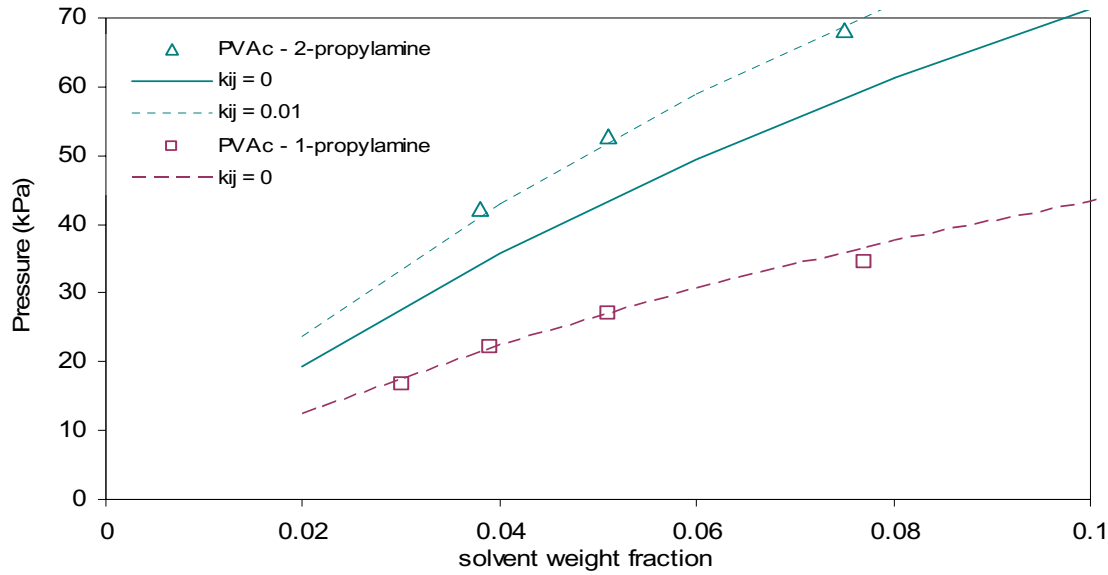

Figure 4.6 Pressure-weight fraction plot of poly(vinyl acetate) with 1-propylamine and 2-propylamine at T = 313 K. Poly(vinyl acetate) molecular weight = 170 000. Experimental data are from Kokes et al.[12]: The dashed line is the simplified PC-SAFT prediction ($k_{ij} = 0$) for the PVAc – 1-propylamine system, the solid line is the simplified PC-SAFT prediction ($k_{ij} = 0$) for the PVAc – 2-propylamine system and the dotted line is the simplified PC-SAFT correlation ($k_{ij} = 0.01$) for the PVAc – 2-propylamine system.

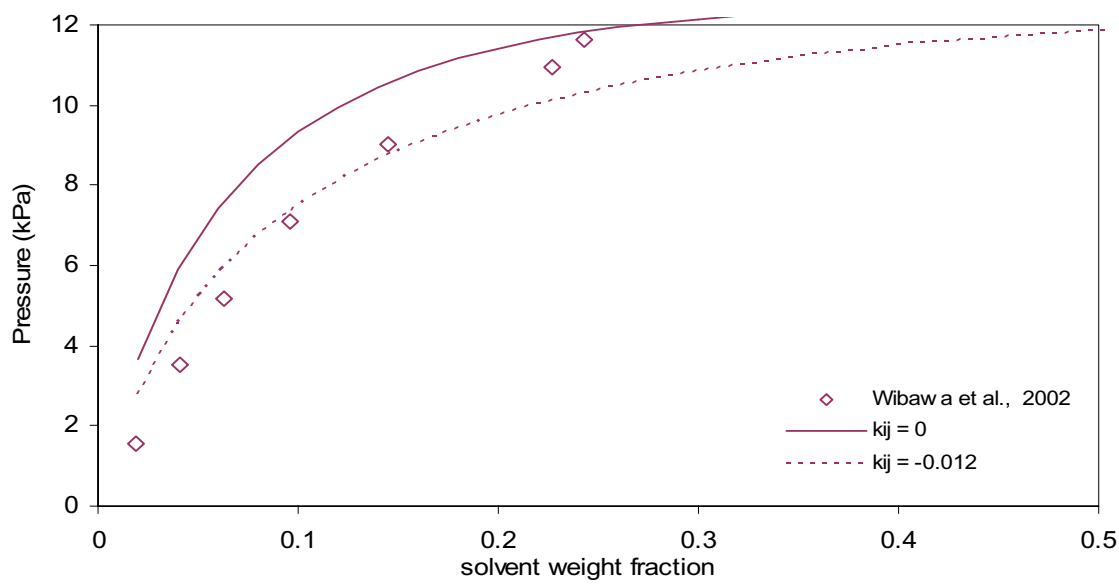

Figure 4.7 Pressure-weight fraction plot of poly(vinyl acetate) – 2-methyl-1-propanol at T = 313 K. Comparison of experimental data with prediction ($k_{ij} = 0$) and correlation ($k_{ij} = -0.012$) results of simplified PC-SAFT. Poly(vinyl acetate) molecular weight = 167 000. Experimental data are from Wibawa et al.[10].

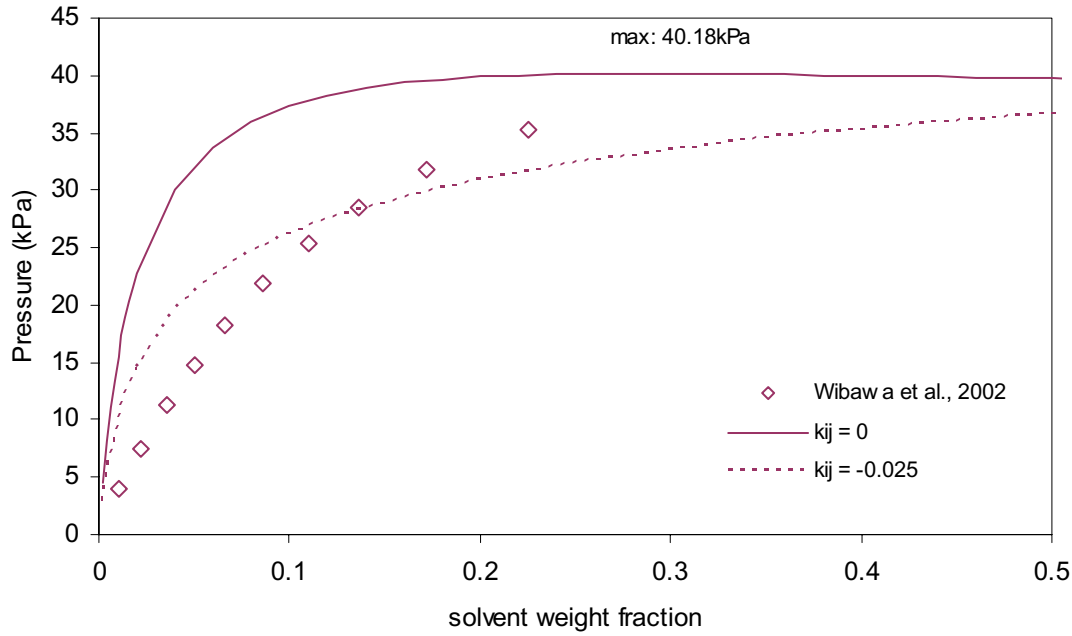

Figure 4.8 Pressure-weight fraction plot of poly(vinyl acetate) – 2-propanol at T = 333 K. Comparison of experimental data with prediction ($k_{ij} = 0$) and correlation ($k_{ij} = -0.025$) results of simplified PC-SAFT. Poly(vinyl acetate) molecular weight = 167 000. Experimental data are from Wibawa et al.[10].

4.4 Conclusions

The simplified PC-SAFT equation of state was applied to vapor-liquid equilibria of polymer mixtures with a variety of solvents. Special attention was given to rather complex systems including polar and self-associating solvents. This area has not been extensively investigated with this model so far and offers a challenge for modern equations of state like PC-SAFT. We have shown that the applied simplification does not have any significant influence on the predicting and correlating capabilities of the model. Thus, it is highly recommended, especially when associating compounds are concerned, and where computational times may become significant.

We have also shown that simplified PC-SAFT has a very good predictive behavior in polymer mixtures with linear, cyclic and chlorinated alkanes, esters and ketones. For associating solvents such as amines and alcohols, a small, negative k_{ij} is needed for an accurate description of the system.

Unlike the method for volatile substances, where the pure-component parameters are obtained by considering only pure liquid-density and vapor-pressure data, in order to find pure-component parameters for polymers, binary experimental data are also used[2,7]. An interesting conclusion that can be drawn from this work is that the method of fitting pure-polymer parameters to experimental binary data with a single solvent provides parameter-sets that can be used in other polymer systems that those that they have been regressed from. Thus, for example, although the pure component parameters for polystyrene are obtained by fitting to experimental phase equilibrium data for the binary system polystyrene-cyclohexane, the parameters obtained are not specific to the solvent used in the fitting procedure and can be used to describe phase behavior in a wide variety of polystyrene systems. However, it hasn't been verified yet whether the resulting polymer parameters are characteristic for the specific polymer or they depend on the selected binary system that is used for their regression. This subject will be further investigated in Chapter 7.

References

1. F. Tumakaka, J. Gross and G. Sadowski, Modeling of polymer phase equilibria using Perturbed-Chain SAFT, *Fluid Phase Equilib.* **2002**, 541, 194.
2. J. Gross and G. Sadowski, Perturbed-Chain SAFT: An Equation of State Based on a Perturbation Theory for Chain Molecules, *Ind. Eng. Chem. Res.* **2001**, 40, 1244.
3. DIPPR Tables of Physical and Thermodynamic Properties of Pure Compounds, AIChE, New York, **1998**.
4. S. H. Huang and M. Radosz, Equation of State for Small, Large, Polydisperse, and Associating Molecules**,** *Ind. Eng. Chem. Res.* **1990,** 29, 2284.
5. J. Gross and G. Sadowski., Application of the Perturbed-Chain SAFT Equation of State to Associating Systems, *Ind. Eng. Chem. Res.* **2002**, 41, 5510.
6. N. von Solms, M. L. Michelsen and G. M. Kontogeorgis, Computational and Physical Performance of a Modified PC-SAFT Equation of State for Highly Asymmetric and Associating Mixtures, *Ind. Eng. Chem. Res.* **2003**, 42, 1098.
7. J. Gross and G. Sadowski, Modeling Polymer Systems Using the Perturbed-Chain Statistical Associating Fluid Theory Equation of State Equation of State, *Ind. Eng. Chem. Res.* **2002,** 41, 1084.
8. W. B. Brown, G. Gee and W. D. Taylor, *Polymer* 1964, 5, 362.
9. J. S. Vrentas, J. L. Duda and S. T. Hsieh, Thermodynamic Properties of some Amorphous Polymer Solvent Systems, *Ind. Eng. Chem. Prod.* **1983**, 22, 326.
10. G. Wibawa, R. Hatano, Y. Sato, S. Tikishima and H. Masuoka, Solubulities of 11 Polar Organic Solvents using the Piezoelectric-Quartz Sorption Method, *J. Chem. Eng. Data* **2002**, 47, 1022.
11. E. C. Baughan, The Absorption of Organic Vapors by Thin Films of Polystyrene, *T. Faraday Soc.*, **1948**, 44, 495.
12. R. J. Kokes, A. R. DiPietro and F. A. Long, Equilibrium Sorption of Several Organic Diluents in Polyvinyl Acetate*J. Am. Chem. Soc.*, **1953**, 75, 6319.

Chapter 5

Application of the Simplified PC-SAFT Equation of State in Binary Liquid-Liquid Equilibria of Polymer Mixtures

Simplified PC-SAFT has been used to calculate binary liquid-liquid equilibria for polymer-solvent systems. A number of different polymers and solvents were examined as part of the study, including both non-associating and associating solvents. In general simplified PC-SAFT is successful in modeling liquid-liquid equilibrium, successfully predicting the correct behavior in many systems exhibiting either upper or lower or both upper and lower critical solution temperatures. Where predictions are not accurate, a small value of the binary interaction parameter is required to correlate experimental data. A novel method, which we call "the method of alternating tangents", has been developed for finding liquid-liquid equilibrium in binary polymer-solvent systems. The algorithm is robust and traces the full temperature composition curve for both UCST and LCST type systems through the critical solution temperature. The algorithm has been successfully applied for a broad range of polymer molecular weights encountered in the literature. The algorithm is applicable to any equation of state for which analytical fugacity coefficients and their derivatives are available, although application was restricted in this study to the simplified PC-SAFT equation of state.

5.1 Introduction

Phase equilibrium calculations in asymmetric mixtures such as those containing polymers can frequently cause computational difficulties. This is particularly true for liquid-liquid equilibrium, where two highly non-ideal liquid phases must be modeled with the same equation of state. Liquid-liquid phase equilibrium is of great importance for systems containing polymers – often as, or even more important than vapor-liquid and solid-liquid equilibrium. Additionally, the presence of two liquid phases is far more common in systems containing polymers than in mixtures containing only substances of low molecular weight.

Here we investigate a method for finding liquid-liquid coexistence (binodal) compositions in binary polymer solvent mixtures. The method finds the spinodal compositions as a starting point for finding the binodals, as well as upper, or lower, or both critical solution

temperatures. The equation of state employed in these calculations is the simplified PC-SAFT[1,2] although it is applicable to any analytic equation of state capable of predicting phase equilibrium in polymer systems. A discussion of the method and its implementation follows, together with results for a variety of different polymers and solvents displaying different types of critical solution temperature behavior.

5.2 The Method of Alternating Tangents

We call the proposed method, "the method of alternating tangents" and it is best illustrated by reference to Figure 5.1.

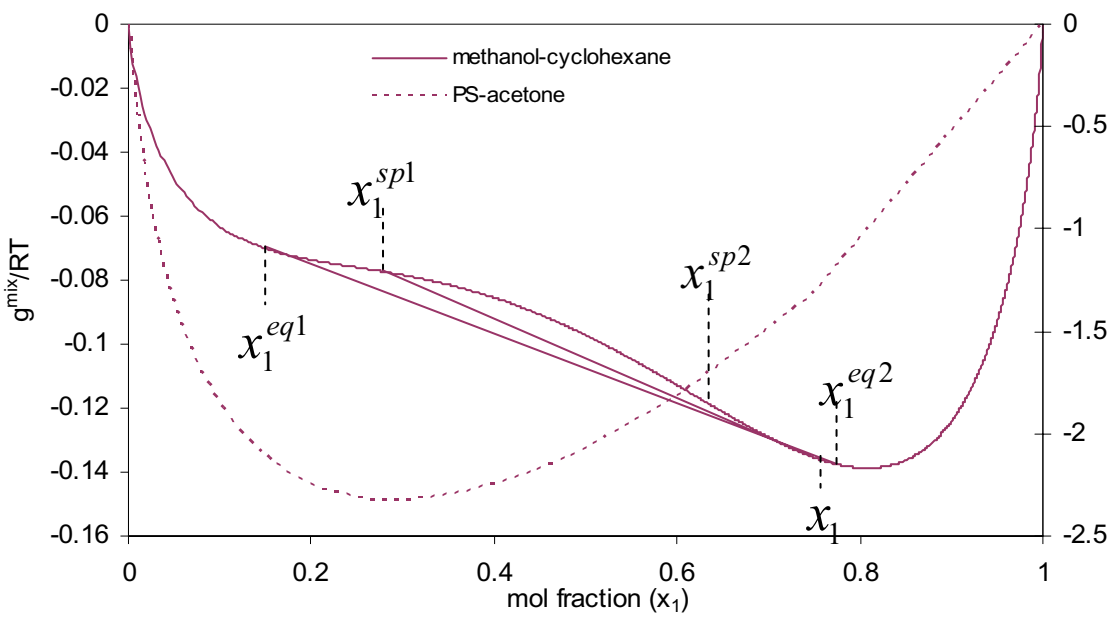

Figure 5.1 Illustration of the method of alternating tangents. The solid line is the system methanol (1)-cyclohexane (2). The dotted line is the system PS (1)-acetone. The two spinodal points are indicated by x_1^{sp1} and x_1^{sp2}. The equilibrium (binodal) points are indicated by x_1^{eq1} and x_1^{eq2}. Starting from a spinodal point, the equilibrium values can be calculated by solving for only one point at a time.

This figure shows the Gibbs energy of mixing for two binary systems as a function of the mole fraction of component 1. The method will be illustrated with reference to the system methanol (1) – cyclohexane (2), since this curve clearly shows the existence of two phases.

The composition of methanol in each phase is found by locating a single line which is a tangent to the curve in two places (the common tangent). In Figure 5.1 these compositions are given by x_1^{eq1} and x_1^{eq2}. In fact the curve for the system PS (1) – acetone (2) also shows the existence of two phases, although this is not visible. The first step in the procedure is to determine whether a spinodal point exists (this is a necessary condition for phase separation). In the figure, the two spinodal points are given by the compositions x_1^{sp1} and x_1^{sp2}. The spinodal condition is given by $\frac{\partial^2 g^{mix}/RT}{\partial x^2} = 0$, i.e. an inflection point on the curve. As shown in the Appendix, this can be translated to a more convenient expression, namely: $\overline{\Phi}_{12} = 1$, where $\overline{\Phi}_{12} = n_T \frac{\partial \hat{\phi}_1}{\partial n_2}$. Therefore, when for a given set of T and P, $\overline{\Phi}_{12}$ is below unity for any composition of the mixture, then the components are fully miscible under these conditions. Once a spinodal point has been found (using a Newton-Raphson method), the next step is to find the point of tangent of a line originating at the spinodal point. In the figure this is the line connecting x_1^{sp1} and x_1. This point is just to the left of x_1^{eq2} (i.e. we are not yet quite at the equilibrium concentration after one step). The equation whose solution gives this point of tangent is:

$$f(x_1) = \frac{g(x_1) - g(x_1^{sp1})}{x_1 - x_1^{sp1}} - \frac{dg}{dx}(x_1) = 0 \qquad (5.1)$$

where $f(x_1)$ is our Newton target function to be solved and $g(x_1)$ is shorthand for $\frac{g^{RES}}{RT}(x_1)$. The derivative is given simply by

$$\frac{dg}{dx}(x_1) = \ln x_1 + \ln \hat{\phi}_1 - \ln(1 - x_1) - \ln \hat{\phi}_2 \qquad (5.2)$$

where $\hat{\phi}_i$ is the fugacity coefficient of *i*. We have implemented a Newton-Raphson routine, which requires that the first derivative of the Newton target function $f(x_1)$ is available. This means that composition derivatives of the fugacity coefficients are required (from Eq. 5.2). Both the fugacities and their composition derivatives have been calculated analytically for the simplified PC-SAFT equation of state. Since only a single equation has to be solved, however, the secant method, which does not require additional derivatives,

would be an excellent alternative. Once the first tangent has been found, the point of tangent opposite is then found in a similar way. This process is repeated until the change in the composition at the tangent point is within a specified tolerance. At this point the equilibrium values have been calculated. It is worthwhile noting that the repeated tangent construction in itself exhibits superlinear convergence behavior, and very few overall calculations are therefore required.

A major benefit of the method is that only one point needs to be found at a time, thereby avoiding simultaneous solution of the two equilibrium compositions. The criterion for the location of the critical solution temperatures (UCST or LCST) is that the two spinodal points (x_1^{sp1}, x_1^{sp2}) have equal values.

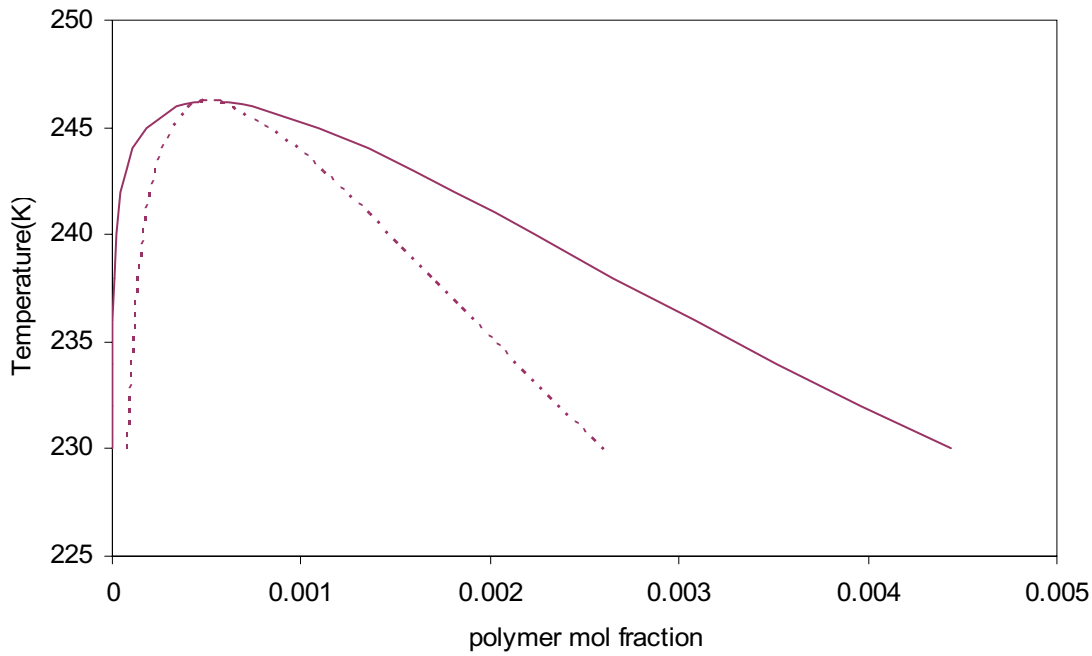

Figure 5.2 Liquid-liquid equilibrium in the system polystyrene-cyclohexane for polystyrene molecular weight 1.270.000, showing both the spinodal and binodal (co-existence) curves. The two curves converge at the critical solution temperature.

Figure 5.2 shows the binodal and the spinodal curve in the system PS (1) – cyclohexane (2). At the UCST all four compositions converge. In the limit, as the critical temperature is approached, use can be made of a universal law which relates the binodal to the spinodal compositions. Taking $x_1^{sp1} = x_1^{eq1} + u(x_1^{eq2} - x_1^{eq1})$, the two spinodal points are found when u

takes the two values obtained as solutions to the 2nd degree shifted Legendre polynomial $6u^2 - 6u + 1 = 0$.

The search for the binodal points is aided by the fact $0 < x_1^{eq1} < x_1^{sp1}$ and $x_1^{sp2} < x_1^{eq2} < 1$, so the solution boundaries are well defined. Another feature which improves the robustness of the algorithm is to use logarithms of the compositions required in the algorithm. This is advantageous since the polymer is often present in the polymer-lean phase in minute amounts, particularly in systems which exhibit LCST behavior. This problem is further exacerbated by the fact that mol fractions (rather than weight fractions) are used in the fugacity calculations. This may be problematic, especially when dealing with very high molecular weight polymers. However, no problems were encountered when using logarithms of compositions, even at the highest polymer molecular weight encountered in systems exhibiting LCST behavior (the most difficult case).

5.3 Results and Discussion

Polymer parameters for PC-SAFT were obtained from Gross and Sadowski[3]. Parameters for most of the solvents were obtained from Gross and Sadowski[4], with the exception of diisobutyl ketone (this work), *n*-alkanols[5] and acetone[2].

Figure 5.3 shows results for the system polystyrene – methylcyclohexane for different molecular weights of polystyrene. The data are reasonably well correlated over a very large range of molecular weight with a single value of the binary interaction parameter, k_{ij}. The binary interaction parameter was adjusted to give the correct upper critical solution temperature. However, the correct critical solution concentration is not obtained, although the experimental trends are correctly predicted by the model: The critical solution temperature increases and the polymer weight fraction at the critical solution temperature decreases with increasing molecular weight.

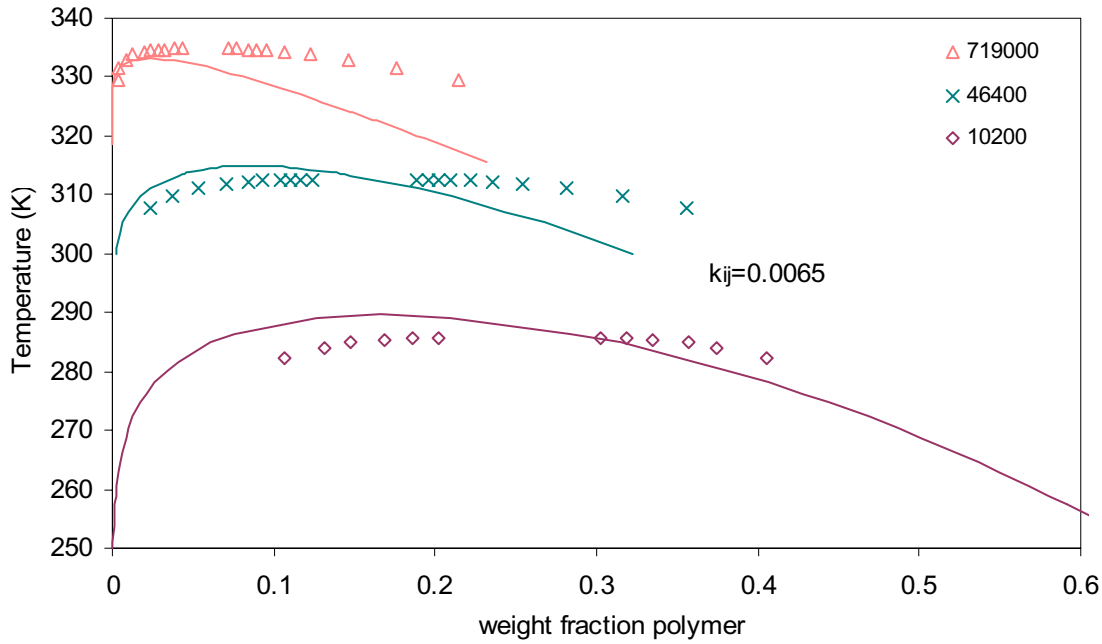

Figure 5.3 Liquid-liquid equilibrium in the system polystyrene-methyl cyclohexane for different molecular weights of polystyrene. The experimental data are from Dobashi et al.[7]. The lines are simplified PC-SAFT correlations with $k_{ij} = 0.0065$.

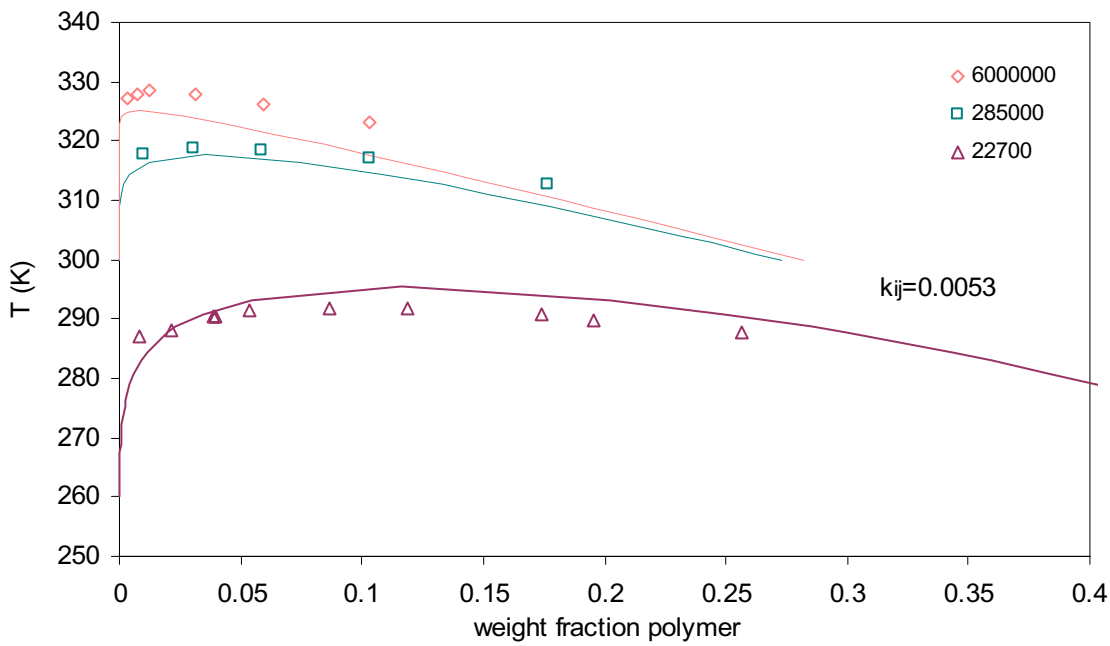

Figure 5.4 Liquid-liquid equilibrium in the system polyisobutylene-diisopropyl ketone. Experimental data are from Shultz and Flory[8]. Lines are simplified PC-SAFT correlations with $k_{ij} = 0.0053$, the same at all three molecular weights.

Figure 5.4 shows results for the system polyisobutylene – diisobutyl ketone at different polymer molecular weights. Pure component parameters for diisobutyl ketone were obtained by fitting to experimental liquid density and vapor pressure data in the temperature range 260 – 600 K. This data was taken from the DIPPR database[6]. The parameters were, $m = 4.6179$, $\varepsilon / k = 243.72$ K and $\sigma = 3.7032$ Å and the average percent deviations were 1.03 % for vapor pressure and 0.64 % for liquid density. A single binary interaction parameter ($k_{ij} = 0.0053$) was used for all three systems, although it seems that there is a weak dependence of molecular weight on k_{ij} . Incorporating a functional dependence of k_{ij} on molecular weight (for example a linear fit) would improve the correlation. It should also be noted that these three systems represent a very large range of molecular weights.

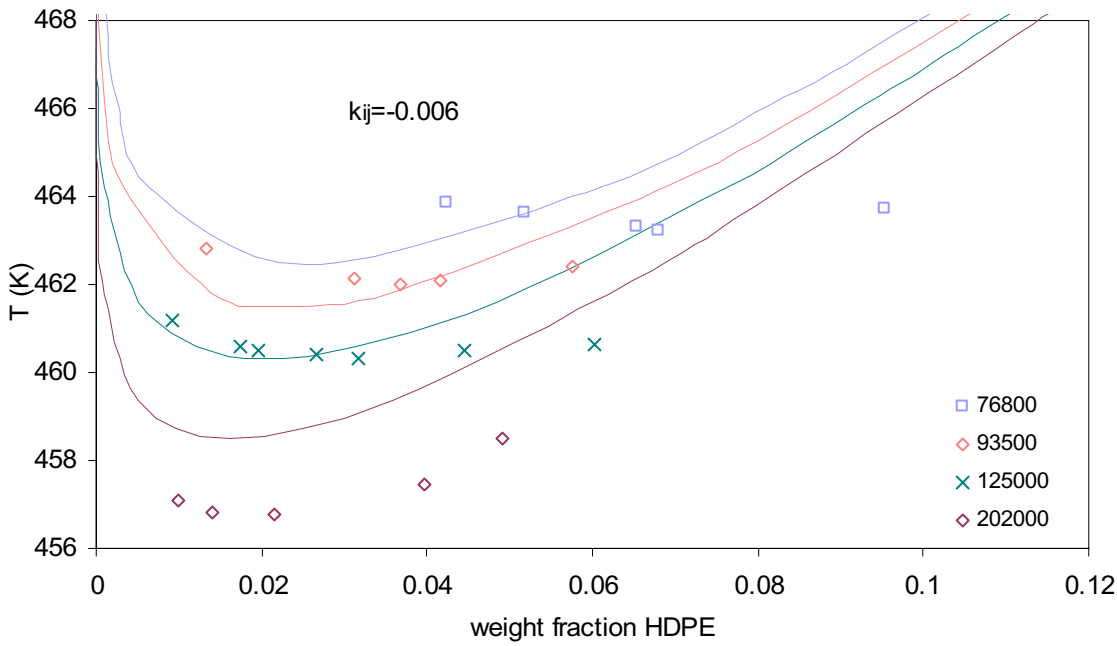

Figure 5.5 Liquid-liquid equilibrium in the system HDPE-*n*-heptane. The experimental data are from Hamada et al.[9]. The lines are simplified PC-SAFT correlations with $k_{ij} = -0.006$ for the molecular weights shown. This system displays lower critical solution temperature (LSCT) behavior.

Figure 5.5 shows the results for HDPE – *n*-heptane, a system which displays lower critical solution temperature (LCST) behavior. The same binary interaction parameter is used for all four molecular weights shown, although this could be fine-tuned. It is worth

noting that the temperature range shown is extremely small (compared with for example Figures 5.3 and 5.4), so this correlation can be considered to be good. An additional point is that generally LCST behavior is rather insensitive to the binary interaction parameter. This is because LCST behavior is usually observed at elevated temperatures, where the effect of the energy parameters is not as marked. Since k_{ij} is a correction to the cross energy parameter ε_{ij}, changing the k_{ij} value generally has only a marginal effect.

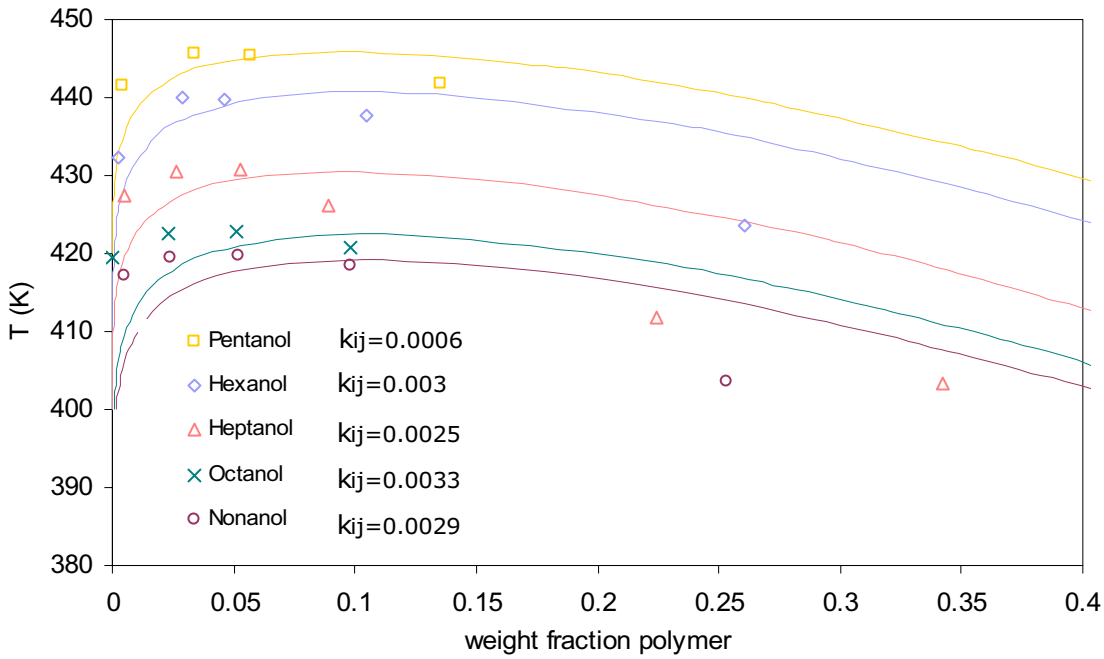

Figure 5.6 Liquid-liquid equilibrium for HDPE with *n*-alkanols. The experimental data are from Nakajima et al.[10]. Lines are simplified PC-SAFT correlations for each of the five solvents (pentanol highest, nonanol lowest). Polymer molecular weight is 20.000.

Figure 5.6 shows the results for a single molecular weight of HDPE in five different *n*-alkanol solvents from *n*-pentanol up to *n*-nonanol. The results are well correlated using simplified PC-SAFT using a small value of the binary interaction parameter k_{ij}. A k_{ij} value of around 0.003 gives a good correlation for all the systems, except HDPE – *n*-pentanol. In the figure, a small value (k_{ij}=0.0006) was used to correlate the data, although the data is also well predicted by simplified PC-SAFT (k_{ij}=0), giving an error in the upper critical solution temperature of 3 K in the case of HDPE – *n*-pentanol.

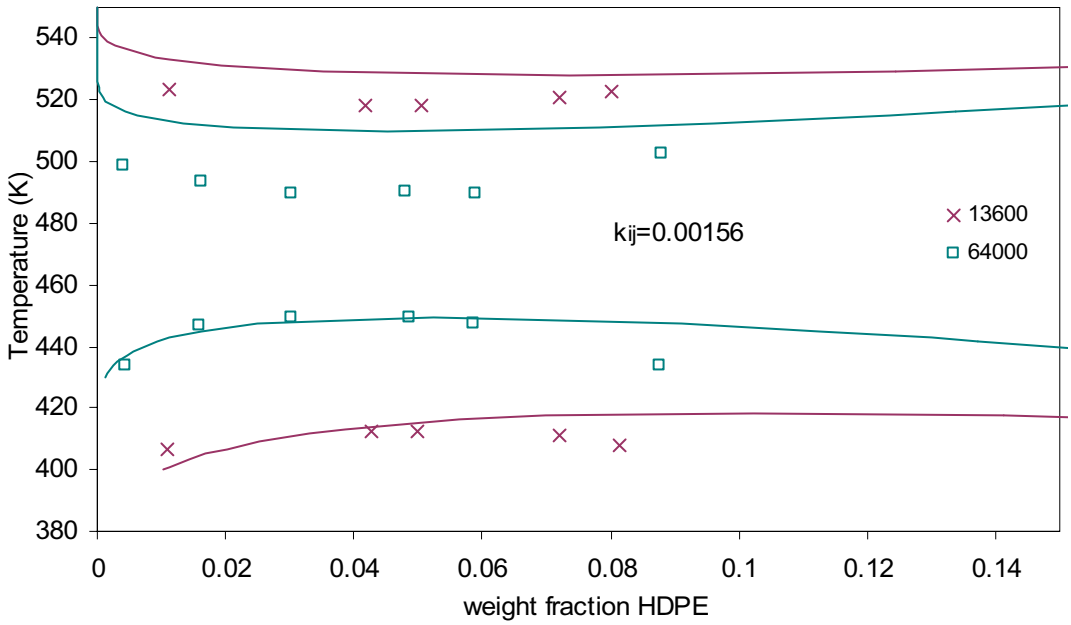

Figure 5.7 Liquid-liquid equilibrium in the system HDPE – butyl acetate. The system displays both upper and lower critical solution temperature behaviour. The experimental data are from Kuwahara et al.[11] for molecular weights 13.600 and 64.000. Lines are simplified PC-SAFT correlations with $k_{ij} = 0.0156$ for both molecular weights.

Figure 5.7 shows the results for the system HDPE – butyl acetate. This system displays both UCST and LCST behavior. A single binary interaction parameter (k_{ij}=0.0156) was used to correlate the data for both molecular weights shown. The binary interaction parameter was adjusted to give a good correlation for the UCST curve at the higher molecular weight (64 000). As mentioned above, the LCST curve is rather insensitive to k_{ij}. Nevertheless, the LCST curve is reasonably well correlated using this value. The prediction (k_{ij}=0) is almost as good for the LCST curve, although the UCST will then be substantially underpredicted.

Finally, Figure 5.8 shows simplified PC-SAFT predictions (k_{ij}=0) in the system PP – diethyl ether. While the effect of molecular weight is captured by the model (decreasing LCST with increasing molecular weight), the magnitude of this effect is not sufficiently accounted for. However the values of the LSCT, the concentration at the LCST and the shape of the curves are generally in good agreement with the experimental data.

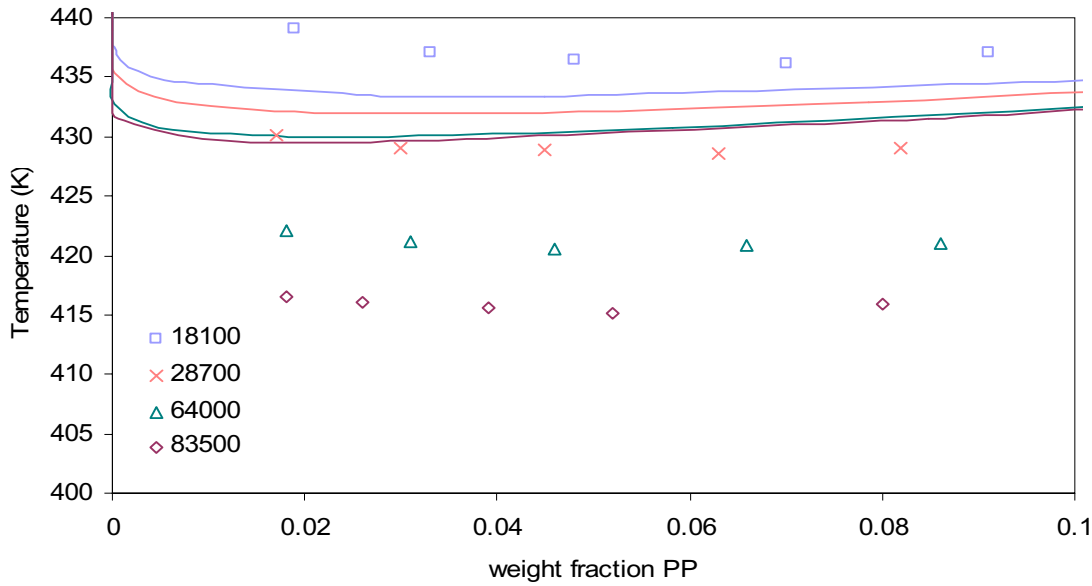

Figure 5.8 Liquid-liquid equilibrium in the system PP – diethyl ether. The system displays lower critical solution temperature behavior. The experimental data are from Cowie and McEwen[12]. The lines are simplified PC-SAFT predictions ($k_{ij} = 0$) for the four molecular weight shown.

5.4 Conclusions

We have developed a novel method, the method of alternating tangents, for calculating liquid-liquid equilibrium in binary polymer-solvent systems. The algorithm is robust and traces the full temperature composition curve for both UCST and LCST type systems through the critical solution temperature. The algorithm worked successfully for all polymer molecular weights encountered in the experimental literature. The algorithm is applicable to any equation of state for which analytical fugacity coefficients and their derivatives are available.

We have tested the simplified PC-SAFT equation of state to predict and correlate LLE in systems containing a range of polymers and solvents, both associating and non-associating. In general simplified PC-SAFT is successful in modeling LLE, successfully predicting the correct behavior in many systems exhibiting upper, lower and both critical solution temperatures. Where predictions are not accurate, a small value of the binary interaction parameter is required to correlate experimental data.

References

1. N. von Solms, M. L. Michelsen and G. M. Kontogeorgis, Computational and Physical Performance of a Modified PC-SAFT Equation of State for Highly Asymmetric and Associating Mixtures, *Ind. Eng. Chem. Res.* **2003**, 42**,** 1098.
2. I. A. Kouskoumvekaki, N. von Solms, M. L. Michelsen and G. M. Kontogeorgis, Application of a Simplified Perturbed Chain SAFT Equation of State to Complex Polymer Systems, *Fluid Phase Equilibria* **2004**, 215, 71.
3. J. Gross and G. Sadowski, Modeling Polymer Systems Using the Perturbed-Chain Statistical Association Fluid Theory Equation of State, *Ind. Eng. Chem. Res.* **2002,** 41, 1084.
4. J. Gross and G. Sadowski, Perturbed-Chain SAFT: An Equation of State Based on a Perturbation Theory for Chain Molecules, *Ind. Eng. Chem. Res.* **2000**, 40, 1244.
5. J. Gross and G. Sadowski, Application of the Perturbed-Chain SAFT Equation of State to Associating Systems, *Ind. Eng. Chem. Res.* **2002**, 41, 5510.
6. DIPPR Tables of Physical and Thermodynamic Properties of Pure Compounds, AIChE, New York, **1998**.
7. T. Dobashi, M. Nakata and M. Kaneko, Coexistence Curve of Polystyrene in Methylcyclohexane. I. Range of Simple Scaling and Critical Exponents, *J.Chem. Phys.* **1980**, 72, 6685.
8. A. R. Shultz and P. J. Flory, Phase Equilibria in Polymer-Solvent Systems, *J. Amer. Chem. Soc.* **1952,** 74, 4760.
9. F. Hamada, K. Fujisawa and A. Nakajima, Lower Critical Solution Temperature in Linear Polyethylene- n-Alkane Systems, *Polymer* **1973**, 4, 316.
10. A. Nakajima, H. Fujiwara and F. Hamada, Phase Relationships and Thermodynamic Interaction in Linear Polyethylene-Diluent Systems. *J. Polym. Sci*. Part A-2. **1966**, 4, 507.
11. N. Kuwahara, S. Saeki, T. Chiba and M. Kaneko, Upper and Lower Critical Solution Temperatures in Polyethylene Solutions, *Polymer* **1974**, 15, 777.
12. J. M. G. Cowie and I. J. McEwen, Lower Critical Solution Temperatures of Polypropylene Solutions, *J. Polym. Sci. Polym. Phys. Ed.* **1974**, 12, 441.

Chapter 6

Application of the simplified PC-SAFT Equation of State to the Vapor Liquid Equilibria of Binary and Ternary Mixtures of Polyamide 6 with Several Solvents

The simplified PC-SAFT equation of state has been applied to the pure-component properties and vapor-liquid equilibria of mixtures of polyamide 6 with several solvents (water, ε-caprolactam, ethyl benzene and toluene). These systems are of interest in the design of the polyamide 6 manufacturing. The optimum binary interaction parameters between polyamide 6, ε-caprolactam and water are estimated based on experimental pressure data from the respective binary mixtures. The obtained parameters are used for the prediction and correlation of the ternary mixture of polyamide 6, ε-caprolactam and water.

In the optimization of the pure-component parameters of polyamide 6, those of ε-caprolactam are taken as initial estimates and only the σ parameter is further fitted to experimental liquid volume data over a wide temperature and pressure range. Furthermore, the densities of several polyamides as a function of temperature and pressure are successfully correlated by fitting only the σ parameter based on experimental liquid density data.

The results show that the simplified PC-SAFT equation of state is a versatile tool for the modeling of multicomponent polyamide systems.

6.1 Introduction

Recent research in the development of modern equations of state such as the simplified PC-SAFT is mainly focused on applications involving multicomponent systems or systems with components with complex structure. Prediction and correlation of the thermodynamic behavior of such systems is of great interest to the industry, since experimental data are often difficult to obtain and they usually do not cover the whole range of desired conditions of temperature, pressure and molecular weight of the polymer.

In the manufacturing of polyamide 6, for instance, knowledge of vapor-liquid equilibrium of the system is essential for the accurate process design and control. Current industrial practice is based on a variety of empirical models that may quite accurately describe the process, but cannot be used as predictive tools or give trustworthy guidelines, when

changes in the process or formulation are required. The difficulties involved in the manufacturing process of polyamide 6 that the model is expected to be able to handle, is from the one hand the structure of the polymer, which includes groups that are self- and cross-associating and from the other hand the presence of water that is a component with unique behavior and properties, which so far even the advanced, theoretically based equations of state such as the simplified PC-SAFT have failed to capture accurately.

6.2 The Manufacturing Process of Polyamide 6

Two routes are available for the manufacture of polyamide 6 from ε-caprolactam[1]. The first, and by far, the predominant method is via hydrolytic polymerization in the melt and results in the opening of the ε-caprolactam ring and formation of aminohexanoic acid.

Ring opening

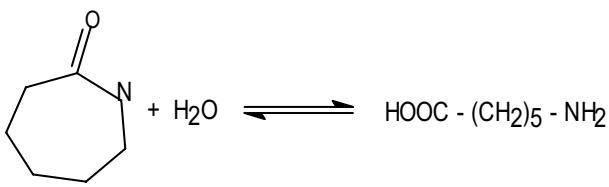

(6.1)

The second route, anionic polymerization, is used for specialty products and accounts for only a small fraction of the worldwide polyamide 6 production.

Ring-opening polymerization is an important method for the synthesis of a broad class of polyamides and copolymers with amide groups in the polymer chain and consists, as seen above, of reactions in which cyclic amide groups are converted into linear ones.

Following the opening of the ring, a polycondensation reaction takes place in the aqueous aminohexanoic acid solution:

Polycondensation

Amide dimer:

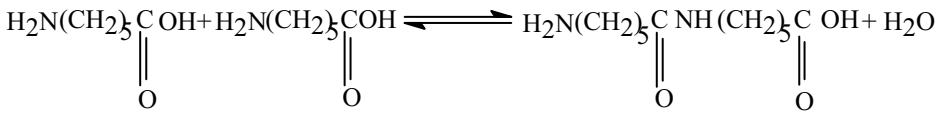

(6.2$_a$)

Polyamide:

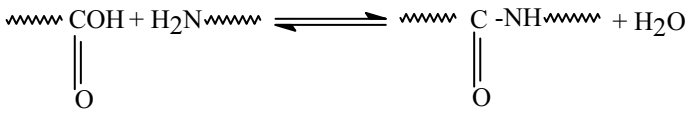

(6.2$_b$)

as well as polyaddition reactions of lactam to the end groups:

Polyaddition

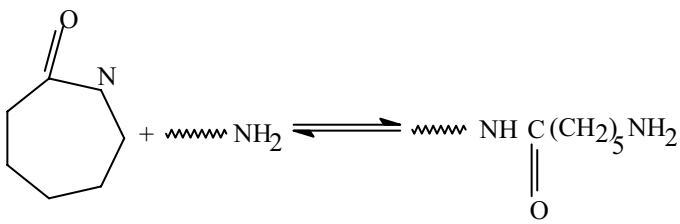

(6.3$_a$)

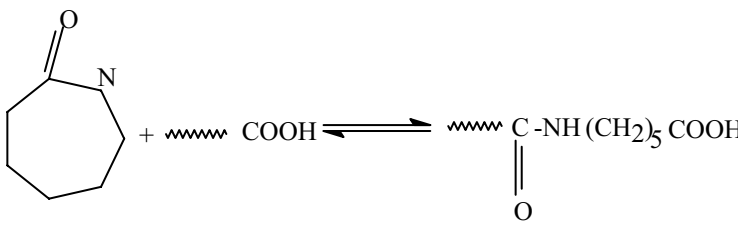

(6.3$_b$)

The end-product (after drying and extraction of nonreacted ε-caprolactam), is polyamide 6 with typically a number average molecular weight (*Mn*) of 15000 – 20000 and a polydispersity (Mw/Mn) of 2 – 2.2.

The phase equilibria of modeling interest to the industry are the VLE of the binary system ε-caprolactam – water and the VLE of the ternary system polyamide 6 – ε-caprolactam – water at low pressures and in the temperature range of the process (500 - 560 K).

An important feature of PC-SAFT is that polymers of different chain lengths can be defined based on the structure of the repeating unit. In this view, ε-caprolactam can be seen as a repeating unit of polyamide 6. Therefore, the modeling of ε-caprolactam is treated first. The pure-component parameters of ε-caprolactam are then used as initial estimates for modeling of the pressure and temperature dependence of the density of polyamide 6 and other polyamides.

Following the determination of the pure-component parameters, simplified PC-SAFT is applied to describe binary and ternary mixtures of polyamide 6 with water and ε-caprolactam.

6.3 Modeling Results and Discussion

6.3.1 ε-Caprolactam

Pure component parameters

The pure-component parameters of ε-caprolactam are regressed based on liquid density and vapor pressure data extracted from the DIPPR correlation[2].

Compound	**PC-SAFT Parameters**					**% Error**		**T range**
	m/MW	*σ* *(Å)*	*ε/k* *(K)*	ε^{AB}/k *(K)*	κ^{AB}	P^{sat}	V_L	*(K)*
ε-caprolactam (no association)	0.038	3.3014	330.112	-	-	0.76	0.77	400-740
ε-caprolactam (2B scheme)	0.036	3.3551	335.374	1623	0.003995	0.32	0.81	400-740

Table 6.1 Pure-component parameters of ε-caprolactam

Initially, ε-caprolactam is assumed to be self-associating (with two associating sites, according to the 2B scheme, as defined by Huang and Radosz[3]), because of the presence of the amide group in the ring, which implies that all five parameters have to be regressed simultaneously. However, the obtained associating parameters (ε^{AB} and κ^{AB}) have quite

low values, so an alternative three-parameter regression is performed (assuming ε-caprolactam to be nonassociating) to explore whether it is possible to apply this simplified approach to VLE calculations. The regressed values for both cases (associating and inert ε-caprolactam) are given in Table 6.1. These results indicate that we can match the experimental accuracy even without the association parameters.

ε-caprolactam - alkanes

Experimental data of binary solutions of ε-caprolactam in three different n- alkanes (octane, decane and dodecane)[4] were chosen for testing the regressed parameters of ε-caprolactam. The pure-component parameters of the alkanes are known and have already been tested in nonpolymer systems[5]. ε-Caprolactam seems to be a weak associating compound, as the correlations of PC-SAFT with and without the association term are rather similar, as shown in Figure 6.1.

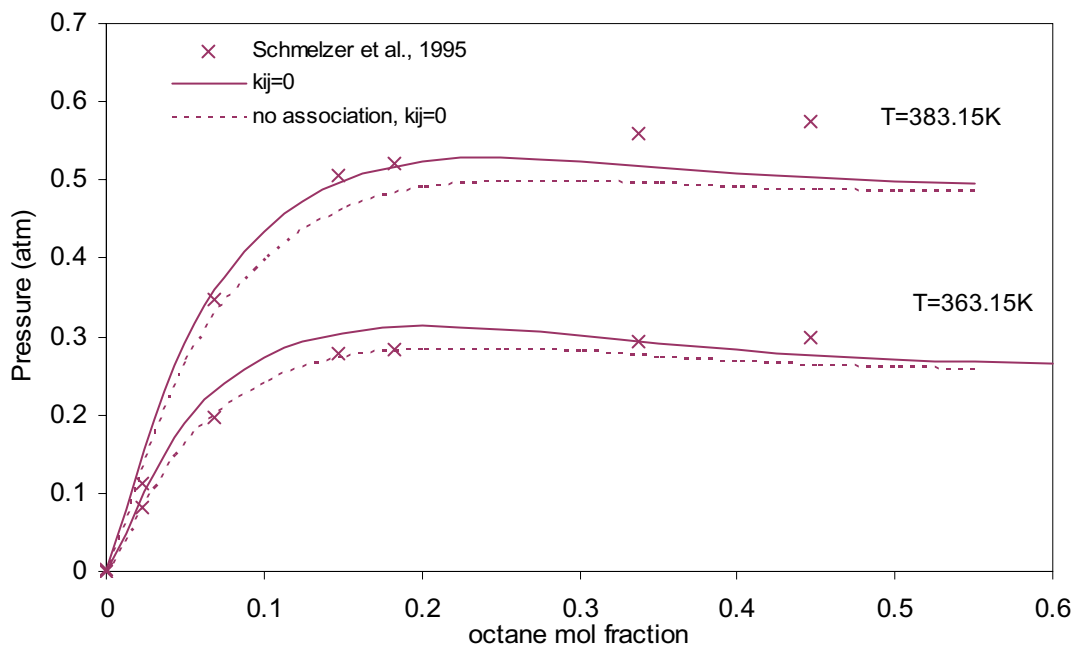

Figure 6.1 Vapor-liquid equilibrium in the system ε-caprolactam – octane. Experimental data are from Schmelzer et al.[4]. Dashed lines are simplified PC-SAFT predictions with ε-caprolactam taken as nonassociating and solid lines are simplified PC-SAFT predictions with ε-caprolactam taken as associating. Both predictions are at 363.15 and 383.15 K.

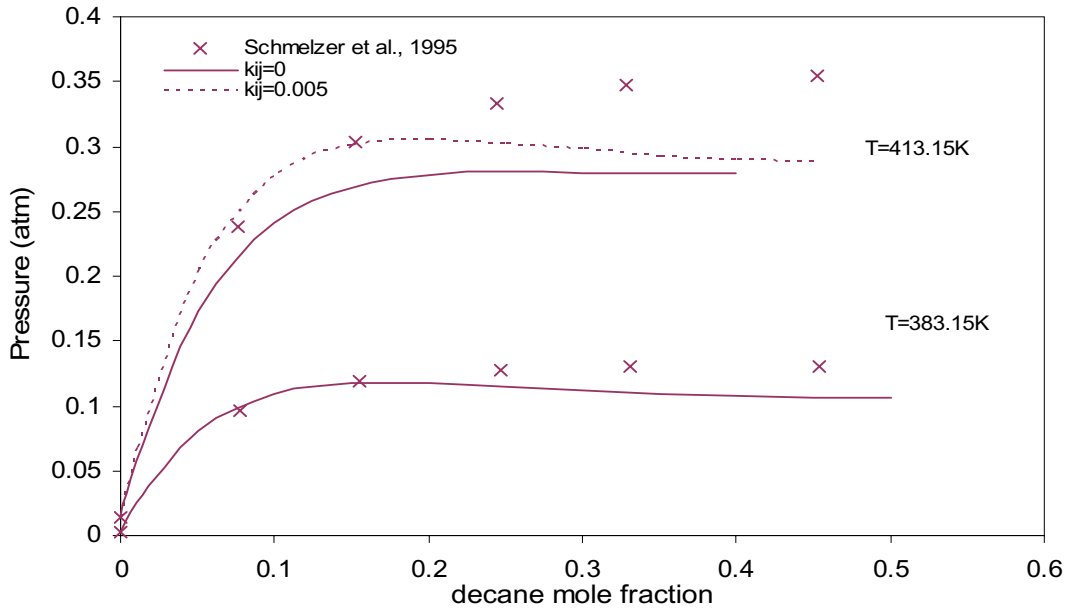

Figure 6.2 Vapor-liquid equilibrium in the system ε-caprolactam – decane. PC-SAFT parameters for ε-caprolactam are $m = 4.0737$, $\varepsilon / k = 335.374$ K, $\sigma = 3.3551$ Å, $\varepsilon^{AB} = 1623$ K and $\kappa^{AB} = 0.003995$. Experimental data are from Schmelzer et al.[4]. Solid lines are simplified PC-SAFT predictions and the dashed line is the simplified PC-SAFT correlation with $k_{ij} = 0.005$.

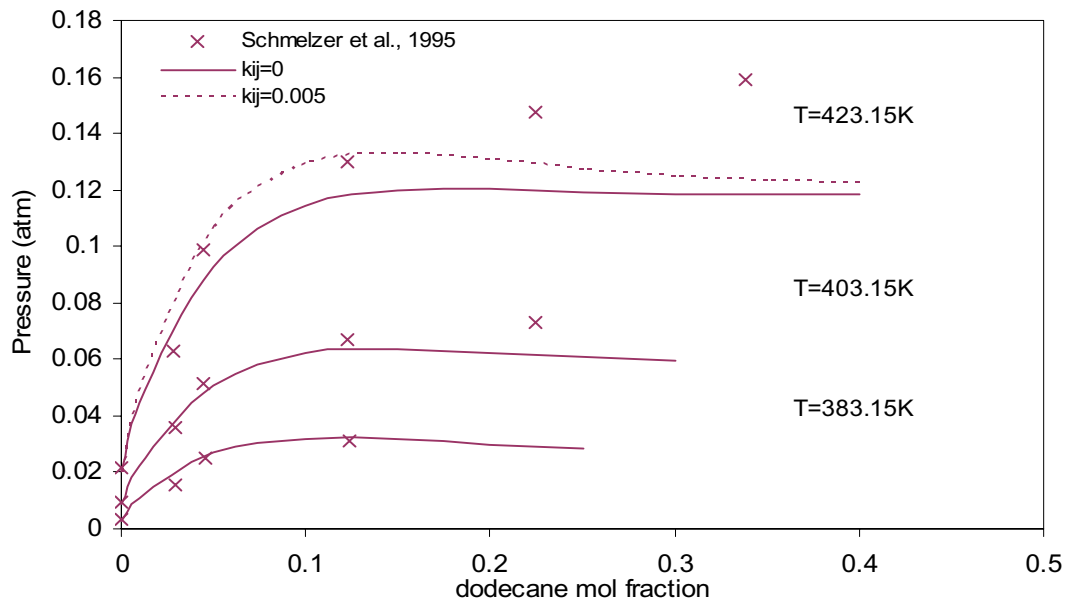

Figure 6.3 Vapor-liquid equilibrium in the system ε-caprolactam – dodecane. PC-SAFT parameters for ε-caprolactam are $m = 4.0737$, $\varepsilon / k = 335.374$ K, $\sigma = 3.3551$ Å, $\varepsilon^{AB} = 1623$ K and $\kappa^{AB} = 0.003995$. Experimental data are from Schmelzer et al.[4]. Solid lines are simplified PC-SAFT predictions and the dashed line is simplified PC-SAFT correlation with $k_{ij} = 0.005$.

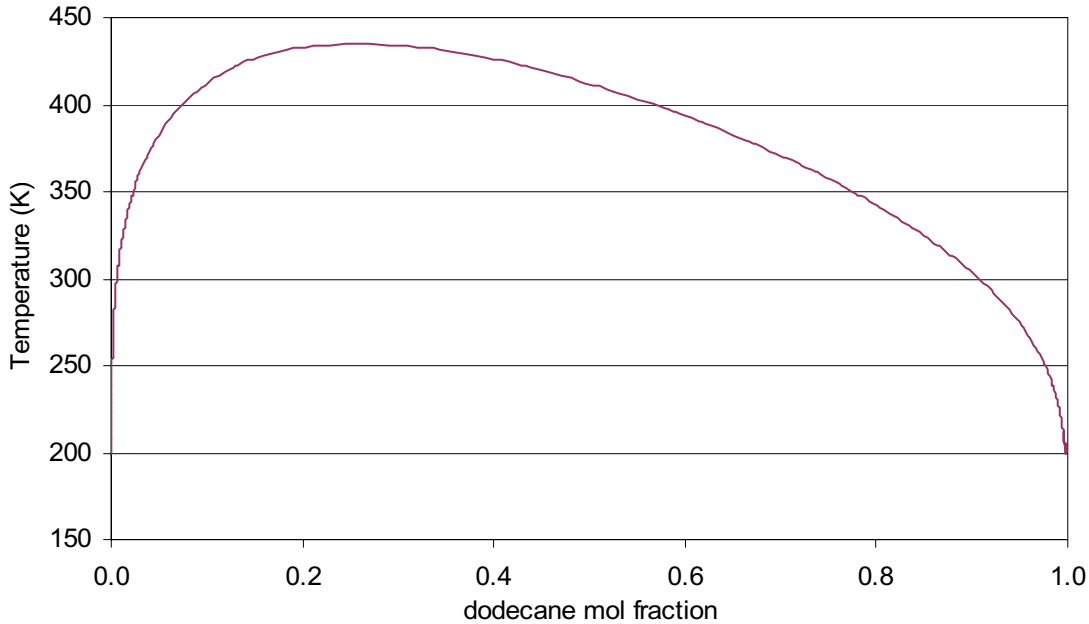

Figure 6.4 Prediction of the liquid-liquid equilibrium in the system ε-caprolactam – dodecane. PC-SAFT parameters for ε-caprolactam are $m = 4.0737$, $\varepsilon / k = 335.374$ K, $\sigma = 3.3551$ Å, $\varepsilon^{AB} = 1623$ K and $\kappa^{AB} = 0.003995$.

The shapes of the PC-SAFT curves for all three alkane systems (Figures 6.1 – 6.3) show that a liquid-liquid phase split will occur. To make this observation clearer, we predicted with PC-SAFT the liquid-liquid split in the system ε-caprolactam – dodecane and obtained the results shown in Figure 6.4. However, only in the case of caprolactam-dodecane do the experimental data indicate a demixing at that temperature range and for these intermediate concentrations of dodecane. Furthermore, as can be seen in Figure 6.3, the demixing covers a higher concentration region as the temperature decreases. PC-SAFT predicts the demixing correctly, but it overestimates the temperature of demixing for a certain concentration of dodecane. The lower the temperature, the more accurate the prediction. This observation (Figure 6.3) helps in understanding the behavior of the model in the first two systems (Figures 6.1 – 6.2): These solutions are unstable at lower temperatures than those covered by the experimental data, but PC-SAFT overestimates the temperature of demixing and, thus, erroneously shows demixing at temperatures where it does not occur. Such LLE overprediction is not uncommon. For example, the Peng-Robinson EOS with the van der Waals mixing rule also shows this behavior[6]. Improvement of the LLE curve could be achieved by using the Wong-Sandler

mixing rule, but further work on this issue is not considered to be of interest at this point, as the purpose of this part of the evaluation is to compare the behavior of the two different parameter sets for pure ε-caprolactam.

ε-caprolactam-acetic acid

Acetic acid is a self-associating compound. The binary solution of ε-caprolactam in acetic acid has been chosen for evaluation purposes, before the possibly more difficult case of a mixture with water is addressed. As can be seen in Figures 6.5 and 6.6, a high value of k_{ij} is needed to correlate the system ε-caprolactam-acetic acid. The same k_{ij} value is adequate at all three temperatures.

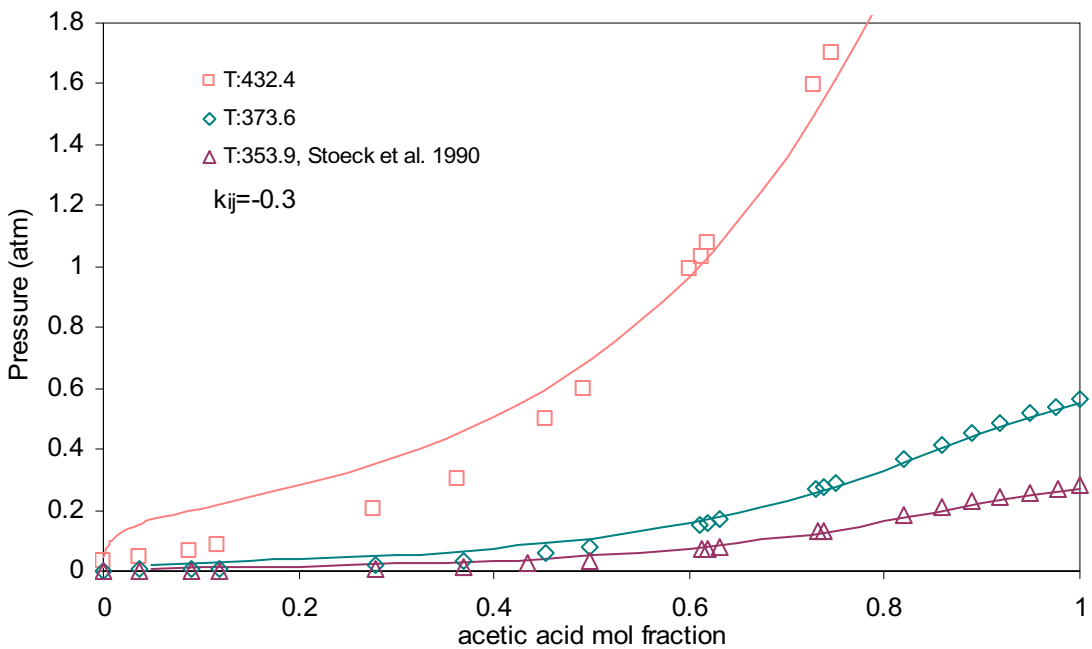

Figure 6.5 Vapor-liquid equilibrium in the system ε-caprolactam – acetic acid. PC-SAFT parameters for ε-caprolactam are $m = 4.3000$, $\varepsilon / k = 330.112$ K and $\sigma = 3.3014$ Å. Acetic acid parameters are $m = 1.3403$, $\varepsilon / k = 211.59$ K, $\sigma = 3.8582$ Å, $\varepsilon^{AB} = 3044.4$ K and $\kappa^{AB} = 0.07555$. Experimental data are from Stoeck et al.[8]. Lines are simplified PC-SAFT correlations with $k_{ij} = -0.30$ at each of the three temperatures.

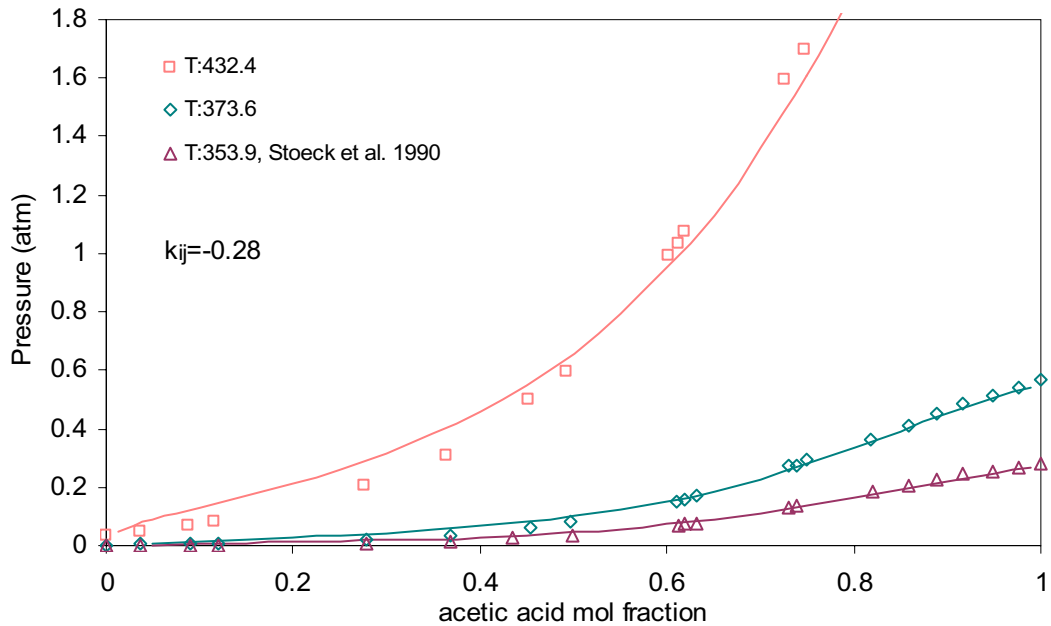

Figure 6.6 Vapor-liquid equilibrium in the system ε-caprolactam – acetic acid. PC-SAFT parameters for ε-caprolactam are $m = 4.0737$, $\varepsilon / k = 335.374$ K, $\sigma = 3.3551$ Å, $\varepsilon^{AB} = 1623$ K and $\kappa^{AB} = 0.003995$. Acetic acid parameters are $m = 1.3403$, $\varepsilon / k = 211.59$ K, $\sigma = 3.8582$ Å, $\varepsilon^{AB} = 3044.4$ K and $\kappa^{AB} = 0.07555$. The Elliot's rule was used as the combining rule for the cross-association strength. Experimental data are from Stoeck et al.[8]. Lines are simplified PC-SAFT correlations with $k_{ij} = -0.28$ at each of the three temperatures.

The results shown in Figure 6.5, are for acetic acid parameters taken from the literature[7], experimental data from Stoeck et al.[8] and caprolactam being treated as a nonassociating compound, whereas in Figure 6.6, both components were taken as associating. In the latter case, a slightly lower – but still high – value of k_{ij} (-0.28 instead of -0.30) is adequate for the correlation, which is furthered improved at high concentrations of ε-caprolactam. This might indicate that the ability of ε-caprolactam to form hydrogen bonds should be taken into account when the second component is self-associating (solvation).

Table 6.4 presents new parameters of acetic acid estimated in this work and the new correlation with PC-SAFT of the ε-caprolactam - acetic acid system is shown in Figure 6.7. The new parameters for acetic acid provide a better fit of vapor pressures and liquid volumes and, moreover, yield a lower interaction parameter (-0.20) and a more accurate correlation of the system.

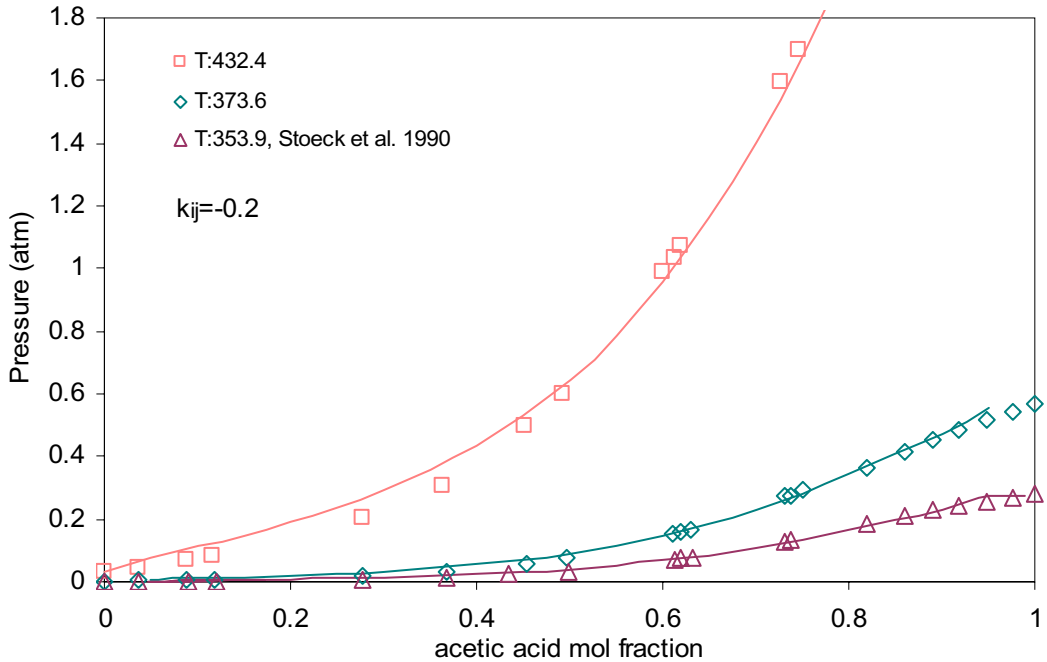

Figure 6.7 Vapor-liquid equilibrium in the system ε-caprolactam – acetic acid. PC-SAFT parameters for ε-caprolactam are $m = 4.0737$, $\varepsilon/k = 335.374$ K, $\sigma = 3.3551$ Å, $\varepsilon^{AB} = 1623$ K and $\kappa^{AB} = 0.003995$. The parameters for acetic acid are $m = 2.3420$, $\varepsilon/k = 199.901$ K, $\sigma = 3.1850$ Å, $\varepsilon^{AB} = 2756.7$ K and $\kappa^{AB} = 0.2599$. Elliot's rule was used as the combining rule for the cross-association strength. Experimental data are from Stoeck et al.[8]. Lines are simplified PC-SAFT correlations with $k_{ij} = -0.20$ at each of the three temperatures.

ε-caprolactam-water

Figure 6.8 shows the correlation of experimental data for the system ε-caprolactam-water at two different temperatures[9,16] (both components were taken as associating and the Elliot's rule[10] was used as the combining rule for the cross-association strength). It is shown that an accurate correlation is possible with a single (moderate-value) temperature-independent $k_{ij} = -0.07$.

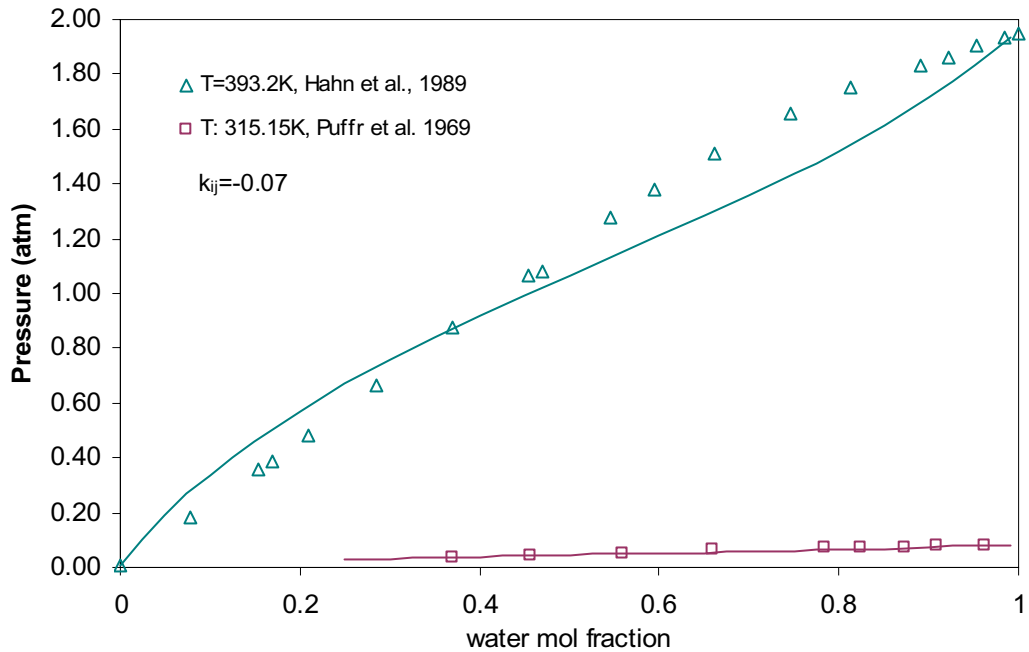

Figure 6.8 Vapor-liquid equilibrium in the system ε-caprolactam – water. PC-SAFT parameters for ε-caprolactam are $m = 4.0737$, $\varepsilon / k = 335.374$ K, $\sigma = 3.3551$ Å, $\varepsilon^{AB} = 1623$ K and $\kappa^{AB} = 0.003995$. The Elliot's rule was used as the combining rule for the cross-association strength. Experimental data are from Hahn et al.[9] and Puffr et al.[16]. Lines are simplified PC-SAFT correlations with $k_{ij} = -0.07$ at each of the two temperatures.

6.3.2 Polyamide 6

Densities of polyamides are reported in the literature as function of pressure and temperature[11]. To obtain the PC-SAFT parameters, only the data above the melting point of polyamide 6 were used, given that the polymer is semicrystalline below the melting temperature. Moreover, the values of the two association parameters of polyamide 6 were assumed to be identical to that of ε-caprolactam. It was further assumed that all of the associating sites of the chain are able to form hydrogen bonds. This means that the number of active sites of each site type per polymer molecule is equal to the number of monomer units in the chain. Figure 6.9 shows the performance of PC-SAFT in correlating the liquid density of polyamide 6 when the segment parameter σ is optimized.

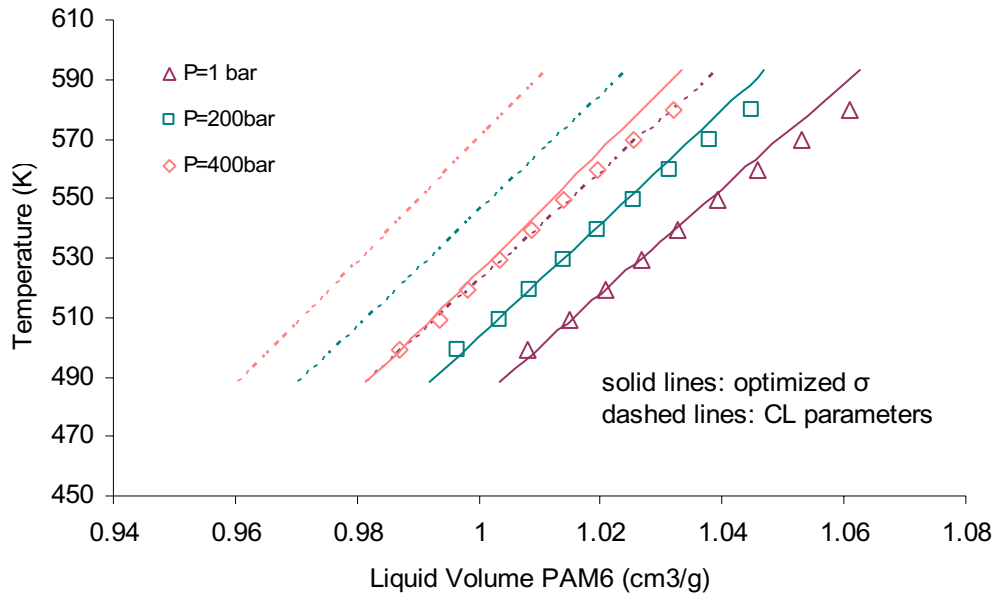

Figure 6.9 Liquid volume of polyamide 6. PC-SAFT parameters for polyamide 6 are $m/MW = 0.036$, $\varepsilon/k = 335.374$ K, $\sigma = 3.3551$ Å, $\varepsilon^{AB} = 1623$ K and $\kappa^{AB} = 0{,}003995$ (prediction-dashed lines) and $m/MW = 0.036$, $\varepsilon/k = 335.374$ K, $\sigma = 3.38$ Å, $\varepsilon^{AB} = 1623$ K and $\kappa^{AB} = 0.003995$ (correlation – solid lines). Comparison of experimental data[11] with the prediction and correlation results with PC-SAFT.

6.3. Polyamide 6 – solvent binary systems

Infinite dilution activity coefficients of toluene and ethyl benzene in polyamide 6

Mixture data of polyamide 6 with toluene and ethyl benzene are used for the testing of the reliability of the pure-component parameters of polyamide 6, estimated as described previously. Both solvents are common in the industry and their pure-component parameters have already been tested for polymer and non-polymer systems[5, 12]. Only data for the weight-based infinite-dilution activity coefficient of the solvent (Ω_1^{∞}) are available in the literature[13] for the two systems of interest. Table 6.2 shows experimental and PC-SAFT predicted values Ω_1^{∞} values for temperatures ranging from 523 to 563 K. The experimental values were calculated in this work based on the experimental retention volumes (V^0_g) presented in the literature and pure component data from the DIPPR compilation[2] using the following equation[13].

$$\ln \Omega_i^{\infty} = \ln \frac{273.2R}{V_g^0 P_i^{sat} M_i} - \frac{P_i^{sat}\left(B_{ii} - V_i\right)}{RT} \qquad (6.6)$$

The prediction results are very close to the experimental data, which is an indication that the pure-component parameters obtained from the monomer can satisfactorily describe the behaviour of the polymer in a solution. One further observation is that, whereas the predicted Ω_1^{∞} values show a decrease with temperature, the experimental values do not show a clear trend with increasing temperature.

	Polyamide 6 (2) – ethylbenzene (1) Ω_1^{∞}	**Polyamide 6 (2) – toluene (1)** Ω_1^{∞}
T= 523 K		
Experimental	10.81	9.62
Predicted	13.34	11.73
T= 533 K		
Experimental	11.99	10.08
Predicted	13.05	11.56
T= 543 K		
Experimental	11.85	10.23
Predicted	12.79	11.45
T= 553 K		
Experimental	11.21	10.66
Predicted	12.58	11.39
T= 563 K		
Experimental	11.48	
Predicted	12.42	

Table 6.2 Infinite-dilution weight-based activity coefficient of ethylbenzene and toluene in polyamide 6. Comparison of experimental data[13] with the prediction results obtained with PC-SAFT.

Polyamide 6 - ε-caprolactam VLE

The next step is the estimation of the interaction parameter between polyamide 6 and ε-caprolactam.

Table 6.3 reports the infinite-dilution weight-based activity coefficient of ε-caprolactam in polyamide 6 at 523 K. The predicted and correlated values are compared with those reported by Bonifaci et al.[14] measured by two different techniques (packed and capillary columns). The predictions made with PC-SAFT in the infinite-dilution region are within

the experimental error and with a small negative k_{ij} (= -0.011), the correlation results are fitted to a mean value of the given data points.

Polyamide 6 (2) - ε-caprolactam (1)	**Ω_1^∞ (predicted)** *T=523K*	**Ω_1^∞ (experimental)** *T=523K*	
		Packed column	*Capillary column*
Prediction (k_{ij} = 0)	3.84	2.68	2.89
Correlation (k_{ij} = -0.011)	2.78		

Table 6.3 Infinite-dilution weight-based activity coefficient of ε-caprolactam in polyamide 6 at 523 K. Comparison of experimental data[14] with the prediction and correlation results with PC-SAFT.

Polyamide 6 - water VLE

The last binary system that needs to be correlated before proceeding to the ternary system is polyamide 6 – water. Figure 6.10 shows the correlated pressure curves of polyamide 6 - water at high temperatures. The plot is given in terms of mole fraction of water, as the weight fraction spans only a very narrow range (1 – 4%). The correlation is satisfactory when a rather large negative – and, moreover temperature dependent – k_{ij} value is used. We believe that this is because the reported experimental data[15] refer to a pseudo-binary system: As stated by the authors, even though the polymer solution was made free of ε-caprolactam and its oligomers by extraction, an amount of acetic acid was still present, reaching mole fractions in the range of 0.13 – 0.18 at the highest temperature (and in the range of 0.05 – 0.1 at the lower temperatures). This might explain the temperature dependence of k_{ij}, as well as the fact that PC-SAFT cannot match the experimental curve at the highest temperature. To account for the presence of acetic acid, the mole fractions of water were corrected according to the amount of acetic acid stated by the authors[15].

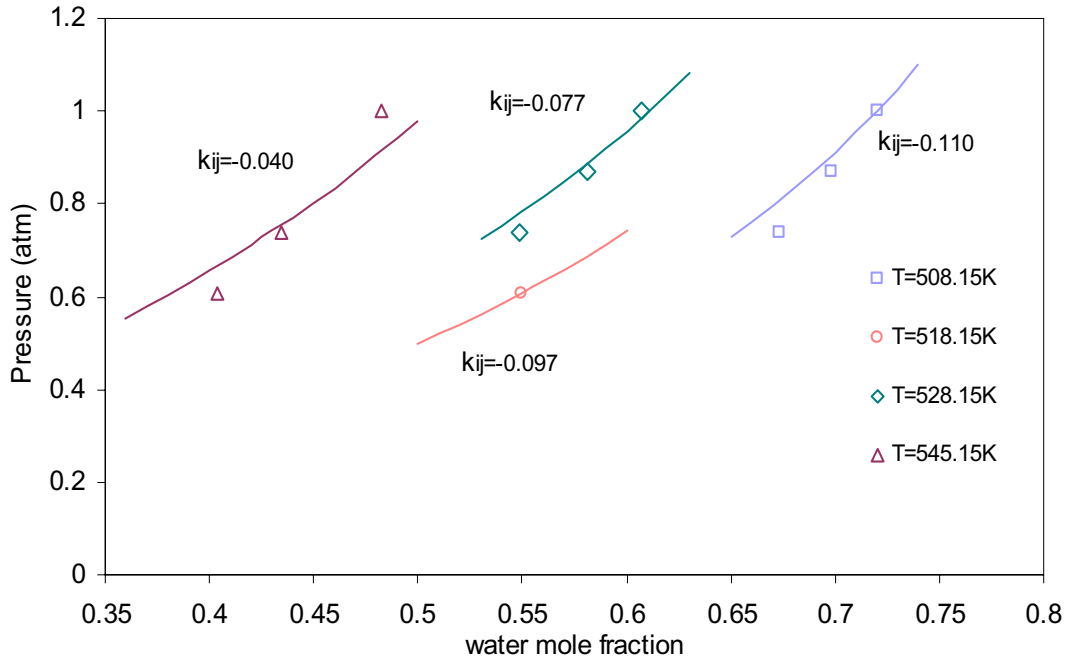

Figure 6.10 Vapor liquid equilibrium in the system polyamide 6 - water. PC-SAFT parameters for polyamide 6 are $m/MW = 0.036$, $\varepsilon/k = 335.374$ K, $\sigma = 3.38$ Å, $\varepsilon^{AB} = 1623$ K and $\kappa^{AB} = 0.003995$. Experimental data are from Fukumoto et al.[15]. Lines are simplified PC-SAFT correlations with temperature-dependent k_{ij}'s.

However, the VLE correlation was based on the binary polyamide 6 - water system, given that experimental data for polyamide 6 - acetic acid are not available. Such data would be required for estimating the binary interaction parameter between the polymer and acetic acid. Judging from the system ε-caprolactam - acetic acid (Figures 6.6 – 6.8), it seems that the interaction parameter between polyamide 6 and acetic acid might have quite a high value and, therefore, might influence significantly the correlation results.

The ambiguity regarding the parameters for water could also be responsible for these poor results. As mentioned by Gross et al [7], it is a considerable simplification to assume the 2B model for water, as there are indications that water is best represented with a four-site treatment. Therefore, in complex aqueous polymer solutions such as the one in the present work, such a simplification could play a major role.

The pure-component parameters employed for each component of the ternary system are provided in Table 6.4.

	m/MW	***σ*** ***(Å)***	***ε/k*** ***(K)***	***ε^{AB}/k*** ***(K)***	***κ^{AB}***
Acetic acid	0.039	3.185	199.901	2757	0.2599
Water	0.059	3.0007	366.510	2501	0.034868
ε-Caprolactam	0.036	3.3551	335.374	1623	0.003995
Polyamide 6	0.036	3.38	335.374	1623	0.003995

Table 6.4 Pure component parameters of PC-SAFT for acetic acid, water, ε-caprolactam and polyamide 6. The associating parameters of all four compounds have been regressed based on the 2B association scheme.

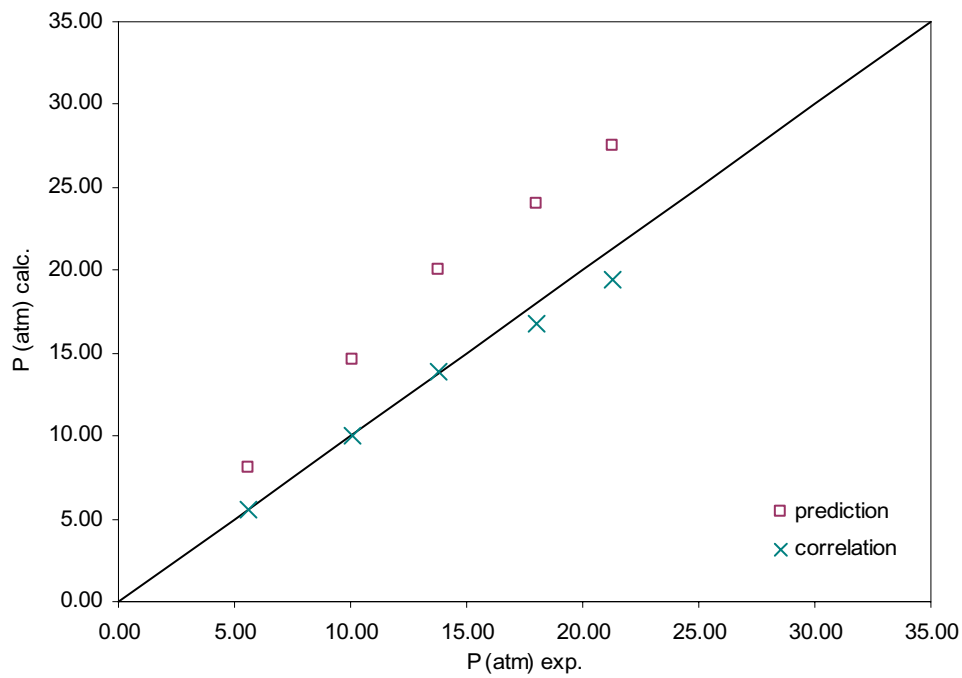

Figure 6.11 Comparison of experimental pressure data[17] with prediction and correlation results obtained with PC-SAFT at 543.15K, for the ternary system polyamide 6 (1) – ε-caprolactam (2) – water (3) (binary interaction parameters are: k_{12}=-0.07, k_{13}=-0.04, k_{23}=-0.011 (prediction) and k_{12}=-0.07, k_{13}=-0.11, k_{23}=-0.011 (correlation).

Figure 6.11 shows the predicted and correlated total pressure for the ternary system polyamide 6 – water -ε-caprolactam. The comparative plot with the experimental data shows that the k_{ij}'s obtained from the respective binary systems predict the ternary system results quite satisfactorily. The k_{ij} of the polyamide 6 - water system was fitted to the value of -0.11, higher than the value obtained from the correlation of the binary data at the temperature of interest (-0.04 at 545.15 K).The correlation of the concentrations of the two components in the vapor phase is shown in Figures 6.12-6.13.

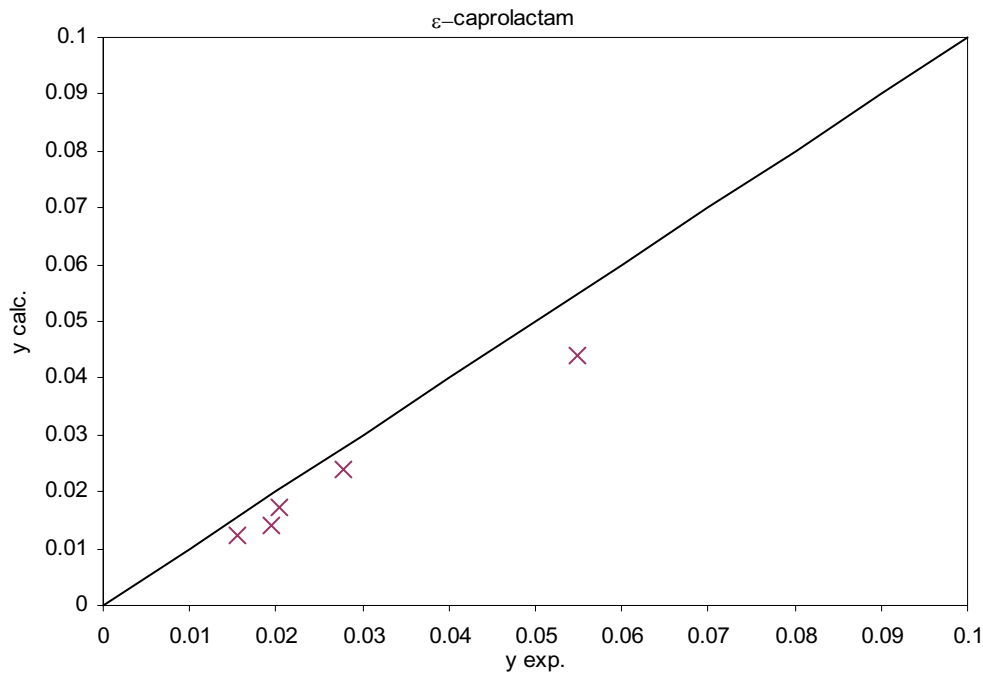

Figure 6.12 Comparison of experimental data for the mole fraction of ε-caprolactam in the vapor phase[17] with correlation results obtained with PC-SAFT at 543.15K for the ternary system polyamide 6 (1) - ε-caprolactam (2) – water (3). (The binary interaction parameters are: k_{12}=-0.07, k_{13}=-0.11, k_{23}=-0.011).

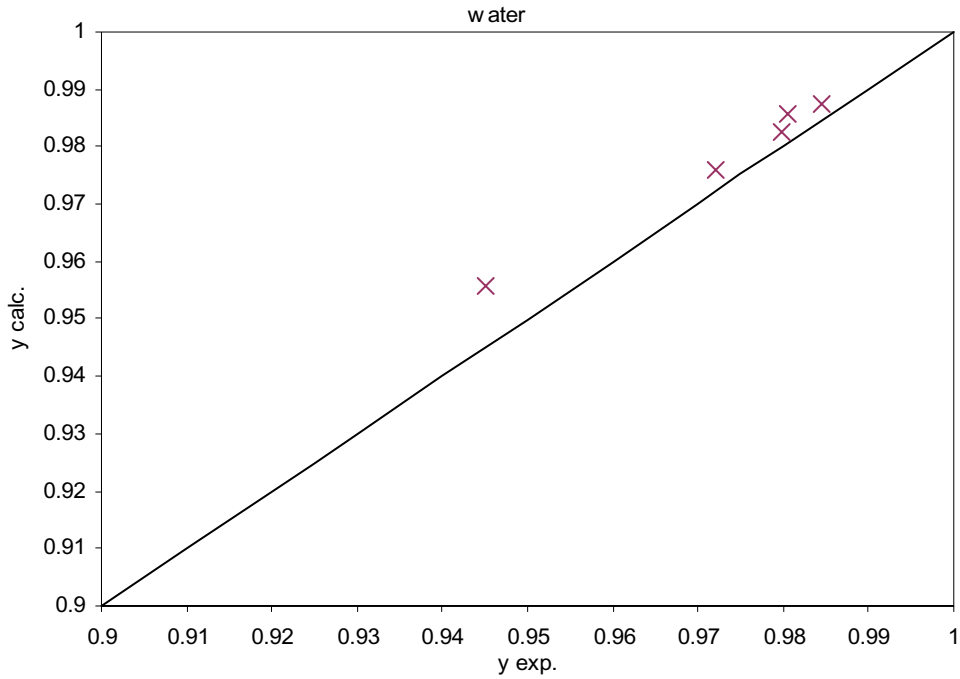

Figure 6.13 Comparison of experimental data for the mole fraction of water in the vapor phase[17] with correlation results obtained with PC-SAFT at 543.15K for the ternary system polyamide 6 (1) - ε-caprolactam (2) – water (3). (The binary interaction parameters are: k_{12}=-0.07, k_{13}=-0.11, k_{23}=-0.011).

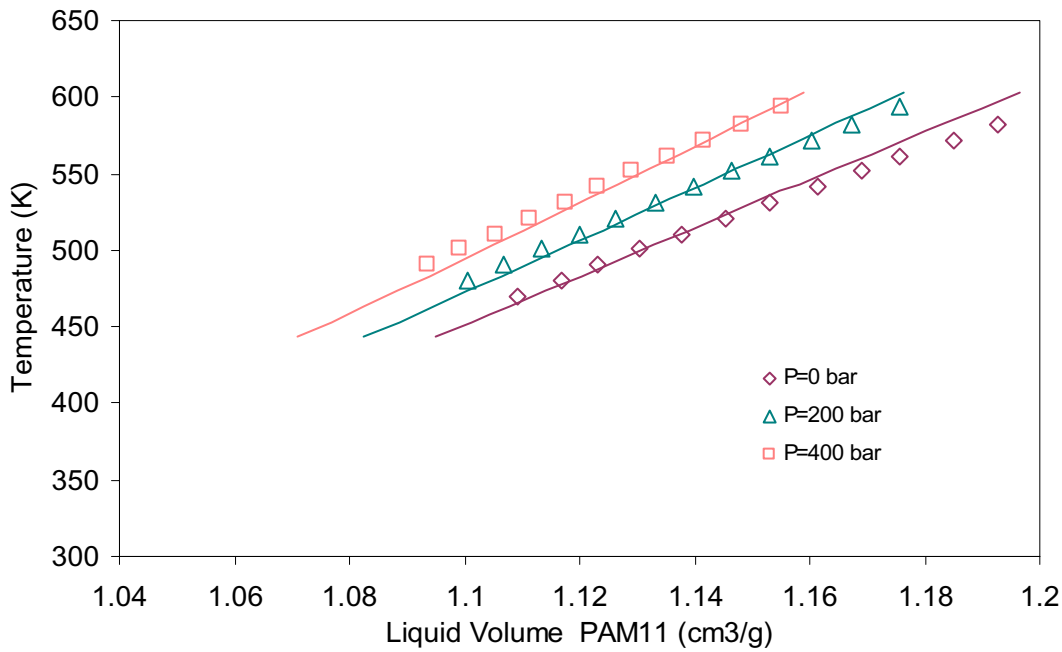

Figure 6.14 Liquid volume of polyamide 11. PC-SAFT parameters for polyamide 11 are $m/MW = 0.036$, $\varepsilon/k = 335.374$ K, $\sigma = 3.51$ Å, $\varepsilon^{AB} = 1623$ K and $\kappa^{AB} = 0.003995$. Comparison of experimental data[11] with correlation results obtained with PC-SAFT.

6.3.5 Extrapolation to other polyamides

Figure 6.14 shows the performance of PC-SAFT in correlating the liquid density of polyamide 11. The figure shows that an excellent correlation of the liquid volume can be obtained by adjusting only the segment parameter value to the alkyl length.

Furthermore, the possibility of whether there is a linear dependency of the segment diameter of polyamides on the percentage of linear polyethylene segment in the polymer was investigated. The percentage of linear polyethylene in each polyamide type was calculated as shown in the following example for the case of polyamide 6:

Polyamide 6: could be also written as:

where the first part, $(CH_2)_4$, represents the polyethylene group and the second part – CH_2CONH – , represents the polyamide group. Because the electronegativity of the carboxyl group influences the neutrality of the neighboring methylene group, one methylene group is not included in the calculation of the polyethylene part.

The weight ratio of polyethylene/polyamide in the polymer chain is then MW_{PE}/MW_{PAM} = 56/57, which corresponds to a weight percentage of 49.5 of the polyethylene segment. The weight percentages of the other polyamide types were calculated accordingly. Results for the other polyamides are presented in Table 6.5.

Figure 6.15 shows that there is indeed a linear increase in the optimum σ value as the weight percentage of the polyethylene segment increases. This can be explained by the fact that, when the ethylene percentage is higher, the hydrogen bonding is weaker, and the polymeric chain becomes more flexible and less dense. Thus, at the same temperature, polyamide 12 has a higher volume and polyamide 4,6 has a lower volume[11]. This increase in volume is responsible for the higher optimum value of the segment diameter σ.

Polyamide Type	*w (PE)*	*σ (Å)*
Polyamide 4,6	0.424	3.32
Polyamide 6	0.495	3.38
Polyamide 6,6	0.495	3.38
Polyamide 7	0.551	3.42
Polyamide 9	0.632	3.48
Polyamide 11	0.688	3.51
Polyamide 12	0.711	3.53

Table 6.5 Weight fraction of linear polyethylene segment in the polymer chain and optimum σ for seven polyamide types.

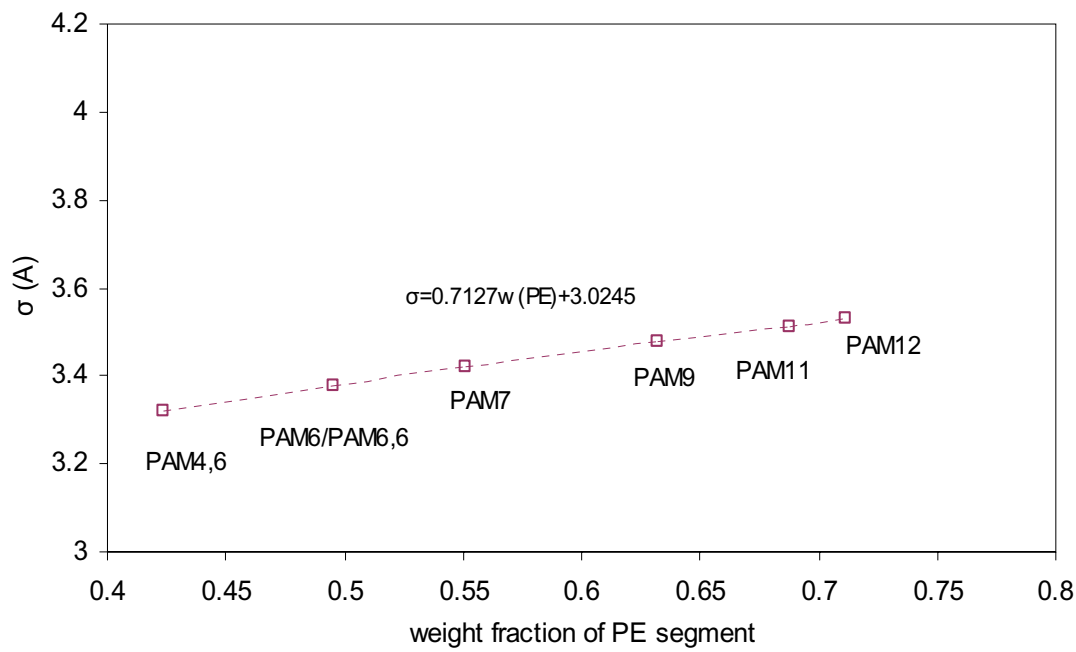

Figure 6.15 Optimum σ values against the weight fraction of linear polyethylene segment in the polyamide chain for seven polyamide types.

6.4 Conclusions

The simplified PC-SAFT equation of state was applied to the vapor-liquid equilibria of binary and ternary systems of polyamide 6 with several solvents (water, caprolactam, ethyl benzene and toluene). Such systems had not been previously investigated with this model and offer a challenge for modern equations of state such as PC-SAFT.

We have shown that simplified PC-SAFT exhibits very good correlative behavior for the above systems, using a small to moderate negative interaction parameter. The system polyamide 6 – water, however, shows increased complexity and correlation is only possible with a rather large negative interaction parameter. This result raises questions as to the correct representation of water by the PC-SAFT parameters and points out the necessity for a more thorough investigation.

ε-Caprolactam was found to be a weakly self-associating compound that is, however, able to cross-associate when present in a solution with a stronger associating compound such as acetic acid and water. The five pure-component parameters of ε-caprolactam were successfully regressed by fitting vapor pressure and liquid volume experimental data. Subsequently, these parameters were used as initial estimates for the parameters of polyamide 6 and the other polyamides: Keeping the four PC-SAFT parameters equal to the values obtained for ε-caprolactam and fitting only the segment diameter to the liquid volume of the polymer, the correlation is very good for all polyamide types over a broad range of temperatures and pressures. The obtained segment diameter σ is higher than that of ε-caprolactam, reflecting the decrease in segment free volume.

It was also found that there is a linear dependency of the segment size parameter σ on the linear polyethylene segment fraction of the polyamide, which can be explained by the fact that the linear polyethylene group adds flexibility to the polymer chain and leads to a higher volume.

The simplified PC-SAFT equation of state was successfully applied to the manufacturing process of polyamide 6 and the results for the final target ternary system (polyamide 6 - ε-caprolactam – water), as well as those for other polyamide types, show that the simplified PC-SAFT equation of state is a versatile tool for the modeling of self- and cross-associating multicomponent polyamide systems of relevance to the design of polyamide processes.

References:

1. R Puffr and V. Kubánek, Lactam-Based Polyamides, Volume I Polymerisation, Structure, Properties, CRC Press, 1991, United States.
2. DIPPR Tables of Physical and Thermodynamic Properties of Pure Compounds, AIChE, New York, 1998.
3. S. H. Huang and M. Radosz**,** Equation of Sate for Small, Large, Polydisperse and Associating Molecules, *Ind. Eng. Chem. Res.* **1990**, 29, 2284.
4. J. Schmelzer and J. Pusch, Phase Equilibria in Binary Systems Containing N-monosubstituted Amides and Hydrocarbons, *Fluid Phase Equilibria*, **1995**, 110, 183.
5. J. Gross and G. Sadowski, Perturbed-Chain SAFT: An Equation of State Based on Perturbation Theory for Chain Molecules, *Ind. Eng. Chem. Res.* **2001,** 40, 1244.
6. S. I. Sandler, Chemical and Engineering Thermodynamics, 3rd ed., John Wiley & Sons: New York, 1998, p 562.
7. J. Gross and G. Sadowski, Application of the Perturbed-Chain SAFT Equation of State to Associating Systems, *Ind. Eng. Chem. Res.* **2002,** 41, 5510.
8. S. Stoeck and K. Moerke, *FIZ Report (DDB)*, **1990**, 2221.
9. J. Hahn and K. Moerke, *FIZ Report (DDB),* **1989,** 5181.
10. S. J. Suresh and J. R. Elliott Jr., Multiphase equilibrium analysis via a generalized equation of state for associating mixtures*, Ind. Eng. Chem. Res.*, **1992,** 31, 2783.
11. P. Zoller and D. J. Walsh, Standard PVT data for polymers, 1995, Technonomic Publ. Comp., ISBN 1-56676-328-2.
12. J. Gross and G. Sadowski, Modeling Polymer Systems Using the Perturbed-Chain Statistical Associating Fluid Theory Equation of State Equation of State, *Ind. Eng. Chem. Res.* **2002,** 41, 1084
13. L. Bonifaci, G. Cavalca, D. Frezzotti, E. Malaguti and G. P. Ravanetti, Thermodynamic Studies of Nylon-6 / solvent Systems by Inverse Gas Chromatography at Elevated Temperatures, *Polymer*, **1992**, 33, 4343.
14. L. Bonifaci and G. P. Ravenetti, Measurement of Infinite Diffusion Coefficients of e-caprolactam in Nylon 6 at Elevated Temperatures by Inverse Gas Chromatography, *J.Chromatography*, **1998**, 607, 145-149.

15. O. Fukumoto, Equilibria between Polycapramide and Water, *Journal of Polymer Science,* **1956,** 22, 263.
16. R. Puffr, *Collect. Czech Chem Commun*., **1969**, 34, 1421.
17. C. Giori and B. T. Hayes, Hydrolytic Polymerization of Caprolactam. II. Vapor-Liquid Equilibria, *Journal of Polymer Science: Part A-1,* **1970,** 8, 351.

Chapter 7

A Novel Method for Estimating Pure-Component Parameters for Polymers: Application to the PC-SAFT Equation of State

In this work we have developed a method for estimating pure-component parameters for polymers for the PC-SAFT equation of state. Our method is based on pure polymer volumetric (PVT) data and extrapolating equations that relate the polymer parameters to those of the corresponding monomer. The obtained parameters are thus unique for each polymer and do not depend on any mixture data. The new pure-component parameters have been used as input in the simplified PC-SAFT equation of state, in order to evaluate both the parameters and the equation of state in a variety of binary polymer mixtures, exhibiting both vapor-liquid and liquid-liquid phase equilibria. In most of the systems studied, satisfactory results have been obtained. Vapour-liquid and upper critical solution temperatures (UCST) in liquid-liquid equilibria are accurately correlated with small values of the interaction parameter.

7.1. Introduction

One limitation, when applying SAFT-family models to polymers is the availability of pure-component parameters for the polymer. Pure-component parameters for PC-SAFT are available for very few polymers.[1,2,3] Furthermore, there is no established, general method for obtaining them. Gross and Sadowski[1] obtained pure-component polymer parameters by simultaneous fitting four parameters - the three pure-component parameters as well as a binary interaction parameter – to pure polymer liquid density and binary phase equilibrium data for a single polymer-solvent system. The polymer parameters determined in this way are then fixed and can then used to predict phase behavior in other mixtures.

In this work we investigate several methodologies for obtaining pure-component polymer parameters for PC-SAFT. We evaluate methods based on simultaneous parameter-fitting to pure polymer PVT data and binary polymer-solvent phase-equilibrium data and we propose a new methodology, whereby the values of the polymer parameters are calculated from extrapolations of monomer parameters. The proposed method does not make use of mixture data.

A discussion of the proposed method and its implementation follows, together with results for a variety of different polymer-solvent mixtures displaying different types of LLE behavior.

7.2. Estimation methods for polymer PC-SAFT parameters

7.2.1 Estimation methods using binary data

In accordance with the molecular model underlying the simplified and the original PC-SAFT equations of state, a three pure-component parameter set is required for non-associating compounds, namely the segment diameter, σ, the segment number, m, and the segment energy, ε. For low molecular-weight compounds, these are typically obtained by simultaneously regressing saturated liquid-density and vapor pressure data. Unfortunately, this is not possible for polymers, since vapor pressure data do not exist. If the pure-component parameters are adjusted only to liquid density data, they can receive unexpected values which lead to unsatisfactory descriptions of phase equilibrium in polymer mixtures[1].
In order to overcome this problem, Gross and Sadowski[1] included both pure polymer PVT data as well as a single binary system for which experimental LLE data were available, in the regression of the polymer parameters. In this way, four parameters (three polymer parameters plus an interaction parameter for the binary system) are simultaneously regressed.
This method has led to successful LLE[1] and VLE[4] correlations for a variety of polymer-solvent systems. Nevertheless, we have observed that the pure-component polymer parameters obtained in this way are not unique for each polymer, but depend on the binary system chosen for the regression as well as the type (VLE / LLE) of experimental phase equilibrium used.
In order to demonstrate this, we compare the pure-component parameters of polystyrene (PS) regressed from pure polymer PVT data and binary phase equilibrium data in five different ways. The five data sets and regression methods used are listed below. The references are to the experimental VLE data sets.

1. A single binary LLE data set for the system PS – cyclohexane (the parameters from Gross and Sadowski[1]);
2. A single binary VLE data set for PS – cyclohexane[5];
3. A single binary VLE data set of PS – cyclohexane, with the binary interaction parameter excluded from the regression[5];
4. A large number of binary VLE data sets of PS with acetone[6], benzene[7,8], toluene[9,10], carbon tetrachloride[7], chloroform[6], MEK[9,11], propylacetate[6], nonane[12] and cyclohexane[5];
5. The same number of binary VLE data sets as above, with the binary interaction parameter excluded from the regression.

The results are summarized in table 7.1 and it can be seen that the values of all the parameters depend to a great extent on the type and number of the binary sets used in combination with the pure polymer PVT data. The effect of the polymer parameters on the LLE of PS with acetone and cyclohexane is also evaluated. These results are discussed in the next section.

Table 7.1 Values of PC-SAFT parameters and average absolute deviation between calculated and experimental liquid density of polystyrene for the five different methods evaluated for the regression of pure-component parameters for polymers. Temperature range: 390 – 470 K, Pressure range: 1 – 1000 bar

	Method of pure polymer parameters' regression	**m/M**	**σ (A)**	**ε/k (K)**	**AAD % ρ**
1.	PVT + single binary LLE	0.0190	4.107	267.0	5.1
2.	PVT + single binary VLE	0.0242	3.939	366.4	0.3
3.	PVT + single binary VLE excl. k_{ij}	0.0214	4.061	312.1	0.9
4.	PVT + all binary VLE	0.0364	3.354	277.9	0.4
5.	PVT + all binary VLE excl. k_{ij}	0.0390	3.243	243.8	0.8

7.2.2 A Novel Estimation Method Using Pure-Component Data

Our aim is to develop a method that will yield unique pure-component polymer parameters, which also give good results when used to describe phase equilibria in polymer mixtures. The basic principle behind this method is to extrapolate from the parameters of similar, lower molecular-weight compounds. This approach has been tried before for polyethylene (based on parameters of the alkane series[13]). Since the alkane series is so well characterized, this seems to be a suitable starting point.

It was noted previously[14] that the following combinations of the pure-component parameters for alkanes are linear functions of molecular weight (MW):

$$m = 0.02537MW + 0.9081 \tag{7.1}$$

$$m\varepsilon / k = 6.918MW + 127.3 \tag{7.2}$$

It may be mentioned that this trend has also been observed for SAFT-VR[15], which suggests that our approach is not solely applicable to PC-SAFT, but might also be suitable to other SAFT-family models, and other segment-based models for polymers. Eqs. (7.1) and (7.2) were obtained by plotting m and $m\varepsilon/k$ against MW for linear alkanes from ethane to eicosane. Although the functional form of Eqs. (7.1) and (7.2) can only be verified against the alkane series, it seems reasonable to assume that it holds for all polymers. We generalize these equations as follows:

$$m = A_m MW + B_m \tag{7.3}$$

$$m\varepsilon / k = A_\varepsilon MW + B_\varepsilon \tag{7.4}$$

Now in order to find the four constants A_m, B_m, A_ε and B_ε we need four equations, i.e. both parameters m and ε for at least two compounds in the series. However, finding properties even for a polymer dimer is problematic. For example, while we have saturated liquid density and vapour-pressure data for ethyl benzene (the monomer of polystyrene), there is virtually no physical property data for the dimer (1,3-diphenyl butane).

We now make the further assumption that in the limit of zero molecular weight polymers become indistinguishable. As can be seen in Figs. 7.1 and 7.2 this is a good approximation for the PP and PIB series, for which information for both the monomer and the dimer of each series is available. Thus we assume the constants B_m and B_ε are universal and can be determined from any homologous series. Using the alkane series (Eqs. (7.1 and (7.2)) and setting *MW* to zero we have:

$$B_m = 0.9081 \tag{7.5}$$

$$B_\varepsilon = 127.3 \tag{7.6}$$

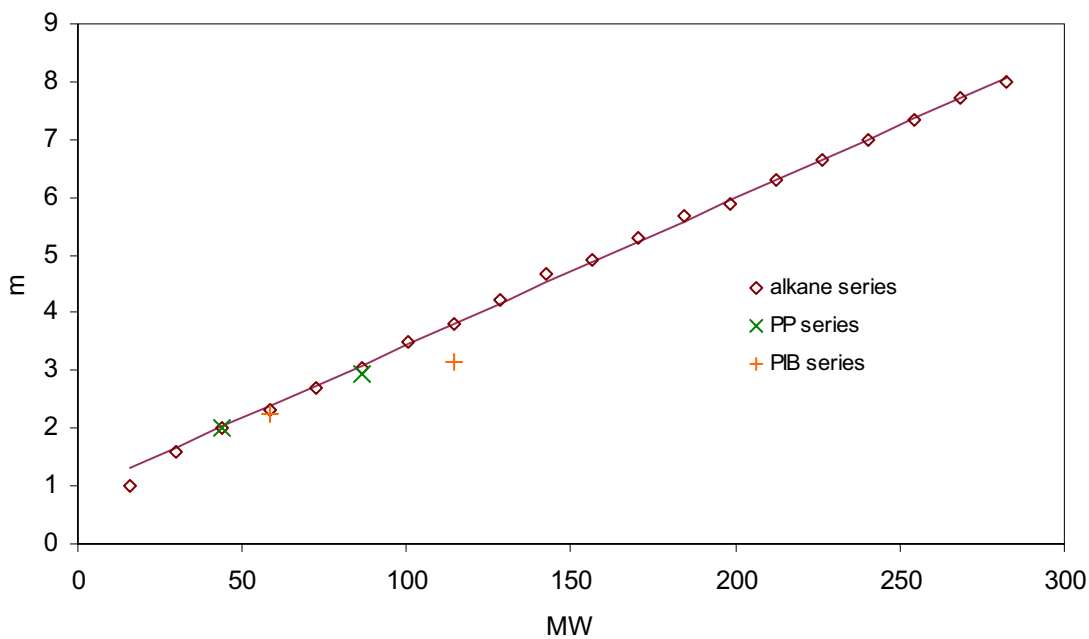

Figure 7.1. m vs. molecular weight for the alkane, the PP and the PIB series. Points are PC-SAFT parameters reported by Gross and Sadowski[17], line is linear fit to the alkane series, excluding methane, described by Eqs. 7.1-7.2.

Now the constants A_m and A_ε can be determined for each polymer using Eqs. (7.3) and (7.4) and the values of the parameters m and ε for the monomer. Dividing Eqs. (7.3) and (7.4) by molecular weight and considering the limit of high molecular weight (as in the case of a typical polymer) we have:

$$\frac{m}{MW} = A_m \tag{7.7}$$

$$\frac{\varepsilon}{k} = \frac{A_\varepsilon}{A_m} \tag{7.8}$$

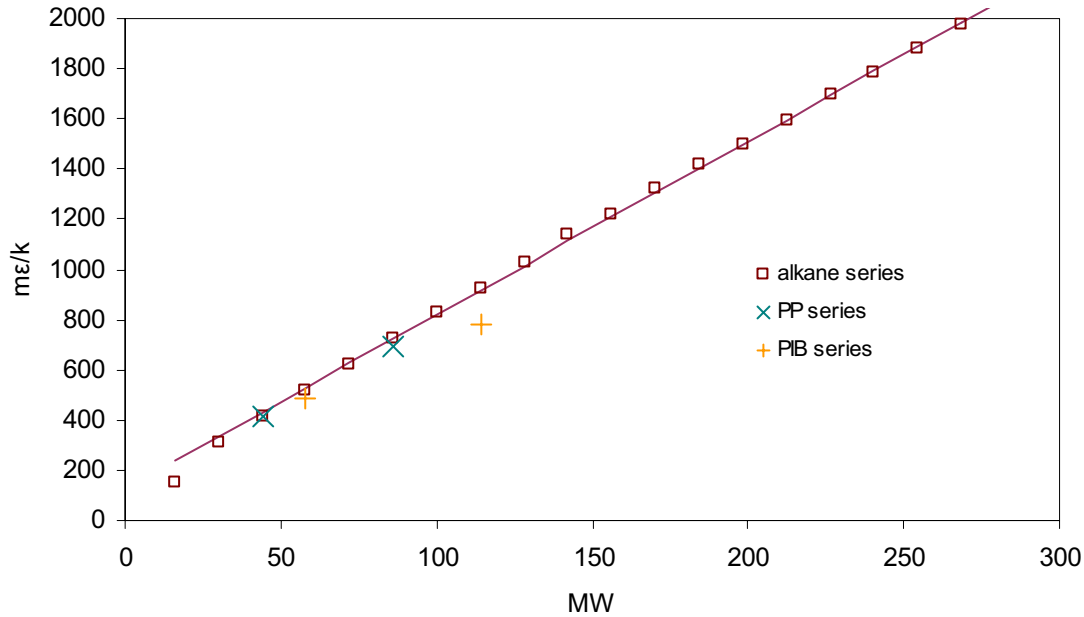

Figure 7.2. $m\varepsilon/k$ vs. molecular weight for the alkane, the PP and the PIB series. Points are PC-SAFT parameters reported by Gross and Sadowski[18], line is linear fit to the alkane series, excluding methane, described by Eqs. 7.1-7.2.

These simple expressions give the chain length and energy parameters of the polymer, respectively. We consider that the first member of the series of a given polymer is the saturated monomer of the repeating unit, e.g. ethylbenzene for PS, isobutane for PIB etc. (see Table 7.2). The last step of this method for obtaining pure-component polymer parameters is to fit the value of the remaining parameter (the size parameter, σ) to the pure polymer PVT data over a wide range of temperature and pressure.

We followed the above procedure for a variety of polymers and the results are summarized in Table 7.3. Our polymer database includes both polymers for which PC-SAFT parameters have already been published, as well as polymers for which parameters are reported here for the first time. In some cases this required obtaining parameters for monomers for which no PC-SAFT parameters are available. Table 7.4 lists the PC-SAFT pure-component parameters for these new monomers. These solvent parameters are

obtained in the usual way (from experimental liquid-density and vapor-pressure data extracted from the DIPPR correlations[16]).

Table 7.2 Corresponding monomer and values of the A_m and the A_ε parameters of Eqs. (7.3) and(7.4) for the studied polymers.

Polymer	Corresponding monomer	A_m	A_ε
PS	ethylbenzene	0.0205	7.1370
PIB	isobutane	0.0233	6.2351
PP	propane	0.0248	6.5615
PVAc	ethylacetate	0.0299	7.8219
PE	ethane	0.0254*	6.918*
PMMA	methylisobutyrate	0.0270	7.1443
PBMA	isobutylisobutyrate**	0.0241	6.3798
BR	2-butene	0.0263	7.3473
PMA	methylpropionate	0.0292	7.8337
PB	butane	0.0245	6.7506

*from the original extrapolation Eqs. (7.1) and (7.2) that are based on the n-alkane series from C_2 to C_{20}.
**isomer, since vapour pressure and liquid density data of butylisobutyrate are not available

Table 7.3 PC-SAFT parameters and average absolute deviation between calculated and experimental liquid density of the studied polymers. These parameters are obtained using the new pure-component extrapolation method.

Polymer	m/M	σ (A)	ε/k (K)	T range (K)	P range (bar)	AAD % ρ
PS	0.0205	4.152	348.2	390-470	1-1000	0.6
PIB	0.0233	4.117	267.6	325-385	1-1000	1.4
PP	0.0248	4.132	264.6	445-565	1-1000	1.1
PVAc	0.0299	3.463	261.6	310-370	1-800	0.4
PE	0.0254	4.107	272.4	410-470	1-1000	1.0
PMMA	0.0270	3.553	264.6	390-430	1-1000	1.0
PBMA	0.0241	3.884	264.7	310-470	1-1000	1.0
BR	0.0263	4.008	279.4	275-325	1-1000	1.0
PMA	0.0292	3.511	268.3	310-490	1-1000	0.5
PB	0.0245	4.144	275.5	410-510	1-1000	0.9

Table 7.4 PC-SAFT pure component parameters and average absolute deviation between calculated and experimental liquid densities and vapor pressures of solvents that have been used in this study for which parameters were not already available in the published literature.

solvent	MW	m	σ (A)	ε/k (K)	T range (K)	AAD % V_L	AAD %P^{sat}
Methylisobutyrate	102.133	3.6605	3.444	234.109	220-510	0.6	0.8
Isobutylisobutyrate	144.214	4.3798	3.7321	239.135	250-560	1.1	1.6
2-butene	56.107	2.3842	3.5640	226.296	150-390	0.4	0.7
heptanone	114.188	3.7965	3.6415	259.346	300-550	1.0	1.3

The new polymer parameters have been evaluated for a variety of polymer-solvent systems exhibiting LLE, some displaying both upper and lower critical solution temperature, as well as one VLE system (for PVAc, for which LLE experimental data were not available). The results are discussed below.

7.3. Results and Discussion

Figures 7.3 to 7.6 show results for simplified PC-SAFT using polymer pure-component parameters obtained from mixture data. Figures 7.3 and 7.4 show LLE in the system PS – acetone. In Figure 7.3 the polymer parameters are from method 1 (the original parameters from Gross and Sadowski). In Figure 7.4 the polymer parameters are obtained from method 4.

The correlations shown in Figure 7.3 give a good representation of the UCST curve at the two lower molecular weights, when different binary interaction parameters are used, but the molecular-weight sensitivity shown experimentally cannot be accounted for. In particular, the calculated LCST curves are almost independent of the molecular weight. For the same reason, it is not possible to obtain the experimentally observed hour-glass behavior for the highest molecular weight.

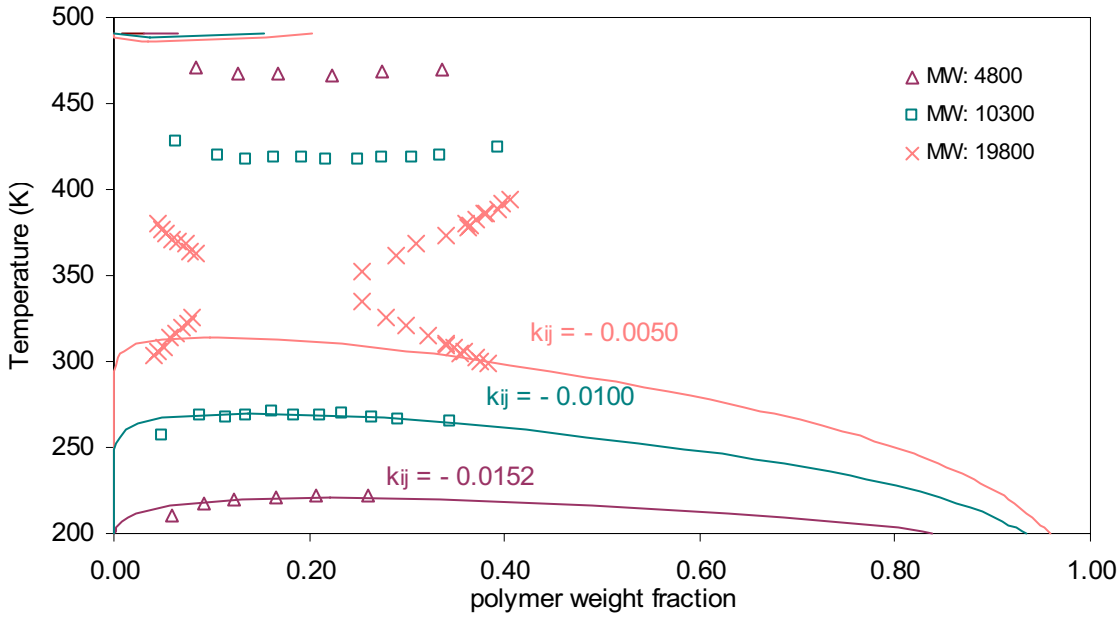

Figure 7.3 Liquid-liquid equilibrium in the system: PS – acetone. Experimental data are from Siow et al[19]. Lines are simplified PC-SAFT correlations with PS parameters obtained according to method 1 (Table 7.1).

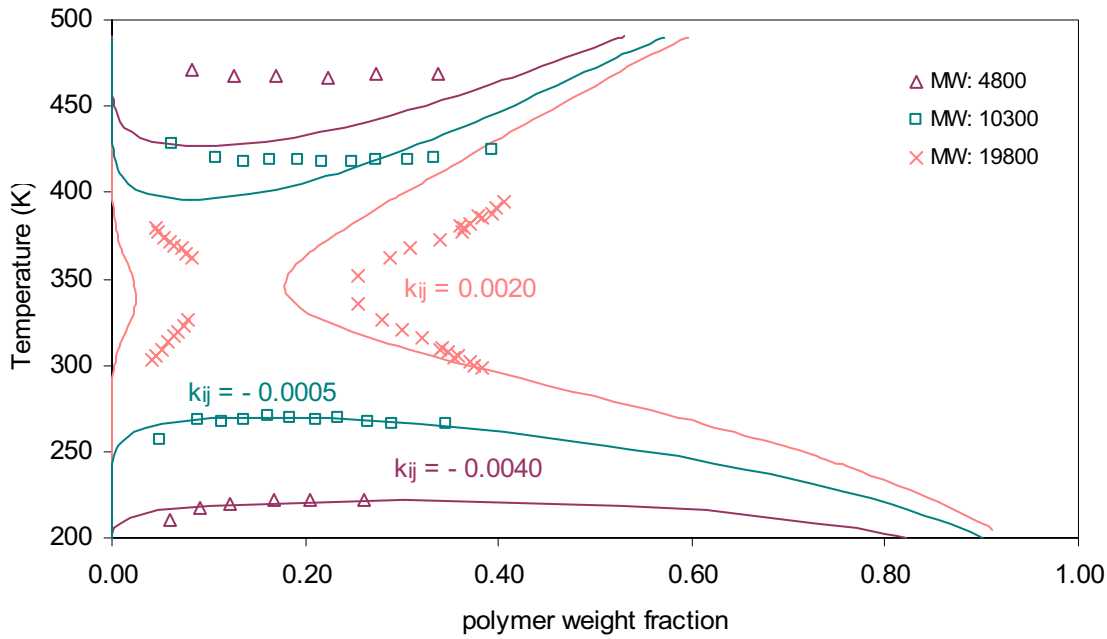

Figure 7.4 Liquid-liquid equilibrium in the system: PS – acetone. Experimental data are from Siow et al[19]. Lines are simplified PC-SAFT correlations with PS parameters obtained according to method 4 (Table 7.1).

Figure 7.4 shows the same system, but with the polymer parameters obtained using method 4 (regression including all three parameters for PS and the interaction parameters

for all binary pairs). The LLE diagram is now correlated much more successfully. The LCST curves now exhibit high sensitivity to the molecular weight and they eventually merge with the UCST curve at the highest molecular weight, with the narrowing of the hour-glass falling in the correct temperature range.

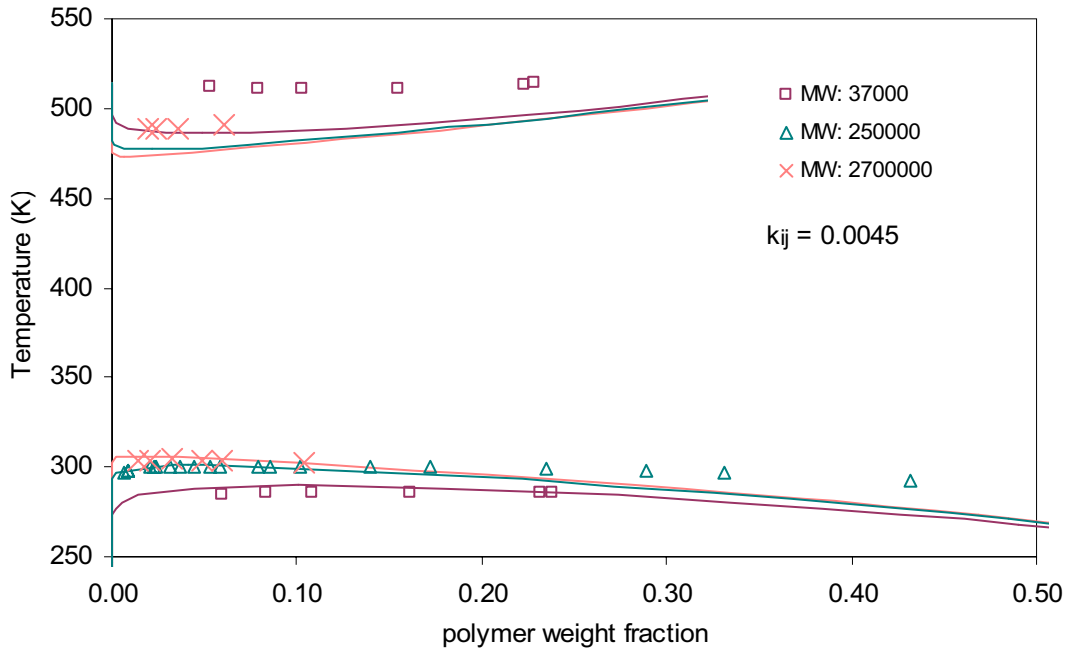

Figure 7.5 Liquid-liquid equilibrium in the system: PS – cyclohexane. Experimental data are from Saeki et al.[20] (MW=37000 and 2700000) and Shultz et al.[21] (MW=250000).Lines are simplified PC-SAFT correlations with PS parameters obtained according to method 1 (Table 7.1).

We now consider the same sets of polymer parameters with the solvent cyclohexane. Figure 7.5 shows that the original parameters for PS (obtained according to method 1 – these are the same parameters used in Figure 7.3) correlate quite satisfactorily both UCST and LCST with the same interaction parameter for all three molecular weights. This is not surprising, since experimental data in the system PS-cyclohexane were used to obtain the pure-component parameters for PS. On the other hand, Figure 7.6 shows that with the parameters obtained according to method 4 (which were so successful in the PS – acetone system of Figure 7.4), the flatness of the curves and the good correlation of the LCST are lost.

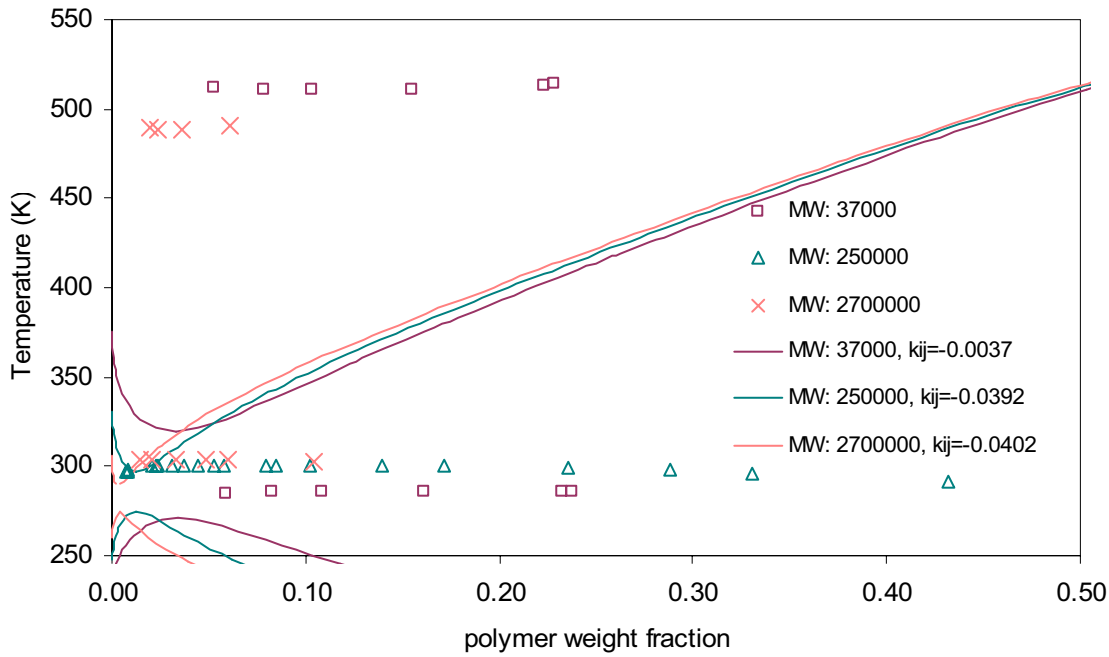

Figure 7.6 Liquid-liquid equilibrium in the system: PS – cyclohexane. Experimental data are from Saeki et al.[20] (MW=37000 & 2700000) and Shultz et al.[21] (MW=250000).Lines are simplified PC-SAFT correlations with PS parameters obtained according to method 4 (Table 7.1).

None of the parameter sets obtained from mixture data (methods 1 to 5) are capable of correlating simultaneously the PS – acetone and the PS – cyclohexane binary LLE diagrams. Parameters that give the experimentally indicated hour-glass behavior for PS-acetone at high PS molecular weight, fail in representing the flatness of the PS-cyclohexane phase diagrams and vice versa.

We now consider the performance of parameters obtained using only pure-component data, as discussed in section 7.2.2 above. Parameters for a number of polymers obtained this way are listed in Table 7.3. The new approach provides sets of pure-component polymer parameters that yield satisfactory results and combine the following advantages:

1. Both m and ε are based on extrapolation equations, different for each homologous series. All that is required are the PC-SAFT parameters of the monomer (the first component of the series), which are either already available or easily regressed from readily available vapor pressures and liquid densities, e.g. generated from the DIPPR correlations[16].

2. The energetic parameter is always higher than that of the corresponding monomer. This is the expected physical behavior. The segments in the polymer are bigger than for the monomer, so there are consequently fewer segments in the polymer per molecular weight unit. This means that each segment carries more of the polymer's interaction energy.
3. The average percent absolute deviations between calculated and experimental liquid densities are very low.
4. The segment parameter, σ has a value of around 4.1Å for many of the studied polymers (apart from PVAc, PMA, PMMA and PBMA, due to the high m value), which has been shown to give good results for polymers[1].

The performance of simplified PC-SAFT using the pure-component polymer parameters estimated with the procedure discussed above has been tested against binary polymer-solvent mixtures exhibiting LLE and VLE phase behaviour. The results are shown in Figures 7.7 – 7.17.

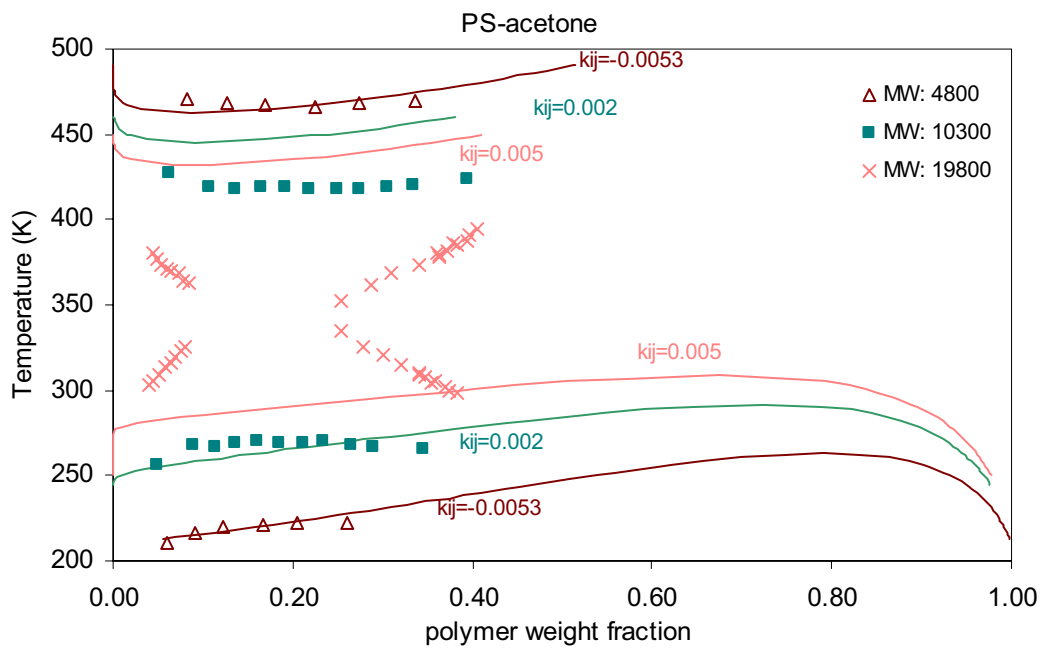

Figure 7.7. Liquid-liquid equilibrium in the system: PS – acetone. Experimental data are from Siow et al[19]. Lines are simplified PC-SAFT correlations with PS parameters obtained according to the proposed novel method (Table 7.3).

Figures 7.7 and 7.8 show the same PS systems as above, this time with PS parameters obtained based on our here proposed method. Figure 7.7 shows the PS – acetone solution, for which the correlation with simplified PC-SAFT is similar to the one shown in Figure 7.3 (that is, with PS parameters according to method 1). Still the hourglass behaviour cannot be captured, even though the model now shows a MW sensitivity. The UCST is satisfactory correlated with low values for the interaction parameter.

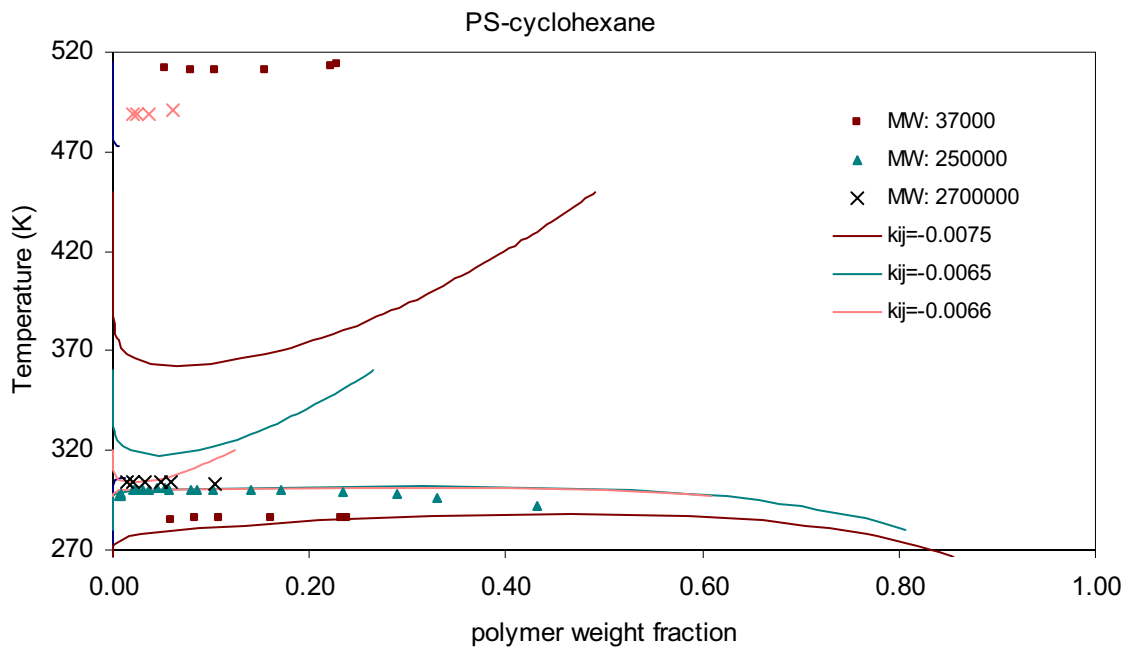

Figure 7.8. Liquid-liquid equilibrium in the system: PS – cyclohexane. Experimental data are from Saeki et al[20] (MW=37000 and 2700000) and Shultz et al. [21] (MW=250000).Lines are simplified PC-SAFT correlations with PS parameters obtained according to the proposed novel method (Table 7.3).

Figure 7.8 shows the PS-cyclohexane solution, for which the UCST is well described, although, - unlike as shown in Figure 7.5- slightly different values for the optimum interaction parameter are now necessary.

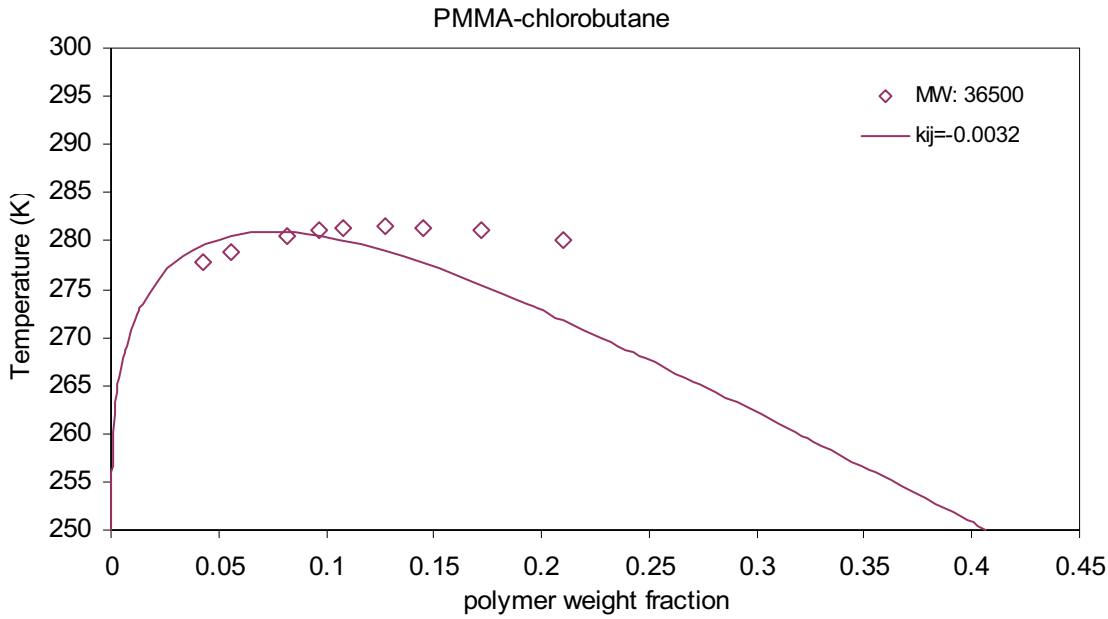

Figure 7.9 Liquid-liquid equilibrium in the system PMMA (MW=36500) – chlorobutane. Experimental data are from Wolf et al.[22] Line is simplified PC-SAFT correlation with k_{ij} = - 0.0032. This system displays upper critical solution temperature (UCST) behavior.

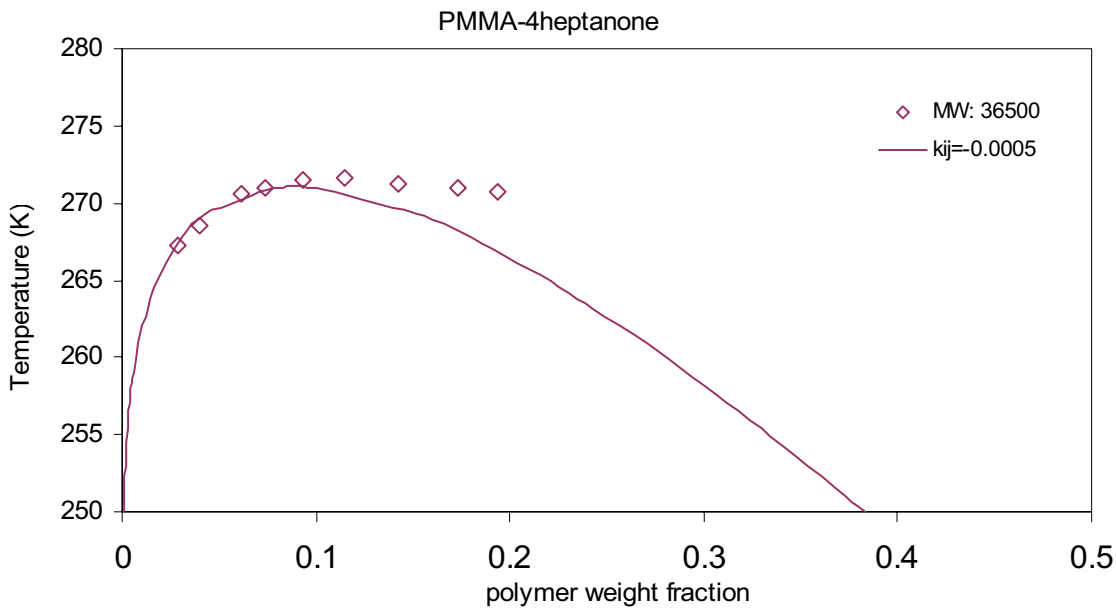

Figure 7.10 Liquid-liquid equilibrium in the system: PMMA (MW=36500) – 4heptanone. Experimental data are from Wolf et al.[22] Line is simplified PC-SAFT correlation with k_{ij} = - 0.0005. This system displays upper critical solution temperature (UCST) behavior.

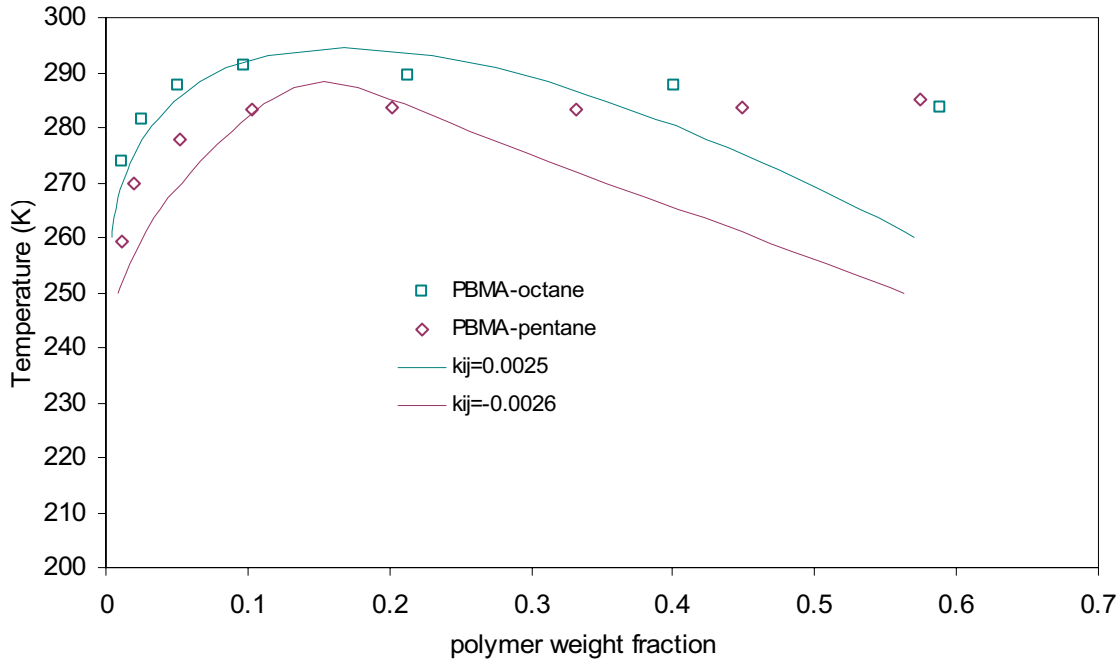

Figure 7.11 Liquid-liquid equilibrium in the systems PBMA – pentane and PBMA – octane. Experimental data are from Saraiva et al.[23] Lines are simplified PC-SAFT correlations with k_{ij} = - 0.0026 (PBMA – pentane) and k_{ij} = 0.0025 (PBMA – octane). The molecular weight of PBMA is 11600. These systems display upper critical solution temperature (UCST) behavior.

Figures 7.9 and 7.10 show two different PMMA solutions with chlorobutane and 4-heptanone respectively, that display upper critical solution temperature behavior. Both systems are satisfactorily correlated with quite small, negative interaction parameters. However, in both cases, the flatness of the experimental data towards the higher polymer weight fractions cannot be accurately described.

The same behavior is shown in Figure 7.11 for two binary solutions of PBMA with pentane and octane, respectively. Both systems display upper critical solution temperature behavior and are very well correlated with small values of the interaction parameters.

Figure 7.12 shows the system PP-diethylether at two different molecular weights of the polymer, which displays lower critical solution temperature behavior. The prediction and correlation with simplified PC-SAFT is very good at the highest molecular weight of the polymer but less so at the lower one.

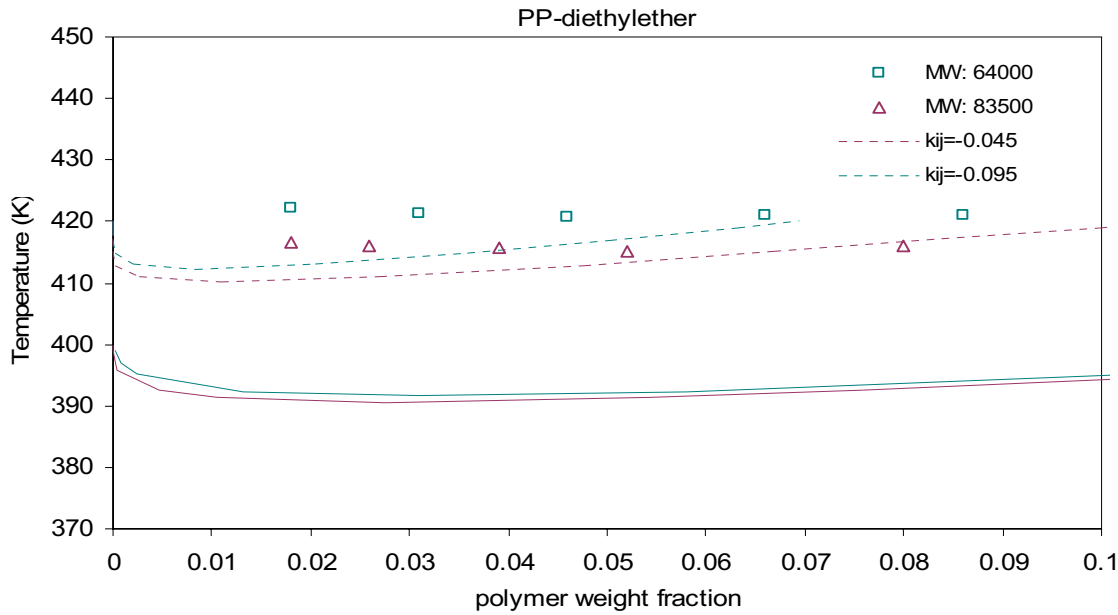

Figure 7.12 Liquid-liquid equilibrium in the system PP – diethylether. Experimental data are from Cowie et al.[24] Solid lines are simplified PC-SAFT predictions and dashed lines are correlations with k_{ij} = - 0.045 (MW = 83500) and k_{ij} = - 0.095 (MW = 64000). This system displays lower critical solution temperature (LCST) behavior.

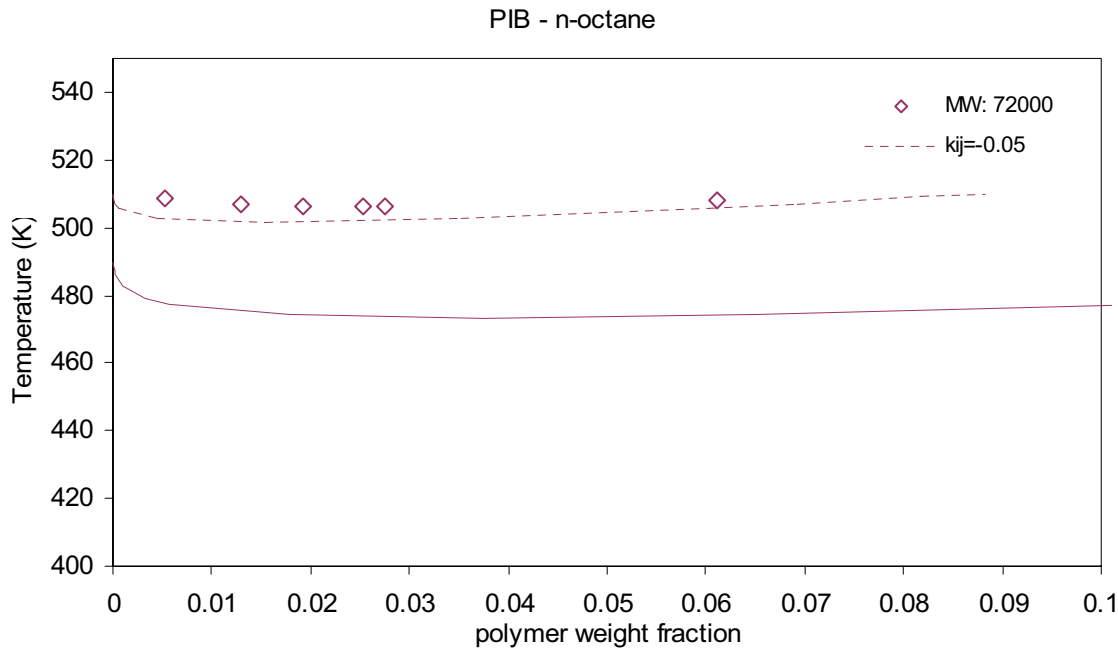

Figure 7.13 Liquid-liquid equilibrium in the system: PIB (MW=72000) – n-octane. Experimental data are from Liddell et al.[25] Lines are simplified PC-SAFT prediction and correlation with k_{ij} = - 0.05. This system displays lower critical solution temperature (LCST) behavior.

Figure 7.13 shows the nearly athermal PIB-octane system, which also displays lower critical solution temperature behavior and is very well predicted ($k_{ij} = 0$) and correlated with simplified PC-SAFT.

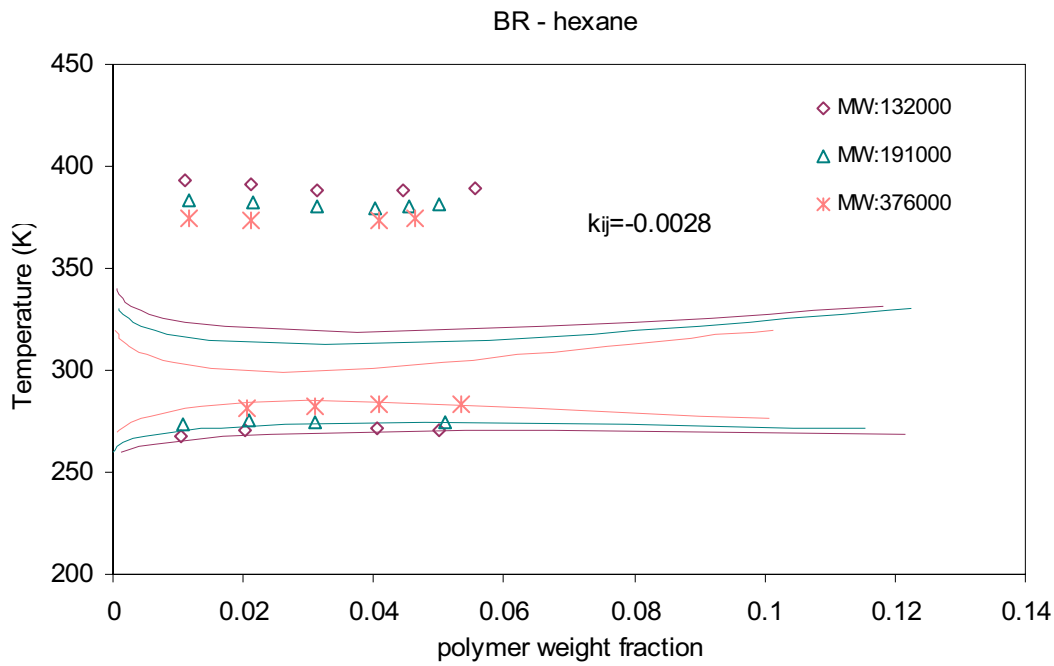

Figure 7.14 Liquid-liquid equilibrium in the system: BR – hexane. Experimental data are from Delmas et al.[26] Lines are simplified PC-SAFT correlation with k_{ij} = - 0.0028, the same for all three molecular weights (132000, 191000 and 376000). This system displays both upper and lower critical solution temperature behavior.

Figure 7.14 shows a more complicated phase diagram, where the BR solution in hexane displays both upper and lower phase split. Unfortunately, even though the correlation of the UCST is possible with a single interaction parameter for the three molecular weights, the LCST is only qualitatively described.

The system BR-2methylhexane, is shown in Figure 7.15, which displays both upper and lower critical solution behavior. The correlated curve successfully matches the experimental UCST data with a small negative binary interaction parameter, but greatly underestimates the LCST.

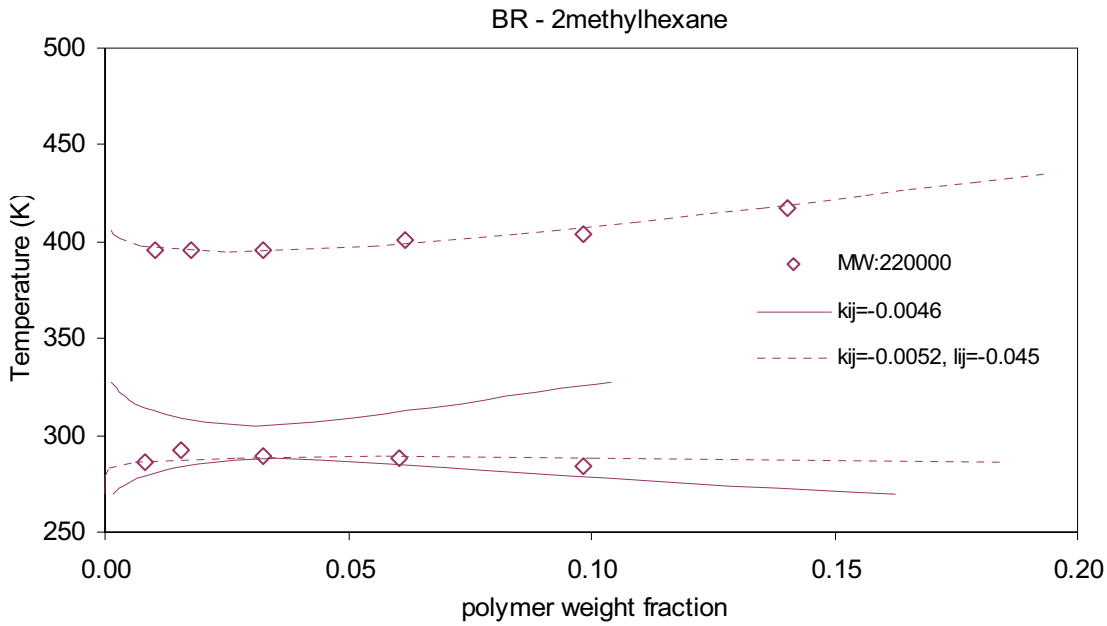

Figure 7.15 Liquid-liquid equilibrium in the system: BR (MW = 220000) – 2-methylhexane. Experimental data are from Delmas et al.[26] Solid lines are simplified PC-SAFT correlation with k_{ij} = - 0.0046. Dashed lines are simplified PC-SAFT correlation with k_{ij} = - 0.0052 and l_{ij} = - 0.045. This system displays both upper and lower critical solution temperature behavior.

As has been observed and discussed previously[17], generally the LCST behavior is rather insensitive to the binary interaction parameter. This is because LCST behavior is usually observed at elevated temperatures, where the effect of the energy parameters is not as marked. Since k_{ij} is a correction to the cross energy parameter ε_{ij}, changing the k_{ij} value generally has only a marginal effect in the LCST. But if a binary interaction parameter l_{ij} is applied in the calculation of the average-segment parameter:

$$\sigma_{ave} = \frac{(\sigma_i + \sigma_j)}{2} \cdot (1 - l_{ij}) \qquad (7.9)$$

as shown in the same figure by the dashed line , then the LCST curve can be successfully fitted as well, without affecting considerably the fit of the UCST (the k_{ij} has to change from -0.0046 to -0.0052).

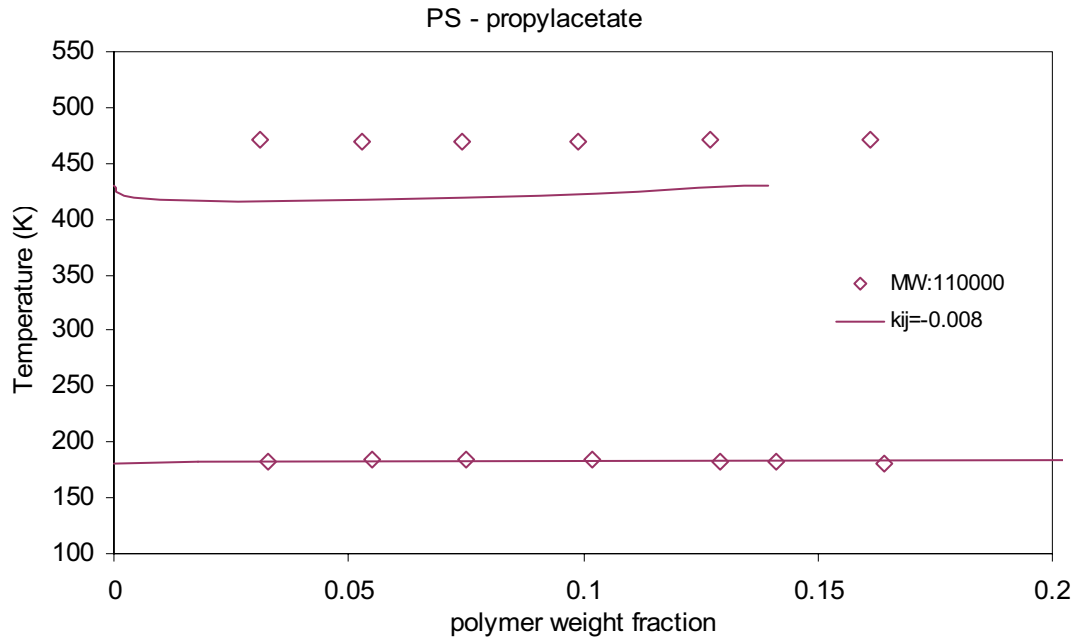

Figure 7.16 Liquid-liquid equilibrium in the system: PS (MW = 110000) – propylacetate. Experimental data are from Saeki et al.[27] Lines are simplified PC-SAFT correlation with k_{ij} = - 0.008. This system displays both upper and lower critical solution temperature behavior.

On the other hand, in the system PS-propylacetate shown in Figure 7.16, the simplified PC-SAFT correlates both UCST and LCST with great accuracy, using the same binary interaction parameter.

Finally, in Figure 7.17, the vapor-liquid phase diagram for the system PVAc-2-methyl-1-propanol is presented at three different temperatures. A comparison with experimental VLE data was chosen in this case for the evaluation of the PVAc parameters, since LLE data of this polymer is not available. This system is very well predicted by simplified PC-SAFT at all three temperatures. Deviations increase, however, as the temperature increases. In general, comparisons with LLE data provide a much stricter test of a model than comparison with VLE data.

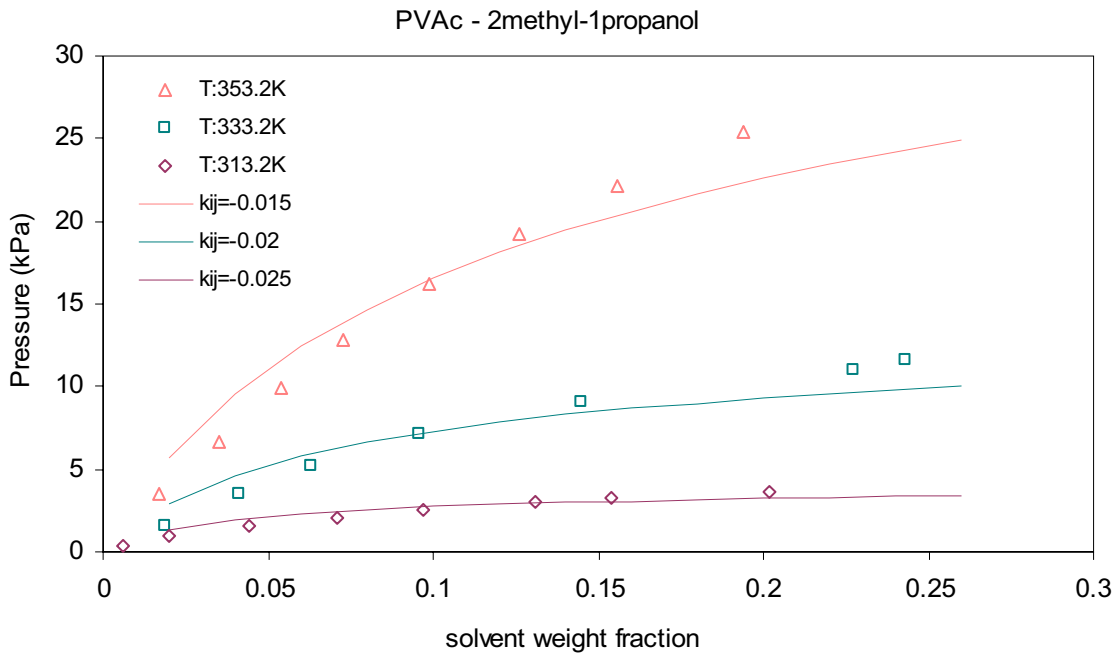

Figure 7.17 Vapour-liquid equilibrium in the system: PVAc (MW = 110000) – 2methyl-1propanol. Experimental data are from Wibawa et al.[28] Lines are simplified PC-SAFT correlations at three different temperatures with k_{ij} = - 0.025 (T = 313.2 K), k_{ij} = - 0.020 (T = 333.2 K) and k_{ij} = - 0.015 (T = 353.2 K).

7.4 Conclusions

In this work we have evaluated a number of different methods of obtaining pure-component polymer parameters from mixture data and pure polymer liquid density data. We have found that these methods do not lead to a unique set of polymer parameters, but depend greatly on the number and the type of the selected binary data used in the regression. Based on this observation, we have directed our efforts to developing a procedure that is only dependent on pure polymer PVT data and extrapolation equations that relate the parameters of the monomer to those of the polymer for each homologous series. This novel method is easy to implement, even in the cases of relatively complex polymers. We have obtained parameters for a number of polymers of varying complexity. Using these parameters, simplified PC-SAFT can successfully describe vapor-liquid and liquid-liquid equilibria in a wide variety of binary polymer-solvent mixtures.

References

1. J. Gross and G. Sadowski, Modeling Polymer Systems Using the Perturbed-Chain Statistical Association Fluid Theory Equation of State. *Ind. Eng. Chem. Res.* **2002,** *41*, 1084.
2. I. A. Kouskoumvekaki, G. Krooshof, M. L. Michelsen and G. M. Kontogeorgis, Application of the simplified perturbed chain SAFT equation of state to the vapor liquid equilibria of binary and ternary mixtures of polyamide 6 with several solvents. *Ind. Eng. Chem. Res*. **2003,** *accepted for publication.*
3. J. Gross, O. Spuhl, F. Tumakaka, and G. Sadowski, Modeling Copolymer Systems Using the Perturbed-Chain SAFT Equation of State. *Ind. Eng. Chem. Res.* **2003,** *42*, 1266.
4. I. A. Kouskoumvekaki, N. von Solms, M. L. Michelsen and G. M. Kontogeorgis, Application of a Simplified Perturbed Chain SAFT Equation of State to Complex Polymer Systems, *Fluid Phase Equilibria,* **2004**, 215, 71..
5. Th. G. Scholte, Determination of Thermodynamic Parameters of Polymer-Solvent Systems by Light Scattering. *Eur. Polym. J.* **1970,** *6*, 1063.
6. C. E. H. Bawn, and M. A. Wajid, High Polymer Solutions. Part 7. Vapor Pressure of Polystyrene Solutions in Acetone, Chloroform and Propyl Acetate. *Trans. Faraday Soc*. **1956,** *52*, 1658.
7. E. C. Baughan, The Absorption of Organic Vapors by Thin Films of Polystyrene. *Trans. Faraday Soc*. **1948,** *44*, 495.
8. I. Noda, Y. Higo, N. Ueno and T. Fujimoto, Semi dilute Region for Linear Polymers in Good Solvents. *Macromolecules* **1984,** *17*, 1055.
9. P. J. T. Tait and A. M. Abushihada, Comparative Studies on the Use of Gas Chromatographic and Vapor Pressure Techniques for the Determination of the Interaction Parameter. *Polymer* **1977,** *18*, 810.
10. Th. G. Scholte, Determination of Thermodynamic Parameters of Polymer-Solvent Systems from Sedimentation-Diffusion Equilibrium in the Ultracentrifuge. *J. Polym. Sci.*, **1970,** *Part A-2 8*, 841.

11. C. E. H. Bawn, R. F. J. Freeman and A. R. Kamaliddin, High Polymer Solutions. Part 1. Vapour Pressure of Polystyrene Solutions. *Trans. Faraday Soc.* **1950,** *46*, 677.
12. Y. Iwai and Y. Arai, Measurement and Prediction of Solubilities of Hydrocarbon Vapors in Molten Polymers. *J. Chem. Engr. Japan* **1989,** *22*, 155.
13. T. Sako, A. H. Wu and J. M.Prausnitz, A Cubic Equation Of State For High-Pressure Phase-Equilibria Of Mixtures Containing Polymers And Volatile Fluids. *J Appl Polym Sci* **1989,** 38, 1839.
14. N. Von Solms, M. L. Michelsen and G. M. Kontogeorgis, Computational and physical performance of a modified PC-SAFT equation of state for highly asymmetric and associating mixtures. *Ind. Eng. Chem. Res.* **2003,** *42,* 1098.
15. J. W. Jiang and J. M. Prausnitz, Equation of State for Thermodynamic Properties of Chain Fluids Near-to and Far-from the Vapor-Liquid Critical Region. *J. Chem. Phys.* **1999,** *111,* 5964.
16. Design Institute for Physical Property Data (DIPPR), AIChE, New York, **1989**.
17. N. Von Solms, I. A. Kouskoumvekaki, T. Lindvig, M. L. Michelsen and G. M. Kontogeorgis, A novel approach to liquid-liquid equilibrium in polymer systems with application to simplified PC-SAFT. *Fluid Phase Equilib*. **2003,** *submitted for publication*
18. Gross; J.; Sadowski, G.; Perturbed-Chain SAFT: An equation of state based on a perturbation theory for chain molecules. *Ind. Eng. Chem. Res.* **2001,** *40*, 1244.
19. K. S. Siow, G. Delmas and D. Patterson, Cloud-point curves in polymer solutions with adjacent upper and lower critical solution temperatures. *Macromolecules* **1972,** *5*, 29.
20. S. Saeki, N. Kuwahara, S. Konno and M. Kaneko, Upper and lower critical solution temperatures in polystyrene solutions. *Macromolecules* **1973,** *6*, 246.
21. A. R. Shultz and P. J. Flory, Phase equilibria in polymer-solvent systems. *J.Amer.Chem.Soc.* **1952,** *74*, 4760.
22. B. A. Wolf and G. Blaum, Measured and calculated solubility of polymers in mixed solvents: monotony and cosolvency. *J.Polym. Sci.* **1975,** *13*, 1115.

23. A. Saraiva, M. Pleuss, O. Persson and Aa. Fredenslund, A Study of the Miscibility/Immiscibility Phenomena in Low Molecular Weight Poly (n-butylmethacrylate)/Single Solvent Systems by Thermo-optical Analysis by Microscopy. SEP 9412, (1994) (Internal Report, Department of Chemical Engineering, Technical University of Denmark).
24. J. M. G. Cowie and I. J. McEwen, Lower critical solution temperatures of polypropylene solutions. *J. Polym. Sci., Polym. Phys. Ed. 12,* **1974,** 441.
25. A. H. Liddell and F. L. Swinton, Thermodynamic properties of some polymer solutions at elevated temperatures. *Disc. Farad. Soc.* **1970,** *49*, 115.
26. G. Delmas and P. D. Saint-Romain, Upper and lower critical solution temperatures in butadiene-alkane systems – Effect of surface-to-volume ratio of polymer. *European Polymer Journal* **1974,** *10*, 1133.
27. S. Saeki, S. Konno, N. Kuwahara, M. Nakata and M. Kaneko, Upper and Lower Critical Solution Temperatures in Polystyrene Solutions. III. Temperature Dependence of the X1 Parameter. *Macromolecules* **1974,** *7*, 521.
28. G. Wibawa, R. Hatano, Y. Sato, S. Tikishima and H. Masuoka, Solubilities of 11 polar organic solvents in four polymers using the piezoelectric-quartz sorption method. *J. Chem. Eng. Data,* **2002,** *47*, 1022.

Chapter 8

Conclusions and Future Challenges with the Application of Simplified PC-SAFT Equation of State in Polymer Systems

The primary target of this thesis was to investigate and improve the performance of activity coefficient models and equations of state in describing fluid phase equilibria in polymer mixtures. The applied modification on the Entropic-FV model corrects the underestimation of the original model in the prediction of both activity coefficients of the solvent and the solute in infinite dilution, as well as at intermediate concentrations. The simplified PC-SAFT equation of state has shown to be applicable in binary and ternary polymer mixtures exhibiting either VLE or LLE behavior. It has been able to handle polymers with complex structure and solutions with polar or associating solvents. The overall good performance of simplified PC-SAFT in the studied areas provides solid ground for extending the evaluation of the model in other areas of industrial interest, such as multicomponent polymer systems, polymer blends and aqueous polymer solutions. Some preliminary results are presented here as a starting point for further research on the subject.

8.1 Conclusions

The main conclusions that can be derived from this thesis are the following:

Free-volume activity coefficient models such as the modified Entropic-FV can be very useful in polymer systems since they provide fast and reliable qualitative answers that are based in limited experimental input.

On the other hand, equations of state can be applied to both low and high pressures and also for properties other than phase equilibria. They normally require pure-component parameters that are characteristic for each component and are usually determined from pure-component properties.

One promising family of equations of state is SAFT and its many versions, which have a strong theoretical basis on statistical mechanics. PC-SAFT has been chosen for evaluation and further improvement, as the one that had been specifically developed to describe polymer chains.

The simplified PC-SAFT equation of state has been applied in a variety of binary polymer mixtures exhibiting VLE behavior, where it has shown very successful performance in polymer systems with either non-associating or associating solvents.
It has been further applied in LLE of polymer systems, successfully predicting and correlating the phase behavior in many systems exhibiting either upper or lower or both upper and lower critical solution temperatures.
The application of simplified PC-SAFT in the manufacturing process of polyamide 6 has revealed the ability of the model to describe pure-component properties, as well as binary and ternary systems of complex polymers, even when experimental data for these systems are limited. It has also shown that the model can treat systems with compounds that self- and cross-associate, even though the correlation of the experimental data is not always accurate and the interaction parameters may get quite high values.
Finally, in the area of pure-polymer parameters, efforts have been made towards developing a method that is only based on pure-component properties and extrapolation equations. The good preliminary results that are presented in the previous chapter broaden the applicability of the model to polymers, for which, pure-component parameters were not available.

8.2 Future Challenges with the Application of Simplified PC-SAFT Equation of State in Polymer Systems

The overall good performance of simplified PC-SAFT in the studied areas provides solid ground for extending the evaluation of the model in other areas. Some characteristic applications of industrial interest, which thermodynamic models often fail to describe satisfactorily or have not been as yet evaluated, are:

a) Multicomponent polymer systems
b) Polymer blends
c) Aqueous polymer solutions

Furthermore, an evaluation of simplified PC-SAFT in calculating various properties (beyond phase equilibria) may provide an indication of the capabilities or limitations of

the model. If, for example, simplified PC-SAFT describes successfully the (infinite dilution) activity coefficient of the solute (γ_2^{∞}), then one can be optimistic about the model's performance in LLE calculations in polymer mixtures, where the activities of all the components in the mixture need to be obtained with accuracy. Additionally, calculation of pure-component properties like the polymer packing fraction gives useful indications regarding the partial calculations that are performed by the model and the influence on them of the separate contribution terms.

Some characteristic results are going to be briefly presented in the following paragraphs, with the primary aim being an inspiration for further work on the extension and improvement of simplified PC-SAFT in polymer systems.

8.2.1 Multicomponent Polymer Systems

Calculation of phase equilibria for multicomponent polymeric systems is becoming increasingly important due to the numerous industrial processes and products involving such systems (paints, pharmaceuticals etc.).

When it comes to multicomponent vapor-liquid and liquid-liquid equilibria of polymer – mixed solvent mixtures, the data available in the literature are very scarce and, so far, have not been used methodically to test thermodynamic models[1].

As shown in Figure 8.1, zero interaction parameters are not expected to represent the experimental data with good accuracy, but serve to give an indication of the sensitivity of the model to the value of the binary interaction parameters.

Simplified PC-SAFT becomes a predictive model for multicomponent systems, when all binary interaction parameters are obtained from correlations of experimental binary VLE or LLE data. For the system shown in the figure, the interaction parameters between the polymer and the two solvents are obtained from the correlations of the corresponding binary systems. The third interaction parameter (chlorobutane – 4-heptanone) has been fitted to the experimental ternary data, due to lack of experimental binary LLE data for this system.

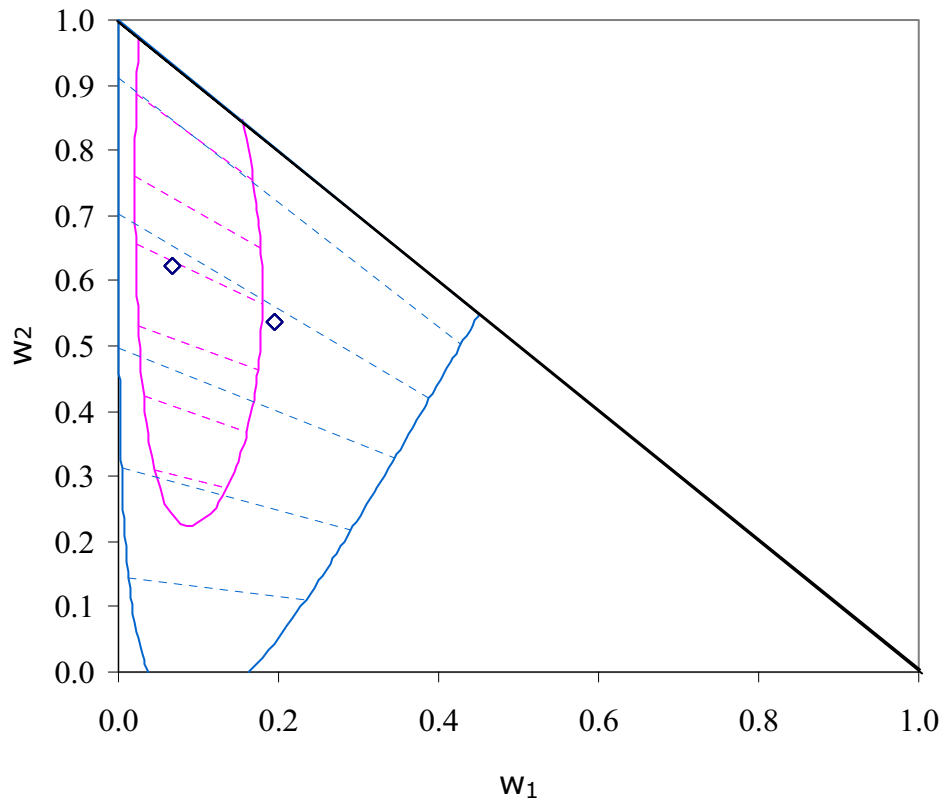

Figure 8.2 Ternary LLE-diagram for polymethylmethacrylate (1) – chlorobutane (2) – 4-heptanone (3) at 277 K. Blue curve: $k_{ij} = 0$. Red curve: Correlation with $k_{12} = -0.0032$, $k_{13} = -0.0005$ and $k_{23} = -0.002$. Experimental data from Wolf et al.[4].

8.2.2 Polymer Blends

A polymer blend is a mixture containing two or more polymers and, perhaps, an additional component to enhance polymer compatibility. Blends, unlike polymer solutions, consist of components that do not differ significantly in size. Therefore, they have similar free volumes, i.e. degrees of expansion and when immiscibility occurs, it is mainly due to enthalpic differences.

A correlation of the polystyrene / butadiene rubber blend is shown in Figure 8.2 for four different molecular weight combinations of the two polymers in the blend.

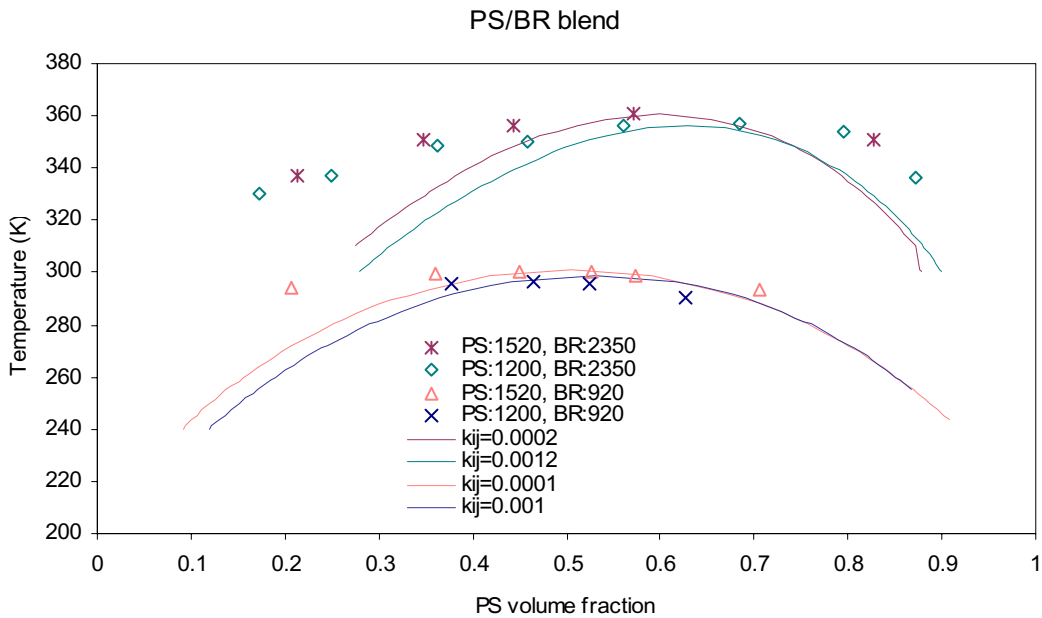

Figure 8.2 Cloud point curves for polystyrene – butadiene rubber blends. Experimental data are from Rostami et al.[3]. Lines are correlations with simplified PC-SAFT.

Unfortunately, the model does not have the necessary molecular weight sensitivity and a different value for the interaction parameter is needed for each system. Especially for the lower molecular weight of polystyrene, the sensitivity of the model is weaker, which is the reason for the higher values of the optimum interaction parameters. Furthermore, the flatness of the experimental points cannot be matched by the correlated curve.

8.2.3 Aqueous Polymer Solutions

Water is a strongly hydrogen-bonding compound, which can both self- and cross-associate in the presence of a second hydrogen-bonding compound. Due to its unique nature, water has been causing many difficulties to equations of state and there are still contradictory views regarding the estimation of the pure-component parameters for water. As mentioned by Gross et al.[2], it is a considerable simplification to assume the 2B model for water, since there are indications that it is best represented with a four-site treatment. Therefore, in complex aqueous polymer solutions such a simplification could play a

major role. Furthermore, one more difficulty arises from the fact that only a few polymers are soluble in water, so experimental data are very limited.

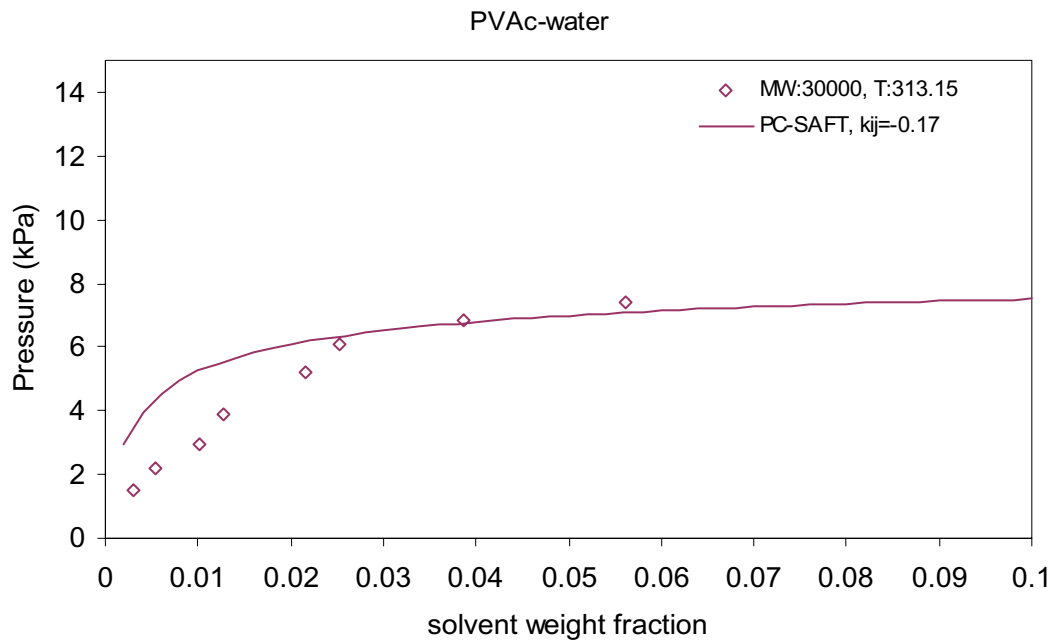

Figure 8.3 Pressure-weight fraction plot of polyvinylacetate – water at T = 313.15 K. Poly(vinylacetate) molecular weight = 30 000. Comparison of experimental data with the correlation of simplified PC-SAFT. ($k_{ij} = 0.17$). Experimental data are from the DECHEMA electronic database[5].

Figure 8.3 presents the vapor-liquid equilibria in the system poly(vinylacetate) – water. Simplified PC-SAFT needs a high, negative interaction parameter in order to be able to calculate pressures in the same range as the experimental. Even so, the pressure at low concentrations of water cannot be matched, which indicates that the model predicts a weaker hydrogen-bonding than what the experimental pressure shows.

8.2.4 Infinite Dilution Activity Coefficient Calculations

Calculations of infinite dilution activity coefficients of the solute (heavy component) in a binary mixture are very important when it comes to the description of liquid-liquid equilibria. Accurate calculations of γ_2^{∞} indicate that a possible good behavior of the

model in liquid-liquid equilibria is not due to cancellation of errors, but due to the ability of the model to calculate with accuracy the activities of both components.

Infinite dilution activity coefficient calculations have been performed with the simplified PC-SAFT equation of state, in athermal mixtures of long-chain hydrocarbons (C_{12}-C_{36}) and PE in short-chain ones (hexane, cyclohexane and heptane).

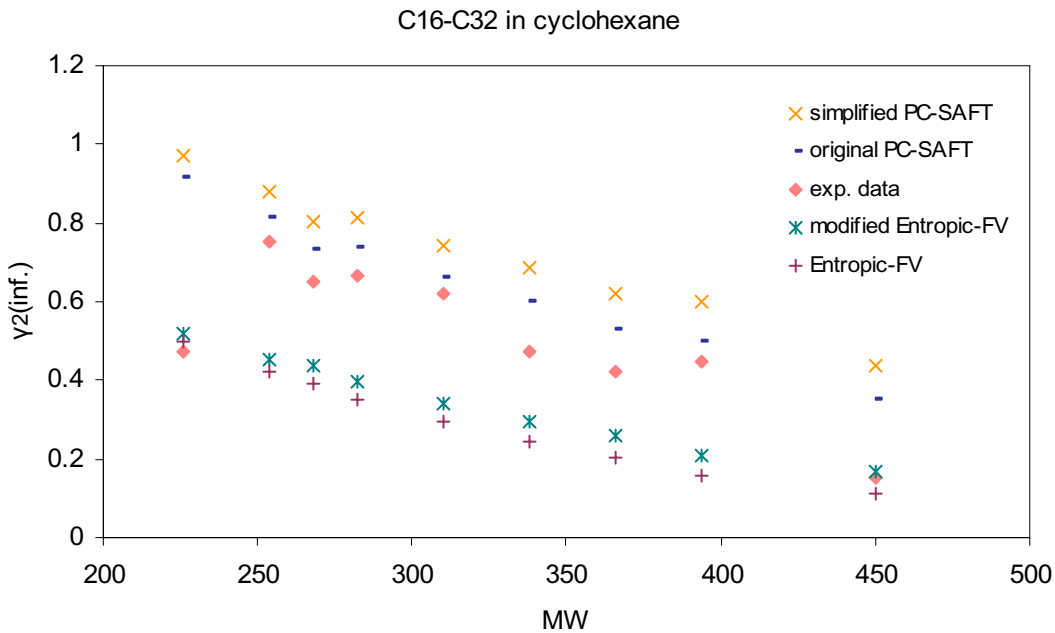

Figure 8.4 Experimental[6,7] and predicted infinite dilution activity coefficients of binary solutions of alkanes C_{16} to C_{30} in cyclohexane.

The purpose is to evaluate the chain-term of simplified PC-SAFT and its ability to describe the activity of a long-chain molecule.

For comparison purposes, calculations with the original PC-SAFT equation of state, the Entropic-FV activity coefficient model and the modified (a = 1.2) Entropic-FV are presented as well (these two models are presented in detail in chapter 2).

All calculations have been performed with the interaction parameter of simplified PC-SAFT set to zero.

Table 8.1 Absolute average deviation (%) between experimental and calculated infinite dilution activity coefficients.

% AAD	**Simplified PC-SAFT**	**Original PC-SAFT**	**Entropic-FV**	**Modified EFV**
$C_{12} - C_{36}$ in hexane	16	8	29	12
PE in hexane	24	15	7	-
$C_{16} - C_{32}$ in cyclohexane	30	15	50	41
PE in cyclohexane	3	10	31	-
$C_{18} - C_{36}$ in heptane	15	6	31	13
PE in heptane	12	2	4	-
$C_4 - C_{10}$ in C_{30}	5	3	7	5
$C_4 - C_{10}$ in C_{36}	6	2	8	5

The conclusions of this evaluation can be summarized as follows:

- The simplified PC-SAFT equation of state gives γ_2^∞ values that are not far from the experimental ones, apart from the cases that very low values of γ_2^∞ have been measured (e.g. C_{24} in C_6, C_{16} in cC_6 and C_{32} in C_7). This is a positive result, considering the difficulty of the studied systems (previous calculations with a variety of activity coefficient models had shown increased deviations in these systems).
- The trend with the MW of the calculated values with the simplified PC-SAFT is in agreement both with the experimental data and with the rest of the evaluated models.
- The simplified PC-SAFT overestimates the experimental data in all cases. Using the original PC-SAFT improves the results, as it is shown in Figures 8.4 – 8.5 and Table 8.1. As expected, the deviation of the simplified PC-SAFT from the original PC-SAFT is more apparent when the MW of the long-chain increases, or in other words, when the size-difference between the two components is greater.
- Table 8.1 shows that the best performance in the majority of the studied systems is of the original PC-SAFT, while the highest deviations are those of Entropic-FV.

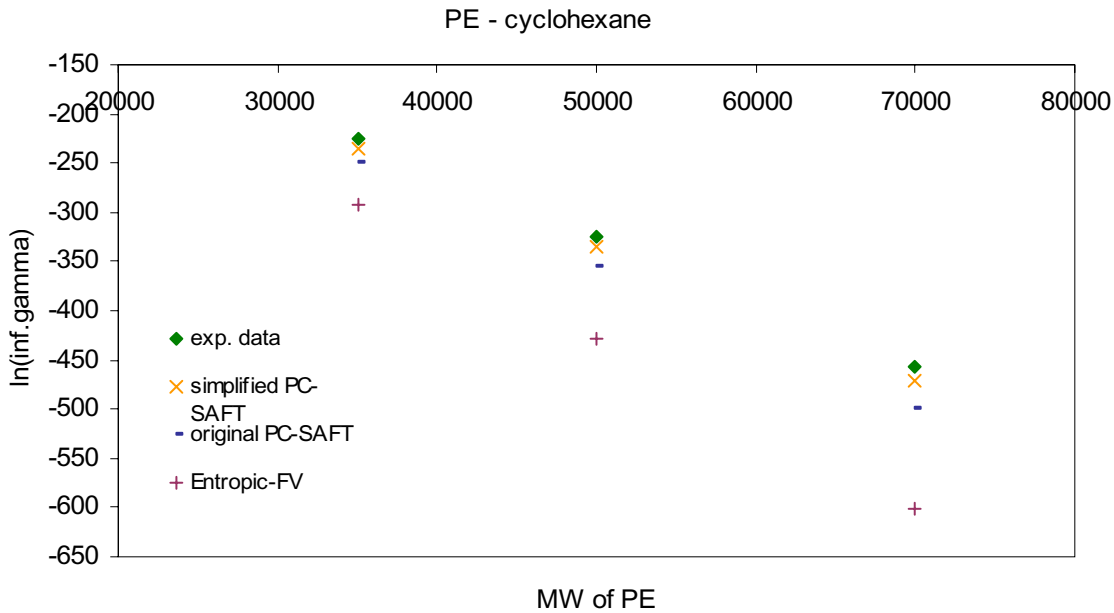

Figure 8.5 Infinite dilution activity coefficient of polyethylene in cyclohexane. Experimental data are data from molecular simulation studies[8].

8.2.5 Polymer Packing Fraction

Calculations with simplified PC-SAFT show that the polymer packing fraction $\zeta_3 = \frac{\pi\rho}{6}\sum_i x_i m_i d_i^3$ is largely independent of the segment number m and it reaches a constant value for very large values of m. This is shown in Figure 8.6, where polystyrene is taken as an example.

Moreover, as shown in Figure 8.7, in the limit of large m, there is a 'universal' density function that holds for all polymers, in the sense that the packing fraction ζ, at low pressure is a unique function of a reduced temperature, T* = T/ε, where ε is the energy parameter. Evaluating and tabulating this function should facilitate the determination of pure component parameters.

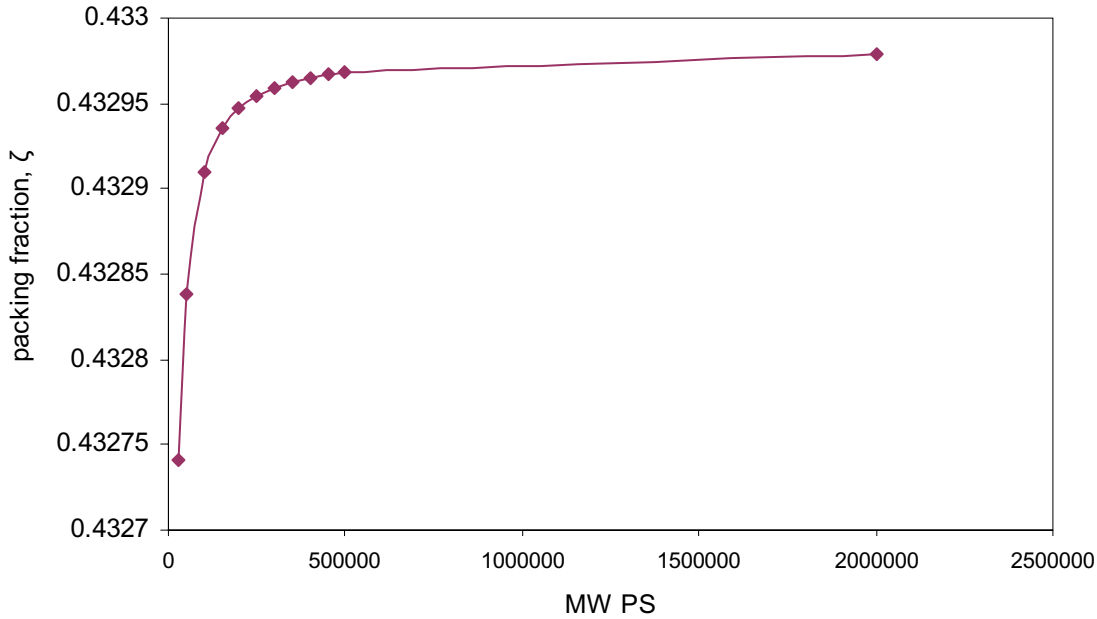

Figure 8.6 Packing fraction versus molecular weight of polystyrene, as calculated by simplified PC-SAFT.

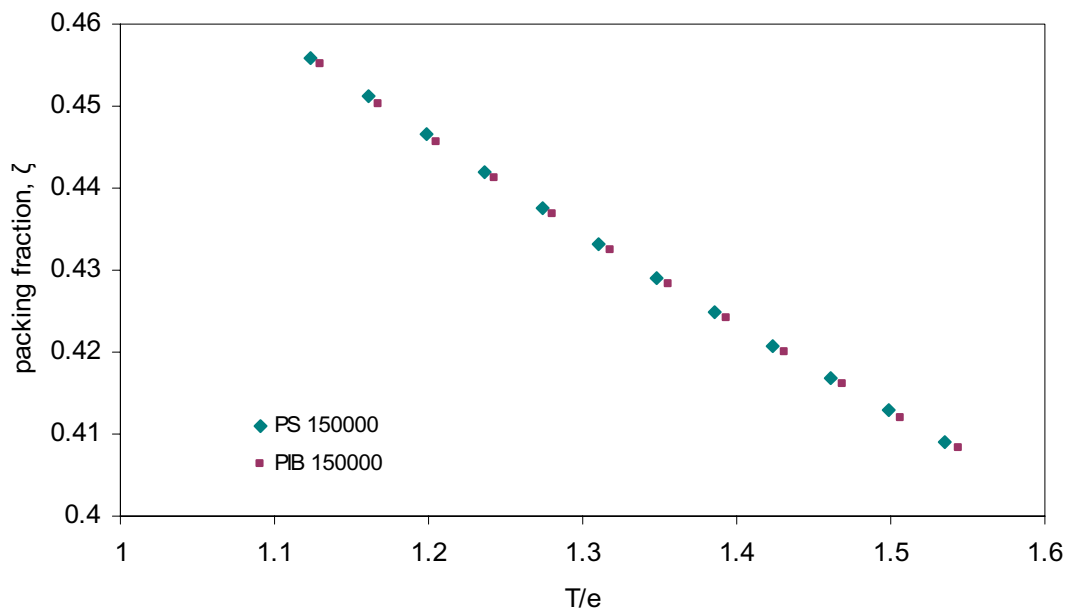

Figure 8.7 Packing fraction – reduced temperature plot for polystyrene (15.000) and polyisobutylene (15.000), as calculated by simplified PC-SAFT.

References:

1. T. Lindvig, M. L. Michelsen and G. M. Kontogeorgis, Phase Equilibria for Complex Polymer Solutions, *Fluid Phase Equilibria,* **2002,** 194-197, 663.
2. J. Gross and G. Sadowski, Application of the Perturbed-Chain SAFT Equation of State to Associating Systems, *Ind. Eng. Chem. Res.* **2002,** 41, 5510.
3. S. Rostami and D. J. Walsh, Simulation of Upper and Lower Critical Phase-Diagrams for Polymer Mixtures at Various Pressures, *Macromolecules,* **1985**, 6, 1228.
4. B. A. Wolf and G. Blaum, Measured and calculated solubility of polymers in mixed solvents: monotony and cosolvency, *J.Polym. Sci.* **1975,** 13, 1115.
5. W. Hao, H. S. Elbro and P. Alessi, Polymer Solution Data Collection Part 1-2, DECHEMA, Chemistry Data Series XIV, **1992.**
6. K. Kniaz, Influence of Size and Shape Effects on the Solubility of Hydrocarbons. The Role of the Combinatorial Entropy, *Fluid Phase Equilibria*, **1991,** 68, 35.
7. K. Kniaz, Solubility of normal-Docosane in normal-Hexane and Cyclohexane, *J. Chem. Eng. Data,* **1991**, 36, 471.
8. G.M. Kontogeorgis, E. Voutsas and D. Tassios, A Molecular Simulation-Based Method for the Estimation of Activity Coefficients for Alkane Solutions, *Chem. Eng. Science*, **1996,** 51 (12), 3247.

List of Symbols

$\tilde{a}$:	reduced Helmholtz energy
A:	Helmholtz energy
A_i, B_i, C_i:	GCVOL parameters
b:	co-volume parameter
B:	second virial coefficient
c:	Flory-FV constant
C:	concentration
d:	density / temperature-dependent segment diameter (Å)
f:	Newton target function
g:	radial distribution function, Gibbs Energy
k:	Boltzmann's constant (1.38066 x 10^{-23} J K^{-1}), binary interaction parameter
m:	segment number
M:	molecular weight
Mn:	number-average molecular weight
Mw:	weight-average molecular weight
N_A:	Avogadro's number
N:	total number of molecules
P:	Pressure
P^{sat}:	saturated vapor pressure
R:	ideal gas constant
r:	radial distance
T:	temperature
u:	composition variable
V:	molar volume
$\tilde{V}$:	reduced volume
V^*:	hard-core volume
V_L:	liquid volume
V^0_g:	specific retention volume at 0^o C
x:	mole fraction

X:	fraction of unbonded sites
u:	internal energy
w:	weight fraction

Greek letters

α*:*	activity
γ:	mole based activity coefficient
Δ*:*	strength of association
ε*:*	dispersion energy parameter, association energy (J)
ζ*:*	partial volume fraction
η*:*	volume fraction
κ*:*	association volume
ρ:	(molar) density
σ*:*	segment diameter (Å)
φ:	(volume/segment) fraction
$\hat{\phi}$ *:*	fugacity coefficient
Ω:	weight based activity coefficient
Ω_1^{∞}	infinite dilution weight based activity coefficient

Polymer Names

AR:	Benzyl Ether dendrimer with aromatic termination ring
BR:	Butadiene rubber (polybutadiene)
C12:	Benzyl Ether dendrimer with dodecyl alkane termination ring
HDPE:	High density polyethylene
PAM:	Polyamide
PAMAM:	Poly(amidoamine) dendrimer
PBMA:	Poly (butyl methacrylate)
PDMS:	Polydimethylsiloxane
PE:	Polyethylene
PIB:	Polyisobutylene
PMA:	Poly (methyl acrylate)

PMMA: Poly (methylmethacrylate)

PP: Polypropylene

PS: Polystyrene

PVAc: Polyvinylacetate

PVAL: Poly(vinyl alcohol)

Abbreviations

A: A-series poly(imidoamine) dendrimer

AAD: Absolute Average Deviation

ACM: Activity Coefficient Model

CL: ε-caprolactam

EoS: Equation of State

FV: Free Volume

G: Generation

GC: Group Contribution

GCLF: Group Contribution Lattice Fluid

LCST: Lower critical solution temperature

LCT: Lattice Cluster Theory

LLE: Liquid-Liquid equilibria

MEK: Methyl ethyl ketone

MW: Molecular Weight

N: number

n: normal

PC-SAFT: Perturbed Chain Statistical Associating Fluid Theory

PVT: Pressure Volume Temperature

SAFT: Statistical Associating Fluid Theory

SINC: Solvent Induced Crystallization

SLE: Solid-Liquid Equilibria

UCST: Upper critical solution temperature

UNIFAC: Universal Functional Activity Coefficient

UNIQUAC: Universal quasi-chemical

vdW: van der Waals

VLE: Vapor-Liquid equilibria

VR: Variable range

ZM: Zhong-Masuoka

Subscripts

1: component index for the solvent/short chain alkane

2: component index for the polymer/long chain alkane

cal: calculated value

DP: data points

exp: experimental value

i,j: component indices

f: free volume

m: mixture

pred: predicted

s: saturated

sys: systems

w: van der Waals

Superscripts

1,2: component 1,2

A,B: association site indices

assoc: association

comb: combinatorial

comb-fv: combinatorial-free volume

disp: dispersion

eq: equilibrium

fv: free volume

hc: hard chain

hs: hard sphere

id: ideal

mix:	mixing
res:	residual
sp:	spinodal
∞*:*	infinite dilution
⁻*:*	average quantity

List of Captions

Figure 4.5 Pressure-weight fraction plot of polystyrene – butyl acetate at T = 293 K Polystyrene molecular weight = 500 000. Comparison of experimental data with the predictions of simplified PC-SAFT. The interaction parameter k_{ij}=0. Experimental data are from Baughan.

Figure 4.6 Pressure-weight fraction plot of poly(vinyl acetate) with 1-propylamine and 2-propylamine at T = 313 K. Poly(vinyl acetate) molecular weight = 170 000. Experimental data are from Kokes et al.: The dashed line is the simplified PC-SAFT prediction ($k_{ij} = 0$) for the PVAc – 1-propylamine system, the solid line is the simplified PC-SAFT prediction ($k_{ij} = 0$) for the PVAc – 2-propylamine system and the dotted line is the simplified PC-SAFT correlation ($k_{ij} = 0.01$) for the PVAc – 2-propylamine system.

Figure 4.7 Pressure-weight fraction plot of poly(vinyl acetate) – 2-methyl-1-propanol at T = 313 K. Comparison of experimental data with prediction ($k_{ij} = 0$) and correlation ($k_{ij} = -0.012$) results of simplified PC-SAFT. Poly(vinyl acetate) molecular weight = 167 000. Experimental data are from Wibawa et al.

Figure 4.8 Pressure-weight fraction plot of poly(vinyl acetate) – 2-propanol at T = 333 K. Comparison of experimental data with prediction ($k_{ij} = 0$) and correlation ($k_{ij} = -0.025$) results of simplified PC-SAFT. Poly(vinyl acetate) molecular weight = 167 000. Experimental data are from Wibawa et al.

Figure 5.1 Illustration of the method of alternating tangents. The solid line is the system methanol (1)-cyclohexane (2). The dotted line is the system PS (1)-acetone. The two spinodal points are indicated by x_1^{sp1} and x_1^{sp2}. The equilibrium (binodal) points are indicated by x_1^{eq1} and x_1^{eq2}. Starting from a spinodal point, the equilibrium values can be calculated by solving for only one point at a time.

Figure 5.2 Liquid-liquid equilibrium in the system polystyrene-cyclohexane for polystyrene molecular weight 1.270.000, showing both the spinodal and binodal (co-existence) curves. The two curves converge at the critical solution temperature.

Figure 5.3 Liquid-liquid equilibrium in the system polystyrene-methyl cyclohexane for different molecular weights of polystyrene. The experimental data are from Dobashi et al. The lines are simplified PC-SAFT correlations with $k_{ij} = 0.0065$.

Figure 5.4 Liquid-liquid equilibrium in the system polyisobutylene-diisopropyl ketone. Experimental data are from Shultz and Flory. Lines are simplified PC-SAFT correlations with $k_{ij} = 0.0053$, the same at all three molecular weights.

Figure 5.5 Liquid-liquid equilibrium in the system HDPE-*n*-heptane. The experimental data are from Hamada et al. The lines are simplified PC-SAFT correlations with $k_{ij} = -0.006$ for the molecular weights shown. This system displays lower critical solution temperature (LSCT) behavior.

Figure 5.6 Liquid-liquid equilibrium for HDPE with *n*-alkanols. The experimental data are from Nakajima et al. Lines are simplified PC-SAFT correlations for each of the five solvents (pentanol highest, nonanol lowest). Polymer molecular weight is 20.000.

Figure 5.7 Liquid-liquid equilibrium in the system HDPE – butyl acetate. The system displays both upper and lower critical solution temperature behaviour. The experimental data are from Kuwahara et al. for molecular weights 13.600 and 64.000. Lines are simplified PC-SAFT correlations with $k_{ij} = 0.0156$ for both molecular weights.

Figure 5.8 Liquid-liquid equilibrium in the system PP – diethyl ether. The system displays lower critical solution temperature behavior. The experimental data are from Cowie and McEwen. The lines are simplified PC-SAFT predictions ($k_{ij} = 0$) for the four molecular weight shown.

Figure 6.1 Vapor-liquid equilibrium in the system ε-caprolactam – octane. Experimental data are from Schmelzer et al. Dashed lines are simplified PC-SAFT predictions with ε-caprolactam taken as nonassociating and solid lines are simplified PC-SAFT predictions with ε-caprolactam taken as associating. Both predictions are at 363.15 and 383.15 K.

Figure 6.2 Vapor-liquid equilibrium in the system ε-caprolactam – decane. PC-SAFT parameters for ε-caprolactam are $m = 4.0737$, $\varepsilon / k = 335.374$ K, $\sigma = 3.3551$ Å, $\varepsilon^{AB} = 1623$ K and $\kappa^{AB} = 0.003995$. Experimental data are from Schmelzer et al. Solid lines are simplified PC-SAFT predictions and the dashed line is the simplified PC-SAFT correlation with $k_{ij} = 0.005$.

Figure 6.3 Vapor-liquid equilibrium in the system ε-caprolactam – dodecane. PC-SAFT parameters for ε-caprolactam are $m = 4.0737$, $\varepsilon / k = 335.374$ K, $\sigma = 3.3551$ Å, $\varepsilon^{AB} = 1623$ K and $\kappa^{AB} = 0.003995$. Experimental data are from Schmelzer et al. Solid lines are simplified PC-SAFT predictions and the dashed line is simplified PC-SAFT correlation with $k_{ij} = 0.005$.

Figure 6.4 Prediction of the liquid-liquid equilibrium in the system ε-caprolactam – dodecane. PC-SAFT parameters for ε-caprolactam are $m = 4.0737$, $\varepsilon / k = 335.374$ K, $\sigma = 3.3551$ Å, $\varepsilon^{AB} = 1623$ K and $\kappa^{AB} = 0.003995$.

Figure 6.5 Vapor-liquid equilibrium in the system ε-caprolactam – acetic acid. PC-SAFT parameters for ε-caprolactam are $m = 4.3000$, $\varepsilon / k = 330.112$ K and $\sigma = 3.3014$ Å. Acetic acid parameters are $m = 1.3403$, $\varepsilon / k = 211.59$ K, $\sigma = 3.8582$ Å, $\varepsilon^{AB} = 3044.4$ K and $\kappa^{AB} = 0.07555$. Experimental data are from Stoeck et al. Lines are simplified PC-SAFT correlations with $k_{ij} = -0.30$ at each of the three temperatures.

Figure 6.6 Vapor-liquid equilibrium in the system ε-caprolactam – acetic acid. PC-SAFT parameters for ε-caprolactam are $m = 4.0737$, $\varepsilon / k = 335.374$ K, $\sigma = 3.3551$ Å, $\varepsilon^{AB} = 1623$ K and $\kappa^{AB} = 0.003995$. Acetic acid parameters are $m = 1.3403$, $\varepsilon / k = 211.59$ K, $\sigma = 3.8582$ Å, $\varepsilon^{AB} = 3044.4$ K and $\kappa^{AB} = 0.07555$. The Elliot's rule was used as the combining rule for the cross-association strength. Experimental data are from Stoeck et al. Lines are simplified PC-SAFT correlations with $k_{ij} = -0.28$ at each of the three temperatures.

Figure 6.7 Vapor-liquid equilibrium in the system ε-caprolactam – acetic acid. PC-SAFT parameters for ε-caprolactam are $m = 4.0737$, $\varepsilon / k = 335.374$ K, $\sigma = 3.3551$ Å, $\varepsilon^{AB} = 1623$ K and $\kappa^{AB} = 0.003995$. The parameters for acetic acid are $m = 2.3420$, $\varepsilon / k = 199.901$ K, $\sigma = 3.1850$ Å, $\varepsilon^{AB} = 2756.7$ K and $\kappa^{AB} = 0.2599$. Elliot's rule was used as the combining rule for the cross-association strength. Experimental data are from Stoeck et al. Lines are simplified PC-SAFT correlations with $k_{ij} = -0.20$ at each of the three temperatures.

Figure 6.8 Vapor-liquid equilibrium in the system ε-caprolactam – water. PC-SAFT parameters for ε-caprolactam are $m = 4.0737$, $\varepsilon / k = 335.374$ K, $\sigma = 3.3551$ Å, $\varepsilon^{AB} = 1623$ K and $\kappa^{AB} = 0.003995$. The Elliot's rule was used as the combining rule for the cross-association strength. Experimental data are from Hahn et al. and Puffr et al. Lines are simplified PC-SAFT correlations with $k_{ij} = -0.07$ at each of the two temperatures.

Figure 6.9 Liquid volume of polyamide 6. PC-SAFT parameters for polyamide 6 are $m / MW = 0.036$, $\varepsilon / k = 335.374$ K, $\sigma = 3.3551$ Å, $\varepsilon^{AB} = 1623$ K and $\kappa^{AB} = 0{,}003995$ (prediction-dashed lines) and $m / MW = 0.036$, $\varepsilon / k = 335.374$ K, $\sigma = 3.38$ Å, $\varepsilon^{AB} = 1623$ K and $\kappa^{AB} = 0.003995$ (correlation – solid lines). Comparison of experimental data with the prediction and correlation results with PC-SAFT.

Figure 6.10 Vapor liquid equilibrium in the system polyamide 6 - water. PC-SAFT parameters for polyamide 6 are $m/MW = 0.036$, $\varepsilon/k = 335.374\,\text{K}$, $\sigma = 3.38\,\text{Å}$, $\varepsilon^{AB} = 1623\,\text{K}$ and $\kappa^{AB} = 0.003995$. Experimental data are from Fukumoto et al. Lines are simplified PC-SAFT correlations with temperature-dependent k_{ij}'s.

Figure 6.11 Comparison of experimental pressure data with prediction and correlation results obtained with PC-SAFT at 543.15K, for the ternary system polyamide 6 (1) – ε-caprolactam (2) – water (3) (binary interaction parameters are: k_{12}=-0.07, k_{13}=-0.04, k_{23}=-0.011 (prediction) and k_{12}=-0.07, k_{13}=-0.11, k_{23}=-0.011 (correlation).

Figure 6.12 Comparison of experimental data for the mole fraction of ε-caprolactam in the vapor phase with correlation results obtained with PC-SAFT at 543.15K for the ternary system polyamide 6 (1) - ε-caprolactam (2) – water (3). (The binary interaction parameters are: k_{12}=-0.07, k_{13}=-0.11, k_{23}=-0.011).

Figure 6.13 Comparison of experimental data for the mole fraction of water in the vapor phase with correlation results obtained with PC-SAFT at 543.15K for the ternary system polyamide 6 (1) - ε-caprolactam (2) – water (3). (The binary interaction parameters are: k_{12}=-0.07, k_{13}=-0.11, k_{23}=-0.011).

Figure 6.14 Liquid volume of polyamide 11. PC-SAFT parameters for polyamide 11 are $m/MW = 0.036$, $\varepsilon/k = 335.374\,\text{K}$, $\sigma = 3.51\,\text{Å}$, $\varepsilon^{AB} = 1623\,\text{K}$ and $\kappa^{AB} = 0.003995$. Comparison of experimental data with correlation results obtained with PC-SAFT.

Figure 6.15 Optimum σ values against the weight fraction of linear polyethylene segment in the polyamide chain for seven polyamide types.

Figure 7.1 m vs. molecular weight for the alkane, the PP and the PIB series. Points are PC-SAFT parameters reported by Gross and Sadowski, line is linear fit to the alkane series, excluding methane, described by Eqs. 7.1-7.2.

Figure 7.2 $m\varepsilon/k$ vs. molecular weight for the alkane, the PP and the PIB series. Points are PC-SAFT parameters reported by Gross and Sadowski, line is linear fit to the alkane series, excluding methane, described by Eqs. 7.1-7.2.

Figure 7.3 Liquid-liquid equilibrium in the system: PS – acetone. Experimental data are from Siow et al. Lines are simplified PC-SAFT correlations with PS parameters obtained according to method 1 (Table 7.1).

Figure 7.4 Liquid-liquid equilibrium in the system: PS – acetone. Experimental data are from Siow et al. Lines are simplified PC-SAFT correlations with PS parameters obtained according to method 4 (Table 7.1).

Figure 7.5 Liquid-liquid equilibrium in the system: PS – cyclohexane. Experimental data are from Saeki et al. (MW=37000 and 2700000) and Shultz et al. (MW=250000).Lines are simplified PC-SAFT correlations with PS parameters obtained according to method 1 (Table 7.1).

Figure 7.6 Liquid-liquid equilibrium in the system: PS – cyclohexane. Experimental data are from Saeki et al. (MW=37000 & 2700000) and Shultz et al. (MW=250000).Lines are simplified PC-SAFT correlations with PS parameters obtained according to method 4 (Table 7.1).

Figure 7.7 Liquid-liquid equilibrium in the system: PS – acetone. Experimental data are from Siow et al. Lines are simplified PC-SAFT correlations with PS parameters obtained according to the proposed novel method (Table 7.3).

Figure 7.8 Liquid-liquid equilibrium in the system: PS – cyclohexane. Experimental data are from Saeki et al. (MW=37000 and 2700000) and Shultz et al. (MW=250000).Lines are simplified PC-SAFT correlations with PS parameters obtained according to the proposed novel method (Table 7.3).

Figure 7.9 Liquid-liquid equilibrium in the system PMMA (MW=36500) – chlorobutane. Experimental data are from Wolf et al. Line is simplified PC-SAFT correlation with k_{ij} = - 0.0032. This system displays upper critical solution temperature (UCST) behavior.

Figure 7.10 Liquid-liquid equilibrium in the system: PMMA (MW=36500) – 4heptanone. Experimental data are from Wolf et al. Line is simplified PC-SAFT correlation with k_{ij} = - 0.0005. This system displays upper critical solution temperature (UCST) behavior.

Figure 7.11 Liquid-liquid equilibrium in the systems PBMA – pentane and PBMA – octane. Experimental data are from Saraiva et al. Lines are simplified PC-SAFT correlations with k_{ij} = - 0.0026 (PBMA – pentane) and k_{ij} = 0.0025 (PBMA – octane). The molecular weight of PBMA is 11600. These systems display upper critical solution temperature (UCST) behavior.

Figure 7.12 Liquid-liquid equilibrium in the system PP – diethylether. Experimental data are from Cowie et al. Solid lines are simplified PC-SAFT predictions and dashed lines are correlations with k_{ij} = - 0.045 (MW = 83500) and k_{ij} = - 0.095 (MW = 64000). This system displays lower critical solution temperature (LCST) behavior.

Figure 7.13 Liquid-liquid equilibrium in the system: PIB (MW=72000) – n-octane. Experimental data are from Liddell et al. Lines are simplified PC-SAFT prediction and correlation with k_{ij} = - 0.05. This system displays lower critical solution temperature (LCST) behavior.

Figure 7.14 Liquid-liquid equilibrium in the system: BR – hexane. Experimental data are from Delmas et al. Lines are simplified PC-SAFT correlation with k_{ij} = - 0.0028, the same for all three molecular weights (132000, 191000 and 376000). This system displays both upper and lower critical solution temperature behavior.

Figure 7.15 Liquid-liquid equilibrium in the system: BR (MW = 220000) – 2-methylhexane. Experimental data are from Delmas et al. Solid lines are simplified PC-SAFT correlation with k_{ij} = - 0.0046. Dashed lines are simplified PC-SAFT correlation with k_{ij} = - 0.0052 and l_{ij} = - 0.045. This system displays both upper and lower critical solution temperature behavior.

Figure 7.16 Liquid-liquid equilibrium in the system: PS (MW = 110000) – propylacetate. Experimental data are from Saeki et al. Lines are simplified PC-SAFT correlation with k_{ij} = - 0.008. This system displays both upper and lower critical solution temperature behavior.

Figure 7.17 Vapour-liquid equilibrium in the system: PVAc (MW = 110000) – 2methyl-1propanol. Experimental data are from Wibawa et al. Lines are simplified PC-SAFT correlations at three different temperatures with k_{ij} = - 0.025 (T = 313.2 K), k_{ij} = - 0.020 (T = 333.2 K) and k_{ij} = - 0.015 (T = 353.2 K).

Figure 8.2 Ternary LLE-diagram for polymethylmethacrylate (1) – chlorobutane (2) – 4-heptanone (3) at 277 K. Blue curve: k_{ij} = 0. Red curve: Correlation with k_{12} = -0.0032, k_{13} = -0.0005 and k_{23} = -0.002. Experimental data from Wolf et al.

Figure 8.2 Cloud point curves for polystyrene – butadiene rubber blends. Experimental data are from Rostami et al. Lines are correlations with simplified PC-SAFT.

Figure 8.3 Pressure-weight fraction plot of polyvinylacetate – water at T = 313.15 K. Poly(vinylacetate) molecular weight = 30 000. Comparison of experimental data with the correlation of simplified PC-SAFT. ($k_{ij} = 0.17$). Experimental data are from the DECHEMA electronic database.

Figure 8.4 Experimental and predicted infinite dilution activity coefficients of binary solutions of alkanes C_{16} to C_{30} in cyclohexane.

Figure 8.5 Infinite dilution activity coefficient of polyethylene in cyclohexane. Experimental data are data from molecular simulation studies.

Figure 8.6 Packing fraction versus molecular weight of polystyrene, as calculated by simplified PC-SAFT.

Figure 8.7 Packing fraction – reduced temperature plot for polystyrene (15.000) and polyisobutylene (15.000), as calculated by simplified PC-SAFT.

Appendix

Derivation of the Equations for the Method of the Alternating Tangents

The reduced Gibbs energy for a binary mixture in terms of the mol fraction of component 1 (x) is:

$$\frac{g_{res}}{RT} = x(\ln x + \ln \hat{\phi}_1) + (1-x)(\ln(1-x) + \ln \hat{\phi}_2) \tag{A1}$$

The first derivative with respect to x is then:

$$\frac{\partial(g_{res}/RT)}{\partial x} = \ln x + \ln \hat{\phi}_1 + x(\frac{1}{x} + \frac{\partial \ln \hat{\phi}_1}{\partial x}) - (\ln(1-x) - \ln \hat{\phi}_2 + (1-x)(-\frac{1}{1-x} + \frac{\partial \ln \hat{\phi}_2}{\partial x}) \tag{A2}$$

We define

$$\phi_{ij} = \left(\frac{\partial \ln \hat{\phi}_i}{n_j} \right)_{T,P,n_{k \neq j}} \tag{A3}$$

and

$$\overline{\Phi}_{ij} = n_t \phi_{ij} \tag{A4}$$

It can be shown in a straightforward way that we then have

$$\frac{\partial \ln \hat{\phi}_1}{\partial x} = \overline{\Phi}_{11} - \overline{\Phi}_{12} \tag{A5$_a$}$$

$$\frac{\partial \ln \hat{\phi}_2}{\partial x} = \overline{\Phi}_{21} - \overline{\Phi}_{22} \tag{A5$_b$}$$

The Gibbs-Duhem relation with these variables is:

$$x\overline{\Phi}_{11} + (1-x)\overline{\Phi}_{12} = 0 \qquad (A6_a)$$

$$x\overline{\Phi}_{21} + (1-x)\overline{\Phi}_{22} = 0 \qquad (A6_b)$$

In addition, from symmetry we have

$$\overline{\Phi}_{12} = \overline{\Phi}_{21} \qquad (A7)$$

and eq. A2 reduces to

$$\frac{\partial(g_{res}/RT)}{\partial x} = \ln x + \ln\hat{\phi}_1 - \ln(1-x) - \ln\hat{\phi}_2 \qquad (A8)$$

Taking the second derivative and utilizing conditions (A6) and (A7) we have:

$$\frac{\partial^2(g_{res}/RT)}{\partial x^2} = \frac{1}{x} + \frac{1}{1-x} + \frac{\partial \ln\hat{\phi}_1}{\partial x} - \frac{\partial \ln\hat{\phi}_2}{\partial x} = \frac{1}{x} + \frac{1}{1-x} + \overline{\Phi}_{11} - \overline{\Phi}_{12} - (\overline{\Phi}_{21} - \overline{\Phi}_{22}) = \frac{1-\overline{\Phi}_{12}}{x(1-x)} \qquad (A9)$$

At the spinodal, the second derivative of the Gibbs energy is zero, which results in the simple condition:

$$\overline{\Phi}_{12} = 1 \qquad (A10)$$